Investigations into the Early Steps of Cobalamin Metabolism

Isabelle Racine Miousse

Doctorate of Philosophy

Department of Human Genetics

McGill University

Montreal, Quebec, Canada

June 6, 2011

A thesis submitted to McGill University in partial fulfillment of the requirements of the degree of Doctorate of Philosophy

DEDICATION

This work is dedicated to the persons living

with cobalamin disorders and their families.

ACKNOWLEDGMENTS

I would like to thank my supervisors David Rosenblatt and James Coulton for their support and inspiration during the years I have spent in their company. I am grateful for all the opportunities they have opened for me, for their time and their patience.

Thank you to my committee members, Dr. Eric Shoubridge and Dr. Rima Slim, for their advice and guidance.

Special thanks also to Drs. David Watkins and Maria Plesa for their technical guidance and their great depth of knowledge. I would also like to thank them for proofreading work.

Thank you to the students, particularly Woranontee Werarpachai for teaching me microcell-mediated chromosome transfer, Abigail Gradinger and Amanda Duval-Loewy for getting me started with PCR and cell culture, and all the other students I had the chance to work with.

TABLE OF CONTENTS

LIST OF TABLES

LIST OF FIGURES

CLAIMS TO ORIGINALITY

1) The gene responsible for the *cblF* form of inborn error of intracellular cobalamin metabolism was located to chromosome 6.
2) Four novel mutations were identified in *cblF* patients, including the first splice mutation and large deletion.
3) Analysis of three new *cblD* patients strengthened the association between the nature and location of mutations in the MMADHC gene with the biochemical phenotype displayed by patients.
4) A tag-free pure MMADHC protein was purified for the first time. Results indicate that interactions between the MMACHC and MMADHC proteins are susceptible to occur mainly at the C-terminus of MMACHC.

LIST OF ABBREVIATIONS

ABC	ATP-binding cassette
AdoCbl	5’-deoxyadenosylcobalamin
ATP	Adenosine-5’-triphosphate
BBB	Blood-brain barrier
Cbl	Cobalamin
CNCbl	Cyanocobalamin
Cob(I)alamin	Oxidation state +1 of the cobalt atom in cobalamin
Cob(II)alamin	Oxidation state +2 of the cobalt atom in cobalamin
Cob(III)alamin	Oxidation state +3 of the cobalt atom in cobalamin
HC	Haptocorrin
IF	Intrinsic factor
LDL	Low-density lipoprotein
LDLR	Low-density lipoprotein receptor
MeCbl	Methylcobalamin
MeTHF	5-methyltetrahydrofolate
MMA	Methylmalonic acid
MMCT	Microcell-mediated chromosome transfer
MS	Methionine synthase

MS/MS	Tandem mass spectrometry
MTHFR	Methylenetetrahydrofolate reductase
MTRR	Methionine synthase reductase
MUT	Methylmalonyl-CoA mutase
NTD	Neural tube defect
OHCbl	Hydroxycobalamin
SPR	Surface plasmon resonance
TC	Transcobalamin
TC-I	Transcobalamin I, haptocorrin
TC-II	Transcobalamin II, transcobalamin
TCA	Tricarboxylic acid
TCblR	Transcobalamin receptor
XMMCT	Irradiated microcell-mediated chromosome transfer

ABSTRACT

Vitamin B_{12} (cobalamin, Cbl) is an essential coenzyme in mammals for two reactions: the conversion of homocysteine to methionine by the enzyme methionine synthase and the conversion of methylmalonyl-CoA to succinyl-CoA by the enzyme methylmalonyl-CoA mutase. In cells, cobalamin is converted to the two active coenzyme forms of the vitamin: methylcobalamin and 5'-deoxyadenosylcobalamin. Eight groups of patients have been described with intracellular disorders of cobalamin metabolism, named *cblA*-*cblG* and *mut*. Three groups of patients present with an inability to produce both methylcobalamin and 5'deoxyadenosylcobalamin: *cblF*, *cblC* and *cblD*. We located the gene responsible for the *cblF* type of cobalamin disorder to chromosome 6 by microcell-mediated chromosome transfer, leading to the discovery of the *LMBRD1* gene. We identified three novel mutations in *LMBRD1* among *cblF* patients. We reviewed phenotypic and genetic data on three *cblD* patients and were able to confirm previous genotype-phenotype correlations. We purified the MMADHC protein defective in the *cblD* group of cobalamin disorder and predicted that interactions with the protein defective in the *cblC* group occur in a domain homologous to a bacterial domain involved also in protein-protein interactions.

ABRÉGÉ

La vitamine B_{12} (cobalamine, Cbl) est une coenzyme essentielle chez les mammifères pour deux réactions : la conversion entre l'homocystéine et la méthionine par l'enzyme méthionine synthase et la conversion entre le méthylmalonyl-CoA et le succinyl-CoA par l'enzyme méthylmalonyl-CoA mutase. Dans les cellules, la cobalamine est transformée en ses deux formes coenzymatiques actives : la méthylcobalamine et l'adénosylcobalamine. Huit groupes de patients ont été décrits qui présentent des défauts intracellulaires de la voie métabolique de la cobalamine, nommés *cblA*-*cblG* et *mut*. Trois groupes de patients présentent une inhabilité à synthétiser la méthylcobalamine et l'adénosylcobalamine : *cblF*, *cblC* et *cblD*. Nous avons localisé le gène responsable de la forme *cblF* de désordre de cobalamine sur le chromosome 6 par transfert de chromosome par microcellules, menant à l'identification du gène *LMBRD1*. Nous avons identifié trois nouvelles mutations dans *LMBRD1* chez des patients *cblF*. Nous avons passé en revue des données phénotypiques et génotypiques pour trois patients *cblD* et avons pu confirmer des corrélations génotype-phénotype observées auparavant. Nous avons purifié la protéine MMADHC défectueuse dans le groupe *cblD* et prédit que l'intéraction avec la

protéine défective dans le group *cblC* implique le domaine homologue à un domaine d'une protéine bactérienne aussi impliqué dans des intéractions protéiques.

CHAPTER 1: LITERATURE REVIEW

Vitamin B_{12} (cobalamin, Cbl) is a complex molecule whose characteristics, metabolism, and uses have slowly been uncovered during the last century, and are still the subject of numerous investigations worldwide. Cobalamin is needed as a coenzyme for two reactions in mammalian cells: The first reaction uses methylcobalamin (MeCbl) to transmethylate homocysteine to the amino acid methionine through the action of methionine synthase. This reaction also requires 5-methyltetrahydrofolate (MeTHF), a derivative of folic acid. The second reaction converts methylmalonyl-CoA to succinyl-CoA, an intermediate for the tricarboxylic acid cycle. This reaction requires the coenzyme 5'deoxyadenosylcobalamin (AdoCbl). Cobalamin is produced in nature by some bacteria and archaea, and is absent from yeast and plants. Meat and dairy products represent sources of cobalamin for humans. Deficiency can appear in people following a vegan diet or in newborns breastfed by a cobalamin-deficient mother. The onset of the symptoms in adults can be delayed because of the accumulation of the vitamin in the liver, which can compensate for a decrease in intake for an extended period of time. Rare inborn disorders of cobalamin absorption and metabolism have been

described and are studied to understand normal processes of cobalamin metabolism. The first section of this work retraces the history of the discovery of this intriguing compound, some characteristics of its chemistry and the description of the disorders of cobalamin metabolism.

1.1 Historical perspectives

1.1.1 First descriptions of pernicious anemia

The history of vitamin B_{12} begins with the first description of pernicious anemia. Pernicious anemia is a life-threatening condition that was first reported by Addison in 1849 [1]. The disease is also referred to as Addison anemia (not to be confused with Addison disease, also described by Addison). The term “pernicious anemia” is used to describe a form of non iron-deficient anemia due to an autoimmune reaction. As is the case for iron-deficient anemia, patients experience general weakness that is fatal if left untreated. In 1880, Ehrlich used newly discovered staining techniques to observe blood samples from patients with pernicious anemia and recognized a characteristic enlargement of red blood cells, macrocytosis [2]. Cabot described the symptoms of pernicious anemia in 1200 patients. Numbness and tingling of the extremities were present in almost all patients, a sore tongue in about 40%, and 10% had ataxia [3].

Untreated pernicious anemia is associated with demyelination of the spinal cord as described by Russell in 1900; subacute combined degeneration of the spinal cord [4].

1.1.2 A cure for pernicious anemia

Initial investigations into the origin of the disorder and its treatment occurred in the 1920s when Whipple observed that bleeding-induced anemia in dogs was overcome more quickly when the animals were fed raw liver [5]. Inspired by Whipple's studies on dogs, Minot and Murphy tried the raw liver therapy on a small group of patients with non iron-deficient anemia with encouraging results [6]. It turned out that the effectiveness of liver in the patients was unrelated to the initial observation- the anemia in dogs being helped by the iron contained in liver. However, their conclusion that liver contained an anti-pernicious anemia factor was correct. This therapy was applied more generally around 1926, followed in 1928 by the intramuscular injection of extracts of raw liver due to understandable poor compliance to the oral treatment. A method of production of a concentrated liver extract was designed by Cohn and proved to be 50 to 100 times more efficient than liver itself, representing a significant improvement in therapy [7]. Whipple, Minot and

Murphy were awarded the Nobel Prize in Medicine and Physiology in 1934 for their effort in developing a cure for the fatal disease.

1.1.3 Cobalamin absorption

Inspired by Whipple, Minot and Murphy, Castle identified the source of the biological factor defective in pernicious anemia patients. He referred to it as the "intrinsic" factor (IF), as opposed to the "extrinsic" factor found in liver. He designed an experiment where partially digested meat was extracted from the stomach of volunteers to be administered to patients. During 10 days, anemic patients received 200 g of steak each day. No response was seen in the appearance of red blood cells. He then fed healthy volunteers 300 g of steak and recovered the gastric content after one hour. The gastric content was incubated a few more hours and 200 g was fed by tube to pernicious anemia patients. After 6 days of this treatment, the number of reticulocytes started rising, followed by a corresponding rise in red blood cell number [8, 9]. These result showed that the anti-pernicious anemia factor is not specific to liver. The response seen in patients indicated that it was an unknown factor present in the gastric juice of healthy volunteers that was defective in patients. These

results are part of a series of 15 articles spanning 25 years that set the foundations for the discovery and study of IF.

1.1.4 Pernicious anemia as an immune disorder

After IF was identified as the missing factor in pernicious anemia, a treatment option was to give patients capsules of purified hog-derived IF. The initial response was excellent. However, Mollin and Ross [10] and Glass et al. [11] noticed a decrease in serum cobalamin with the return of macrocytosis and neuropathy after one year of treatment. Over time, patients developed antibodies against IF, cancelling the effect of the treatment. This is not the only link between pernicious anemia and the immune system. Pernicious anemia is an autoimmune disorder [12]. Patients produce antibodies directed at parietal cells in the stomach [13]. These cells are responsible for the production of IF [14]. Parietal cells also secrete hydrochloric acid, explaining the finding of achlorhydria in pernicious anemia patients [15]. Antibodies can also be directed at IF. Pernicious anemia is also sometimes found in association with other immune disorders, such as multiple sclerosis [16] and type I diabetes [17].

1.1.5 Cobalamin-binding proteins

By the end of the Second World War, labeled cobalamin was widely available. Using radio-labeled vitamin B_{12}, Gräsbeck was able to identify two vitamin B_{12}-binding factors in gastric juice on starch-gel electrophoresis [18]. The heavier fragment corresponded to IF defective in patients and he designated the second, rapidly migrating band Rapidly moving-binder (R-binder). Several R-binders were later found in human saliva (reviewed in [19]). Plasma proteins that bind vitamin B_{12} were discovered during the 1950s. They were originally designated transcobalamin I, II, and III (TC-I, II and III) but the accepted modern designation is now haptocorrin (HC) for TC-I and III and TC for TC-II (see section 1.3.1) [20, 21].

1.1.6 Cobalamin malabsorption

In 1953, Schilling described what was to become the reference in cobalamin absorption tests [22]. An oral dose of radioactive cyanocobalamin (CNCbl) was given to the patient and radioactive counts in urine over the next 24 hours were determined. About 10% of the radioactive dose is recovered in normal subjects, as compared to less than 1% in patients with pernicious anemia. If absorption is low, a second

dose of cobalamin containing purified IF is administered. In pernicious anemia patients, there is a characteristic correction of absorption in the presence of exogenous IF. This test allows the differential diagnosis of pernicious anemia versus other forms of cobalamin malabsorption. A new form of inherited macrocytosis due to cobalamin malabsorption similar to pernicious anemia was described in 1960 by two physicians who gave their name to the syndrome, Imerslund and Gräsbeck [23, 24]. Patients with this disease have a defect in the IF receptor complex in the distal ileum, composed of the proteins cubilin and amnionless [25-27].

1.1.7 Isolation of cobalamin

In the 30s and 40s, although a treatment for pernicious anemia was available, the nature of the active factor in liver extract, extrinsic factor, was still unknown. The discovery of the exact nature of the anti-pernicious anemia factor would wait until 1948, when Folkers at Merck in the United States and Smith at Glaxo in the UK simultaneously isolated the compound, which was named vitamin B_{12} [28]. The American group was helped by the development of an assay to test the liver fractions for the presence of the anti-pernicious anemia factor using the bacterium *Lactobacillus lactis* [29]. Isolation quickly shifted from liver extracts to

microbial production. Large quantities of cobalamin could be isolated from fermentation flasks, and radiolabeled cobalamin could be obtained by adding ^{60}Co to the culture media [30]. Cobalamin is still produced in this manner today. Naturally-producing strains such as *Propionibacterium shermanii* and *Pseudomonas denitrificans* are typically modified through random mutagenesis to increase the biosynthetic fermentation process leading to vitamin B_{12} production [31]. The main world producer of cobalamin is Aventis. The company is the result of a fusion including the French company RPR that first described the bacterial pathway leading to B_{12} synthesis.

1.1.8 Structure and synthesis of cobalamin

In 1956, the chemist Dorothy Hodgkin solved the structure of the molecule by X-ray diffraction [32]. She was awarded the Nobel Prize of Chemistry for this achievement in 1964. Her work revealed a heme-like structure called corrin ring with a cobalt atom in its center and a benzimidazole base. The presence of this cobalt atom in the vitamin is at the origin of the technical name of the molecule: cobalamin. In Hodgkin's own words: "To be able to write down a chemical structure very largely from purely crystallographic evidence on the arrangement of atoms in space – and the

chemical structure of a quite formidably large molecule at that – is for any crystallographer, something of a dream-like situation."[33]. Complete synthesis of the cobalamin molecule was achieved for the first time in 1973 after eleven years of effort by a team of over one hundred scientists. The published total synthesis by Woodward and Eschenmoser comprises over 100 steps [34].

1.1.9 Discovery of complementation groups

Inherited disorders of intracellular cobalamin metabolism were first described in the 1960s. Patients show normal enteral absorption of the vitamin but fail to metabolize cobalamin properly within cells. They compose a heterogeneous class of disorders with overlapping features that was separated into gene-based groups using somatic cell complementation. Cultured fibroblasts from two patients within the same complementation group cannot rescue each other's biochemical phenotype when fused *in vitro*, indicating that all patients in this group have a defect in the same gene. On the other hand, fibroblasts from patients belonging to different complementation groups show a normalized behavior biochemically, indicating that the defects are located in different genes. This classification proved to be useful subsequently in providing

homogeneous groups of patients for identification of the genes underlying the different conditions.

1.1.10 Genetic era

The gene encoding the methylmalonyl-CoA mutase (MUT) enzyme had been identified as early as 1989 [35], methionine synthase in 1996 and methionine synthase reductase in 1998 [36]. The completion of the Human Genome Project in 2003 facilitated the identification and characterization of genes and gene products defective in patients. In the last ten years, six genes have been identified, most of them without any previous information about their function. Linkage, comparison with prokaryotic genes, microcell-mediated chromosome transfer (MMCT), and identification of cobalamin-binding proteins are techniques that have been used to locate genes responsible for these inborn errors of cobalamin metabolism [37-42]. These developments allowed for cheaper and faster diagnoses. An important proportion of patients with cobalamin disorders are now offered gene sequencing as a diagnosis method, rather than more complex biochemical studies. This has contributed to dramatically decrease the costs of testing. These advances have also made prenatal testing on the basis of mutation analysis available.

Animal models deficient for the genes encoding methionine synthase [43], methionine synthase reductase [44], and methylmalonyl-CoA mutase [45] have been developed in recent years. The main goals of these models are to reproduce the phenotypes observed in humans, study the etiology of abnormalities, and develop better treatments.

Large populational studies have provided further information on cobalamin metabolism. Low cobalamin levels have been associated with impairment of cognition and dementia in the elderly (reviewed in [46]). The introduction of folate supplementation in flour in several countries has raised concerns as to the potential masking effect of high folate levels on cobalamin deficiency [47]. Widespread cobalamin supplementation is also a subject of debate. Finally, some new reports on the utilization of cobalamin as a delivery molecule for anti-cancer agents opened up a whole new field of study of the vitamin B_{12} [48, 49].

1.2 The cobalamin molecule

1.2.1 Coordination chemistry

As its name indicates, cobalamin is a vitamin that contains in its center a cobalt atom. The chemistry of metals such as cobalt is termed coordination chemistry. In cobalamin, the cobalt atom forms divalent bonds with other atoms, such as the carbon atom of the methyl group in methylcobalamin (MeCbl). However, the proper designation is that the cobalt is "coordinated" rather than "bound" to the carbon atom. The reason for this is that in regular covalent bonds, each atom provides one electron so that the pair can be shared between the two atoms. However, the cobalt atom has an empty outer orbital. Both electrons are provided by the ligand and are shared between the ligand and the cobalt atom. This bond is named a coordinated covalent bond and ligands are said to be coordinated rather than bound to the cobalt. The chemistry of cobalt was in great part solved by Alfred Werner at the turn of the 20th century.

1.2.2 Cobalamin structure

Cobalamins are a class of closely related compounds ranging from 1.3 to 1.5 kDa. The cobalt atom in the cobalamin molecule is located inside a corrin ring, a macrocycle related to the porphyrin ring of hemoglobin and consisting of four pyrrole subunits (Fig. 1). The nitrogen residue in each of these four pyrrole subunits is coordinated to the central cobalt atom. A fifth

and sixth coordination positions are located below (α-axial ligand) and above (β-axial ligand) the corrin ring. A dimethylbenzimidazole group attaches to the corrin ring through a linker constituted of a five-carbon sugar, a phosphate group and seven amide groups. This linker between the corrin ring and the benzimidazole moiety provides the flexibility necessary for a nitrogen residue in the dimethylbenzimidazole group to provide a fifth coordinate to the cobalt atom. This arrangement is referred to as the “base-on” conformation. At acidic pH, the α-axial ligand at the fifth coordinate position is released and the structure opens up into a stable base-off conformation. When the cobalamin molecule is associated with a protein at neutral pH, the dimethylbenzimidazole moiety can be replaced by a histidine residue in the binding pocket of the protein [50]. This histidine residue is found in the conserved sequence DDXHXXG shared by cobalamin-dependant enzymes [51]. This new conformation is then called base-off/His-on. Finally, the sixth and last coordinate for the cobalt atom is provided by a variable upper β-axial ligand, also known as R group. Methyl, deoxyadenosyl, or hydroxy groups are examples of R groups giving rise to the methyl-, adenosyl- or hydroxycobalamin forms of the vitamin, respectively. A number of other ligands can constitute the R group but their significance is not clear.

Figure 1: The structure of cobalamin

The cobalt atom is found in the center of the corrin ring (Co^{3+}), coordinated with four nitrogen atoms. The benzimidazole moiety is coordinated to the cobalt atom, as indicated by the dashed arrow. The variable upper axial ligand is indicated as R. Taken from Watkins et al. [52]

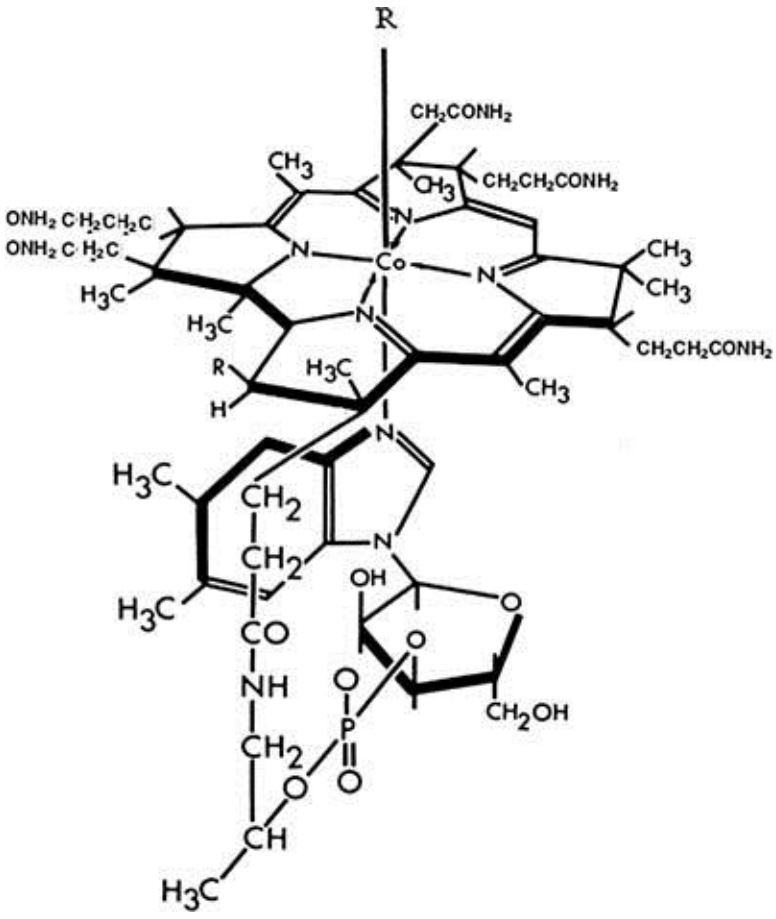

Figure 1: The structure of cobalamin

1.2.3 Oxidation states of cobalamin

The cobalt in the cobalamin molecule has three possible oxidation states: cob(III), (II) and (I)alamin. In cob(III)alamin, the cobalt atom is in the +3 oxidation state and has six coordinates. The vitamin is stable in this form, in the base-on conformation. Cob(II)alamin, the 2+ oxidation form, is generally base-on and lacks the upper axial ligand. However, an alternative form has been detected during the adenosyltransferase reaction where the molecule is transiently in the 2+ oxidation state with a water molecule occupying the lower axial position instead of the benzimidazole group [53]. Finally, cob(I)alamin has four coordinates and lacks the upper axial ligand. It is found in the base-off conformation. The most stable form of cobalamin at neutral pH is cob(III)alamin and reduction to the highly reactive cob(I)alamin form is necessary for the molecule to perform its catalytic role (reviewed in [54, 55]).

1.2.4 Cobalt-carbon bond

The link between the cobalt atom and the upper axial ligand in the two active forms of vitamin B_{12}, AdoCbl and MeCbl, is a cobalt-carbon (Co-C) bond. This type of metal-carbon bond is rare in nature; cobalamin-dependant enzymes catalyze the only known reactions involving such a

structure. This bond is at the center of every biological reaction involving cobalamin. The methionine synthase reaction involves the heterolytic cleavage of the Co-C bond to transfer the methyl group at the upper axial position of MeCbl to homocysteine to form methionine. In methylmalonyl-CoA mutase, the homolytic cleavage of the Co-C bond generates cob(II)alamin and a 5'-deoxyadenosyl radical. The 5'-deoxyadenosyl radical removes a hydrogen atom from methylmalonyl-CoA to form 5'-deoxyadenosine and a methylmalonyl-CoA radical. A rearrangement occurs within the methylmalonyl-CoA radical, and the hydrogen is transferred back to 5'-deoxyadenosine, leaving as products succinyl-CoA and AdoCbl. These reactions were reviewed in more detail by Ludwig and Matthews [54].

1.2.5 Cobalamin-related compounds

Although cobalamin is the only molecule of its family to be utilized by mammals, bacteria produce a variety of cobalamin derivatives. Corrinoids are compounds that contain a corrin ring. Cobamides are corrinoids similar to cobalamin but that harbor substitutions in nucleotide bases, while cobinamides are nucleotide-free (reviewed in [54]). Some cobamide derivatives of cobalamin found in food are designated pseudo-$B_{12,}$ where

the benzimidazole group in the α-axial position is replaced by an alternative nucleotide; adenine. These forms generally have a low affinity for cobalamin-binding proteins and cannot be utilized by cobalamin-dependant enzymes in humans, although some represent the natural form of the cofactor used by bacterial species [56]. It is postulated that haptocorrin present in serum acts as a scavengers for inactive forms of cobalamin [57].

1.2.6 Cobalamin synthesis in bacteria

Notably, higher plants and fungi do not utilize cobalamin and do not synthesize it. Only some bacteria and archaea have the ability to synthesize the vitamin. Microorganisms synthesize cobalamin as well as a variety of cobalamin-related compounds. The synthesis process involves over 30 genes in an aerobic (cob genes) or anaerobic (cbi genes) process. Cobalt incorporation happens earlier in the anaerobic than in the aerobic pathway, and the corresponding enzymes for most steps of the synthesis have different substrate specificity. There are three main types of cobalamin-dependant enzymes in bacteria: the AdoCbl-dependant mutases (with three subclasses: isomerases, eliminases and

aminomutases), the MeCbl-dependant methyltransferases, and the cobalamin-dependant reductive halogenases (reviewed in [54]).

1.2.7 Cobalamin import in bacteria

Bacteria that do not synthesize cobalamin but possess cobalamin-dependant enzymes must acquire the vitamin from the environment. This is the case in the model organism *Escherichia coli*. Gram-negative bacteria such as *E. coli* are surrounded by two membranes separated by a space called the periplasm. The cobalamin molecule must cross both these membranes to reach the cytoplasmic cobalamin-dependant enzymes. On the outer membrane is located a receptor called BtuB [58]. BtuB is a barrel-shaped protein that directly binds cobalamin [59]. Upon binding, the TonB component of the inner-membrane anchored, energy transducing complex TonB/ExbB/ExbD establishes a contact with a domain called the TonB box on the periplasmic face of BtuB. This action triggers the removal of the cork domain, opening the lumen of BtuB for the passage of the molecule [60]. Inside the periplasm, cobalamin is taken up by the periplasmic carrier BtuF and delivered to the inner membrane complex. In the inner membrane, an ABC transporter is composed of a heterotetramer containing two molecules of BtuC with 10 α-helical

membrane spanning domain each, and two molecules of the ATPase BtuD. BtuF docks on the periplasmic surface created by the transmembrane protein BtuC. The cytoplasmically located BtuD molecules provide the energy required for translocation. The import mechanism relies on a sequence of protein-protein interactions and requires ATP [61, 62].

1.3 Cobalamin absorption in humans

1.3.1 Cobalamin binding in the GI tract

Cobalamin forms found in food items of animal and bacterial origins bind to haptocorrin (HC) secreted in the saliva. The HC gene is expressed in several tissues and compartments where it can adopt a variety of glycosylation patterns, altering the properties of the protein [63]. It is referred to in older literature as transcobalamin I, transcobalamin III or R-binders. As all these forms are generated from a single gene, the term haptocorrin is now used uniformly. HC binds cobalamin in the upper part of the GI tract and the action of pancreatic proteases is required to release the vitamin from this carrier once in the ileum. Failure to release cobalamin from HC, a process requiring acidic gastric pH, is thought to impair cobalamin absorption and cause neurological manifestations, a

condition referred to as food cobalamin malabsorption [64, 65]. This hypothesis could explain the high frequency of low serum cobalamin seen in the elderly population. Once cobalamin is free from HC, it can then associate with IF. IF is secreted in the parietal cells of the stomach and the interaction with cobalamin occurs in the ileum. As stated before, auto-antibodies directed at the gastric parietal cells are responsible for IF deficiency and the development of pernicious anemia. Pernicious anemia can also be the result of rare mutations in the IF gene, IF deficiency (MIM# 261000) [66]. IF is a heavily glycosylated and sialylated 45 kDa protein, resulting in a net apparent weight of 58 to 60 kDa. In contrast to HC that binds a wide variety of cobalamin analogues, IF specifically binds cobalamin.

1.3.2 Crossing of the enteric epithelium

The IF-Cbl complex is recognized by a receptor on cells of the distal ileum epithelium. The IF-Cbl receptor is a complex made of the proteins cubilin and amnionless (cubam) that internalizes IF-Cbl [67, 68]. Mutations in cubilin or amnionless lead to a form of cobalamin malabsorption called Imerslund-Gräsbeck syndrome, or selective cobalamin malabsorption (MIM# 261100). Cubilin is a 460 kDa protein containing eight epidermal

growth factor-like repeats and 27 copies of the 110 amino acid CUB domain. Amnionless is a 45 to 50 kDa membrane protein. It forms complex with cubilin and is required in the apical targeting and processing of cubilin [67, 69, 70]. Cubilin and amnionless are co-expressed in the kidney, intestine, and mouse visceral yolk sac [26, 71]. In the kidney, the apical localization of the receptor suggests a role in reabsorption, limiting cobalamin losses in urine.

Megalin is a member of the LDL receptor gene family encoded by the gene *LRP2*. It involved in the internalization of the cubam complex but its exact role is still debated [68]. It is expressed in the intestinal and renal epithelium [72]. Megalin is a transporter for several protein ligands in addition to IF-Cbl, such as hemoglobin [73], myoglobin [74], transferrin [75], albumin [76], and insulin [77]. Mutations in *LRP2* are associated with Donnai-Barrow syndrome [78]. It is characterized by hypertelorism, an enlarged fontanelle, high myopia with progressive vision loss, hearing loss, agenesis of the corpus callosum, cognitive impairment, and congenital diaphragmatic and/or umbilical hernia. The disorder is diagnosed on the basis of excretion of high levels of low-molecular-weight proteins in urine.

As depicted in figure 2, the IF-Cbl complex enters the enterocyte through receptor-mediated endocytosis and the endosome formed is directed to the lysosomal pathway [27]. The IF-Cbl complex dissociates inside the lysosome and cobalamin is exported into the portal circulation through the ATP-binding cassette (ABC) transporter ABCC1 (MRP1). Mice deficient in ABCC1 have low serum, liver and kidney cobalamin levels. No elevations of homocysteine or methylmalonic acid were detected. These animals accumulate cobalamin in the distal ileum and colon epithelium [79].

Figure 2: Cobalamin absorption through the enteric epithelium

Cobalamin (red) is associated with intrinsic factor (IF, blue) in the ileum. The IF-Cbl complex is recognized by the receptor made of the megalin, cubilin and amnionless protein. After receptor-mediated endocytosis, the complex is directed to the lysosomal pathway where it dissociates. The receptor is recycled to the membrane and the cobalamin molecule exits the cell through the transporter ABCC1. Once in the blood, cobalamin is found associated with transcobalamin (TC) and haptocorrin (HC).

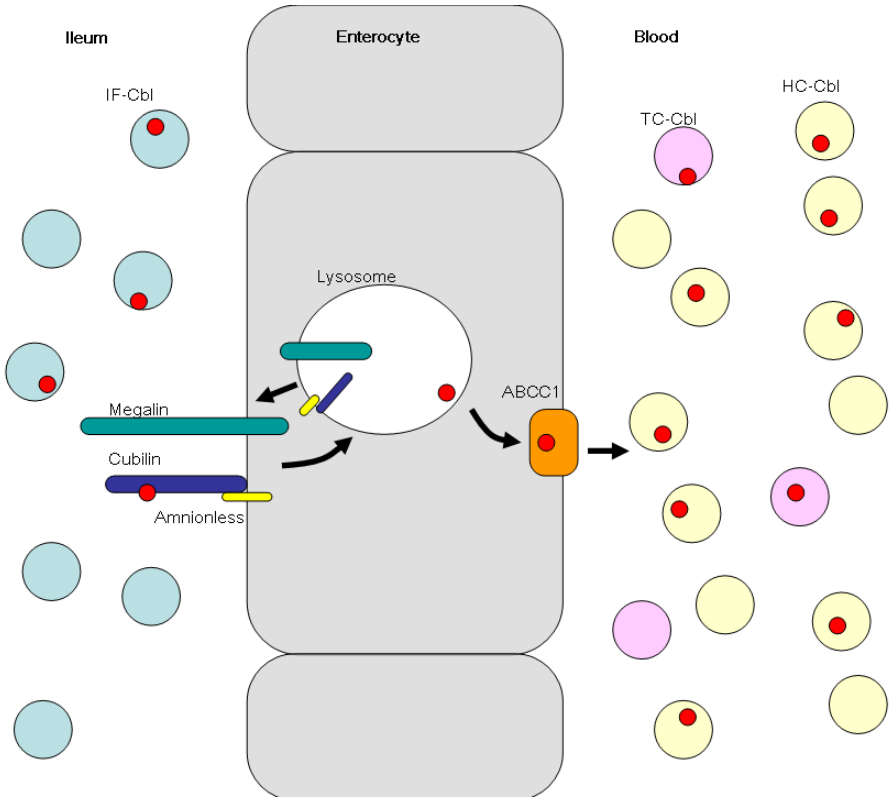

Figure 2: Cobalamin absorption through the enteric epithelium

1.3.3 Cobalamin in the circulation

In the blood, cobalamin is found associated with two proteins: 80% of it is bound to HC and the remaining associates with transcobalamin (TC, formerly transcobalamin II or TCII) [80]. TC shows a greater specificity for the physiologically relevant forms of cobalamin, while the wide ligand spectrum of HC is postulated to act as a scavenger for non-physiologically relevant forms of vitamin B_{12} [81]. Holo-HC is taken up by the liver through the plasma membrane receptor for asialoglycoproteins [82, 83]. The receptor for TC is encoded by a gene identified as *CD320*, described in the next section [42]. IF, TC, and HC share similarities in their sequences and gene organizations, suggesting a common origin for these genes [84, 85]. TC deficiency (MIM# 275350) usually presents in early life with failure-to-thrive, macrocytosis, and immunological and neurological involvements [86, 87]. Serum cobalamin levels are normal in these patients, as most cobalamin is bound to HC. On the other hand, HC deficiency is associated with low serum cobalamin [88]. However, these individuals do not present elevations of methylmalonic acid or homocysteine and do not benefit from cobalamin therapy. The current view is that these patients come to medical attention due to unrelated

causes and their alarmingly low serum cobalamin, though benign in this rare condition, cause them to be unnecessarily treated with cobalamin [89].

1.3.4 Entry into the cells

The TC receptor (TCblR) is a relatively small protein of 282 amino acids encoded by the *CD320* gene [42]. It belongs to the low-density lipoprotein (LDL) receptor family. It is a single pass type 1 membrane protein. TCblR possesses two 38 amino acid long LDL receptor class A domains containing cysteine-rich repeats, and a 55 amino acid long domain sharing similarities with the CUB domain. N- and potentially O-glycosylation, as in IF, significantly increases the apparent weight of the molecule.

Once the TC-Cbl complex binds the TC receptor on the cell surface, a process of receptor-mediated endocytosis is triggered. The endocytic vesicle is directed to the lysosomal pathway and the acidification of the compartment leads to a dissociation of the complex. Free cobalamin is translocated to the cytoplasm. Mutations in the TC receptor were identified in five infants with a positive newborn screen for methylmalonic acid. Cobalamin therapy was initiated in all five patients shortly after newborn

screen and they remain asymptomatic [90, 91]. It is thus not known if TC receptor deficiency is associated with a clinical phenotype.

1.3.5 Cobalamin-dependant enzymes in human

Inside the cells, cobalamin is transformed into its two active coenzyme forms: MeCbl and AdoCbl. MeCbl is utilized as a cofactor in the cytoplasm by the enzyme methionine synthase. Methionine synthase is a 140 kDa protein that catalyzes the transmethylation of homocysteine into the essential amino acid methionine [92]. The methyl group is provided by MeTHF from the folate pathway and the reaction is dependant on cobalamin. Every 200 to 2000 cycles, methionine synthase is inactivated and it is through the action of methionine synthase reductase that it can be reactivated by a reduction reaction. Disturbances in the function of methionine synthase lead to an accumulation of homocysteine in blood and urine.

The other cobalamin-dependant enzyme in humans is located in the mitochondrion, methylmalonyl-CoA mutase. MUTis a 83 kDa protein that converts methylmalonyl-CoA, a product of the catabolism of certain amino acids and odd chain fatty acids, to succinyl-CoA, a key molecule in the

tricarboxylic acid cycle. This reaction is dependant on the presence of AdoCbl. Disturbances in the function of methylmalonyl-CoA mutase lead to an accumulation of methylmalonic acid (MMA) in blood and urine. Both methionine synthase and methylmalonyl-CoA mutase have homologues in bacteria.

1.4 Homocysteine: an overview

Homocysteine is an amino acid that is not present in proteins. It is produced as a result of the metabolism of methionine and cysteine (Fig. 3). It differs from methionine by one methyl group and from cysteine by one methylene group. Pathological elevations of homocysteine are found in inborn errors of metabolism affecting enzymes or coenzymes responsible for homocysteine metabolism. These lead to the excretion of large amounts of homocysteine in blood and urine. Modest elevations of homocysteine in adults are associated with more common conditions such as cardiovascular diseases. Finally, polymorphisms in genes involved in the metabolism of homocysteine are associated with an increased risk for neural tube defects and cardiac malformations in the fetus.

Figure 3: Homocysteine in humans

The two homocysteine remethylation pathways and the transsulfuration pathway. The three key enzymes are in bold: MS: methionine synthase, BHM: betaine-homocysteine S-methyltransferase, CBS: cystathionine beta-synthase. The cofactors vitamin B_{12} and vitamin B_6 are displayed in red. The enzyme methylenetetrahydrofolate reductase (MTHFR) is also displayed for its key role in providing the MeTHF coenzyme necessary for the MS reaction. Figure adapted from [93].

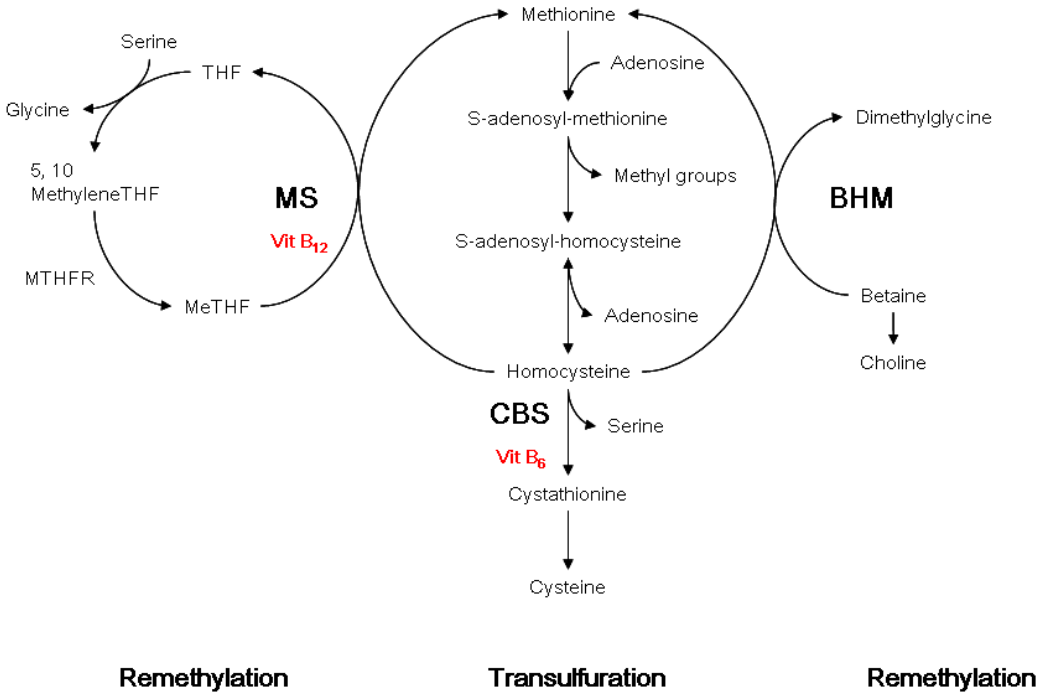

Figure 3: Homocysteine in humans

1.4.1 Inborn errors of homocysteine metabolism

Impairment in three enzymatic reactions can lead to elevations of homocysteine: methionine synthase, betaine-homocysteine methyltransferase, and cystathionine ß-synthase. Methionine synthase and betaine-homocysteine methyltransferase both remethylate homocysteine to methionine while cystathionine ß-synthase is the first step of the transsulfuration pathway to irreversibly convert homocysteine to cysteine. Methionine synthase is ubiquitously expressed and the reaction requires MeCbl and MeTHF. This reaction is detailed in other parts of this manuscript. Any deficiency in acquisition or the synthesis of the MeCbl coenzyme or MeTHF, or in the accessory protein methionine synthase reductase will also lead to an impaired activity of methionine synthase. Betaine-homocysteine methyltransferase is exclusively expressed in the liver. This reaction requires betaine, which is converted to dimethylglycine in the process. Defects in the remethylation pathway lead to systemic levels of methionine in the low to low-normal range in patients, in addition to elevated homocysteine [52]. In the transsulfuration pathway, cystathionine β-synthase is expressed in adult liver, kidney, muscle, brain and ovary and in embryonic neural and cardiac systems

[94]. This enzyme irreversibly transforms homocysteine to cystathionine to be later converted to cysteine through cystathionine γ-lyase. Cystathionine β-synthase uses a coenzyme, pyridoxine (vitamin B_6). High homocysteine due to impaired transsulfuration is accompanied by high levels of methionine, providing a diagnostic criterion to distinguish the two disorders. Elevations of homocysteine due to either the remethylation or the transsulfuration pathway defects have been linked to similar manifestations, including mental retardation, arterial and venous occlusive disease, and neural tube defects.

1.4.2 Folic acid and cobalamin

The cobalamin-dependant enzyme methionine synthase requires a second co-factor to perform the transmethylation of homocysteine. MeTHF provides a methyl group to form MeCbl, which is then transferred to homocysteine. Consequently, disturbances of both folate and cobalamin metabolism, result in an impaired function of methionine synthase. In addition, cobalamin deficiency also affects the folate cycle and the other functions of folates in the cell, such as purine nucleotide synthesis, thymidine synthesis, and histidine and serine metabolism. When methionine synthase is impaired, folate intermediates remain trapped in

the form of MeTHF between the irreversible MTHFR and the deficient methionine synthase reactions. This situation leads to the depletion of the other biologically active forms of folate in the cell, forming the basis for the now widely accepted “methylfolate trap” hypothesis [95]. This situation impairs DNA biosynthesis and causes the characteristic megaloblastosis of defects affecting methionine synthase.

1.4.3 Cardiovascular disease in adults

In 1969, McCully published the observation that severe elevations of homocysteine in several different inborn disorders caused vascular lesions in children [96]. It led to the hypothesis that homocysteine causes tissue damage in the vascular endothelial wall [97]. Subsequent studies found an association between mild elevations of homocysteine and increased risk of vascular disease in adults [98-101]. Homocysteine is an independent risk factor for coronary arterial disease. However, several studies demonstrated that folic acid-based therapies that successfully lowered homocysteine levels failed to have any clear impact on cardiovascular morbidity [102-106]. Meta-analyses confirmed these negative results [107-109]. One current hypothesis is that the pro-inflammatory properties of folic acid would cancel out the benefits of the homocysteine lowering in

patients [110]. Homocysteine might also be an innocent bystander in a pathological process yet to be identified.

1.4.4 Neural tube defects- Folic acid

Low levels of folic acid in pregnant women during the first trimester are a now well-recognized risk factor for neural tube defects (NTD) in the fetus [111]. For example, up to 85% of NTD-affected pregnancies in Northern China can be prevented by meeting a 400 μg daily folate requirement [112]. This has led to the supplementation of grain products in North America, and a subsequent 26% decrease of in NTD-affected pregnancies in the United States [113]. However, just as NTD rates vary by geographic area, socioeconomic status and ethnicity, outcomes from fortification have been variable by location and ethnic group [114-119]. In addition to dietary deficiency, polymorphisms in genes related to the folate metabolism in mothers and babies have been associated with an increased risk of NTD-affected pregnancies [120-124]. The current consensus is that the hypomethylation resulting from the deficiency in methyl groups normally provided through the folate pathway rather than toxicity from homocysteine itself is responsible for the phenotype [125]. Studies in mice have demonstrated that inactivation of methyltransferases cause an

increased frequency of NTDs [126]. The association between the MTHFR 677C>T polymorphism and neural tube defects and other birth defects has been replicated several times in different populations and appears as a risk factor [122, 124, 127-132], although it is important to note that not all studies have observed that effect [123, 133, 134]. Other studies have shown that high levels of homocysteine induced in chick embryos led to neural tube defects, as well as congenital cardiac malformations [135]. However, these results have not been replicated in mice [136].

1.4.5 Neural tube defects- Cobalamin

Because methionine synthase is common to both folate and cobalamin metabolism, it has been postulated that marginally low levels of cobalamin or polymorphisms in cobalamin metabolism genes could increase the risk of having a neural tube defect-affected pregnancy. Low concentrations of cobalamin in the mother's serum have been linked with an increased risk of NTD in Irish, Canadian, Chinese, and Egyptian populations [137-141]. Others have found no effect of cobalamin status [142-145]. Results have been reviewed by Ray and Blom [146]. Polymorphism in the *CUBN* gene has been linked with an increased risk of spina bifida in one study [147]. Polymorphisms in the recently identified TC receptor gene [120] have

been linked with increased risk of NTD-affected pregnancy in the Irish population. Most studies looking at the 776C>G polymorphism in the *TCN2* gene have found no association with neural tube defects [128, 129, 133, 148, 149]. One study have found an association of the G allele with spina bifida [150]. Studies have also looked at the c.66A>G (p.I22M) polymorphism in the gene methionine synthase reductase (MTRR). Some have found an association between neural tube defect risk and the GG or AG allele [127, 130, 131, 151, 152] but others did not [129, 133, 134, 153].

1.4.6 Cardiac malformations

Several inborn errors of folate and cobalamin metabolism with elevations of homocysteine have been linked to congenital heart defects. Malformations are seen both in patients and in the corresponding mouse models. Mouse embryos from *Mthfr* hypomorphic mothers display heart defects [154]. Defects in the reduced folate carrier protein 1 (*Rfc1*) gene in mice also lead to cardiac anomalies [155]. *Mtrr* homozygous mutant embryos display an increased risk of ventricular septal defects [44]. Children with the *cblC* and *cblF* types of inborn error of cobalamin metabolism have an increased risk of congenital heart disease [156, 157]. Polymorphisms in the genes *MTHFR*, *BHMT*, and *TCN2* have been

associated with an increased risk of congenital heart disease when associated with lifestyle factors [132]. Congenital heart disease has also been linked to high homocysteine and evidence suggests that folic acid supplementation during the first trimester of pregnancy decreases the incidence of such malformations [158-160]. Studies in chicken embryos demonstrated that the injection of homocysteine into embryos induces the development of cardiac malformations [161]. Such malformations can be rescued by folic acid supplementation [162]. It has also been shown that choline deficiency in mice lead to cardiac malformations [163]. Choline is converted to betaine, utilized for the betaine-homocysteine methyltransferase reaction, through choline dehydrogenase and betaine aldehyde dehydrogenase.

1.5 Methylmalonic acid: an overview

Methylmalonic acid (MMA) is a biochemical intermediate related to propionic acid. Elevations of MMA in blood or urine (methylmalonic acidemia or aciduria) are part of a group of disorders referred to as organic acidurias, which comprises also propionic aciduria and isovaleric aciduria. MMA has an incidence estimated at 1 per 100 000 births [164-166].

Figure 4: Classical organic acidurias

Metabolic pathways involved in classical organic acidurias. Nutrients at the source of the pathway are indicated in italics. PCC: propionyl-CoA carboxylase, racemase is also known as methylmalonyl-CoA epimerase,MUT: methylmalonyl-CoA mutase.

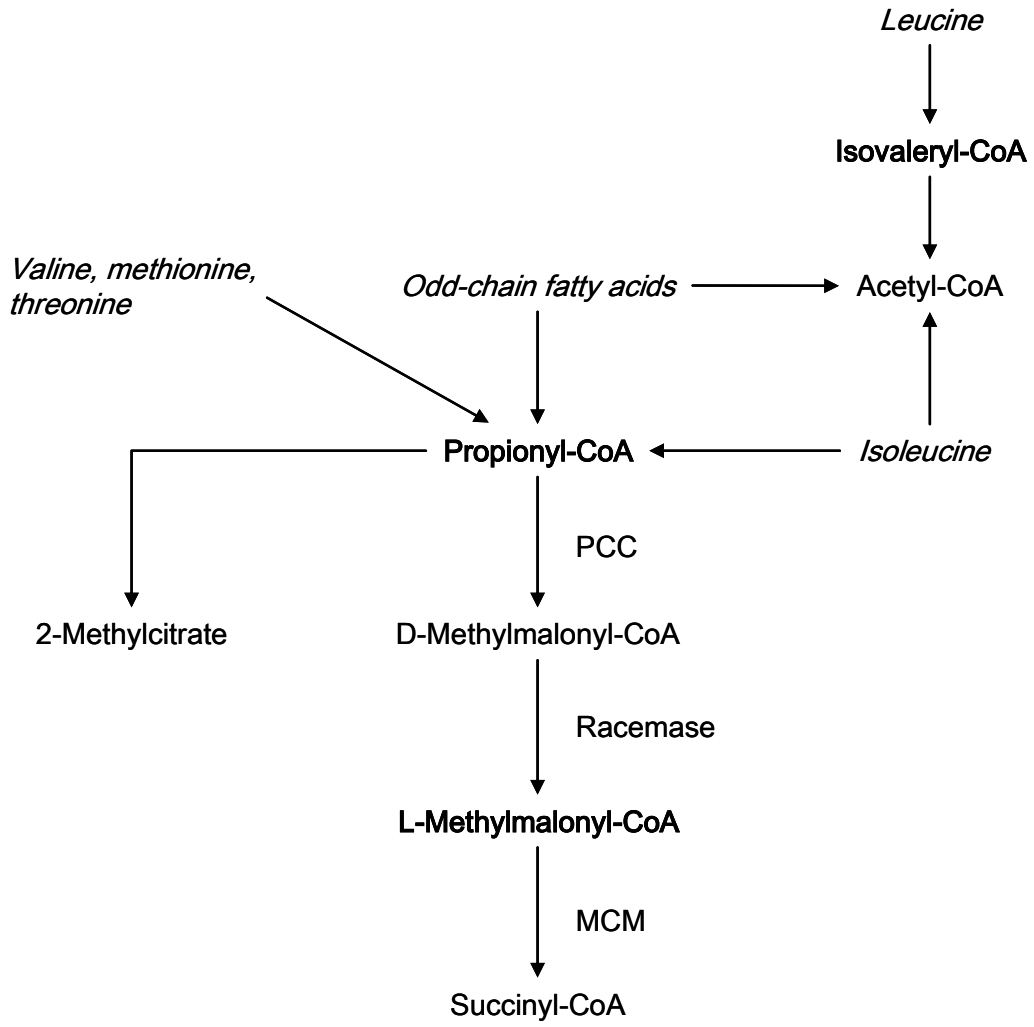

Figure 4: Classical organic acidurias

1.5.1 Metabolic pathways leading to methylmalonic aciduria

Methylmalonic aciduria is the result of the degradation of odd chain fatty acids and certain amino acids (Fig. 4). Odd-chain fatty acids are degraded into the 2-carbon molecule acetyl-CoA and the 3-carbon molecule propionyl-CoA (reviewed in [167]). Propionyl-CoA is also produced during the catabolism of the branched-chain amino acids valine and isoleucine and the propiogenic amino acids methionine and threonine. Propionyl-CoA is then converted to D-methylmalonyl-CoA by the enzyme propionyl-CoA carboxylase [168]. D-methylmalonyl-CoA is converted to L-methylmalonyl-CoA by the enzyme methylmalonyl-CoA epimerase [169]. MMA is a normal intermediate of this pathway prior to the conversion of methylmalonyl-CoA to succinyl-CoA by the enzyme methylmalonyl-CoA mutase. Succinyl-CoA is subsequently integrated into the tricarboxylic acid (TCA) cycle.

1.5.2 Genetic causes of methylmalonic aciduria

Methylmalonic aciduria is frequently found in combination with homocystinuria. Nutritional deficiencies and impaired absorption of cobalamin and genetic defects can lead to the condition. However, genetic

disorders of the mitochondrial branch of cobalamin metabolism are the main cause of isolated elevations of MMA. Mutations in the genes *MMAA, MMAB*, *MUT*, and certain mutations in *MMADHC*, corresponding to the *cblA*, *cblB, mut* and *cblD variant 2* groups of cobalamin disorders, result in an elevation of MMA without elevation of homocysteine. They affect the production of the coenzyme AdoCbl or the methylmalonyl-CoA mutase enzyme itself. Mild elevations of MMA can also be the result of mutations affecting the enzyme methylmalonyl-CoA epimerase (*MCEE*) responsible for the racemization of D- to L-methylmalonyl-CoA [170-172].

Rarer defects in mitochondrial metabolism can also lead to elevations of MMA in patients. Mutations in the alpha (*SUCLG1*) [173, 174] and beta (*SUCLA2*) [175, 176] subunits of the TCA cycle enzyme succinyl-CoA synthetase have been shown to cause elevations of the metabolite. Elevated MMA can be associated with elevated malonic acid in malonyl-CoA decarboxylase (*MLYCD*) deficiency [177]. This enzyme is involved in fatty acid metabolism and catalyses the reversible conversion between malonyl-CoA and acetyl-CoA. It is thought that an excess of malonyl-CoA in the mitochondrion exerts an inhibitory effect on methylmalonyl-CoA mutase, leading to the elevation of MMA [178].

1.5.3 Presentation

Clinical manifestations among the three classes of classical organic acidurias present a significant overlap but observations relating specifically to MMA are described here. Particularities of each type of cobalamin disorder can be found in sections 1.7.1-3. Patients are generally classified into early-onset (neonatal) or late-onset. In early-onset patients, there are often no symptoms at birth. The classical presentation is a neonatal encephalopathy in the presence of hyperammonemia. There is often a refusal to feed and vomiting. This is followed by weight loss and hypotonia. Abnormal posturing and movement is often noted. Lethargy is a common finding, as well as seizures. Coma can ensue, leading in some cases to death or severe brain damage. Late-onset patients often develop an acute, life-threatening encephalopathy in childhood or even adulthood. Patients display ataxia and abnormal behaviors. Poor feeding, refusal of protein-rich food and vomiting are common. Patients have failure-to-thrive and neurodevelopmental delay (reviewed in [179]).

The most characteristic symptoms associated with MMA are neurological disturbances. This can manifest as mental retardation, epilepsy or motor dysfunction. Symmetrical lesions to the basal ganglia, mostly in the globus

pallidum, have been recognized in these patients [180-183]. They are thought to occur during acute metabolic decompensation [167]. Survival is low in patients with MMA [184, 185]. Progressive renal failure is frequent in patients who reach their teenage years [186-190], along with progressive neurocognitive deterioration [179, 190].

1.5.4 Suspected etiologies

The symptoms associated with elevations of MMA have been studied by several groups. The most consistent finding is an inhibition of the respiratory chain, particularly complex II and IV, associated with elevations of MMA [191-194]. MMA is not the only suspect. Propionyl-CoA also has a cytotoxic role. It induces hyperammonemia through the inhibition of N-acetylglutamate synthase [195]. It also decreases oxidative phosphorylation through the inhibition of the pyruvate dehydrogenase complex [196, 197] and the TCA cycle enzymes succinyl-CoA synthetase [198] and α-ketoglutarate dehydrogenase [199]. 2-methylcitrate is another possible culprit in the inhibition of the respiratory chain [200].
Mitochondrial DNA has been demonstrated to be depleted in *SUCLA2* patients and in patients with propionic aciduria [201]. Mitochondrial DNA depletion has also been reported in two patients with methylmalonic and

propionic acidemia [202]. Studies are needed to determine if depletion of mitochondrial DNA can be identified in other patients with MMA. One last possible explanation for the neurological phenotype in patients with methylmalonic acidemia is trapping and accumulation of toxic compounds in the brain by the blood-brain barrier (BBB). Some dicarboxylic acids, unable to cross the BBB, accumulate in the brain and have been linked to toxicity [204-206].

1.5.5 Treatment

Survival in patients with organic aciduria has improved in the last 30 years [207]. This is in large part due to early diagnosis and better treatment. Patients are now routinely identified by newborn screening with tandem mass spectrometry (MS/MS) [208]. Treatment includes a high-energy, low protein diet supplemented with non-propiogenic amino acids. Enteral feeding may be necessary in some cases as prolonged fasting induces the release of odd-chain fatty acids through lipolysis. Patients excrete high levels of acylcarnitine and supplementation with L-carnitine is recommended. Several treatment centers also prescribe the antibiotic metronidazole to prevent the production of propionate by the gut microflora [207, 209]. Liver and kidney transplant has been explored as a

therapy and although some improvements have been noticed, complications are frequent and neurological deficits remain [210, 211]. Advances have been made toward gene therapy for *mut*^{0} patients [212-215].

1.6 Intracellular defects of cobalamin

1.6.1 Biochemical signs of cobalamin disorders

The intracellular pathway of cobalamin metabolism was uncovered in large part through the study of patients presenting inborn errors of cobalamin metabolism. Clinical symptoms are non-specific but two metabolites represent the hallmark of cobalamin disorders: homocysteine and MMA. Some patients present with elevations of both these compounds in blood and urine. This is indicative of a defect of both the cytoplasmic (methionine synthase) and mitochondrial (methylmalonyl-CoA mutase) branches of the pathway. Other patients present with isolated elevations of homocysteine or MMA, affecting only one branch of the pathway.

1.6.2 Newborn screening

With the expansion of newborn screening programs, an increasing proportion of patients are detected and treated before the onset of symptoms. The most common method of testing is blood spot analysis by tandem mass spectrometry (MS/MS). The first indication for methylmalonic aciduria is an elevation in propionylcarnitine (C3) or an elevated ratio of propionylcarnitine to acetylcarnitine (C2). A specific test to detect MMA is then performed. While testing for organic acids is widely spread, testing for homocysteine levels is possible but because of the need for a reducing agent for the mass spectrometry analysis, costs currently limits its availability [208]. An alternative is to screen for low methionine levels, although these frequently fall in the low-normal range in patients. Consequently, cobalamin disorders, with the exception of *cblE* and *cblG*, are identified on the basis of an elevated C3 or C3/C2 ratio on newborn screening, and subsequent testing for elevated methylmalonic acid and homocysteine levels is performed upon the request of the treating physician. If a nutritional deficiency can be excluded, cell-based biochemical testing is performed at one of the two diagnosis centers, located in Zurich (formerly Basel), Switzerland and Montreal, Canada.

More recently, DNA sequencing has been used both as an adjunct and an alternative to traditional cellular assays.

1.6.3 Biochemical characterization

Biochemically, the activity of the methionine synthase and methylmalonyl-CoA mutase pathways can be indirectly assessed by detecting the incorporation of label from specific metabolites into cellular macromolecules by fibroblasts from patients. In cultured human cells with normal methionine synthase activity, a radioactive label in the CH_3 group of MeTHF is metabolized by the cell and incorporated into macromolecules. Cellular radioactive counts are markedly decreased when this reaction is impaired [216]. Similarly, radiolabeled propionate is used to indirectly assess activity of the methylmalonyl-CoA mutase reaction [217]. Cells cultured from patients with defects in the methionine synthase branch of the intracellular cobalamin pathway show a decrease in their ability to incorporate label from MeTHF. Cells cultured from patients with defects in the methylmalonyl-CoA mutase branch of the pathway show a decrease in their ability to take up label from propionate. Patients are classified into three groups; impaired propionate

incorporation, impaired MeTHF incorporation, and combined. However, mutations in at least three genes can explain every class of defect.

1.6.4 Somatic cell complementation

To separate patients on the basis of the affected gene, somatic cell complementation is used [218, 219]. Cultured cells from two patients are fused using polyethylene glycol. The resulting heterokaryons show improvement in their biochemical parameters if the defect is located on different genes (complementation) while cells with defects affecting the same gene are not able to complement each other. Eight complementation groups were established within which cells do not complement each other but complement cells from the other seven groups. These groups were designated *cblA* through *cblG* and *mut* (Fig. 5). Interallelic complementation, i.e. complementation between cell lines with defects in the same gene, can occasionally be observed so testing with more than one cell line is recommended. Based on biochemical analysis, characteristics of each complementation group allowed understanding the function of some of the unknown genes under the complementation groups. For example, in cells from patients of the *cblF* group, cobalamin is found free (not protein bound) and largely in the

lysosomal fraction. This points to a defect in the process by which cobalamin exits the lysosome. However, it is with the development of methods to identify the genes involved in the different groups of cobalamin disorders that more could be understood about the function of each step of the cobalamin pathway.

Figure 5: Intracellular cobalamin metabolism

Cobalamin carried in blood by transcobalamin (TC-Cbl) is recognized by the transcobalamin receptor (TCblR). Receptor-mediated endocytosis directs the vesicle to the lysosomal pathway. Inside the lysosome, the complex dissociates and the cobalamin molecule is exported to the cytoplasm, a process impaired in *cblF* patients. Patients with the *cblC* and *cblD classical* disorders show a defect in the synthesis of both methylcobalamin (MeCbl) 5'-deoxyadenosylcobalamin (AdoCbl). Patients with the *cblD variant 1* and *cblE* defect have a deficient synthesis of MeCbl, patients with the *cblD variant 2*, *cblA* and *cblB* defects show a defect in the synthesis of AdoCbl. *cblG* and *mut* represent a defect in the methionine synthase and methylmalonyl-CoA mutase enzyme, respectively. Defects in the methionine synthase branch of the pathway lead to elevations of homocysteine in plasma (homocysteinemia) and urine (homocystinuria). Defects in the methylmalonyl-CoA mutase branch of the pathway leads to elevations of methylmalonic acid in plasma (methylmalonic acidemia) and urine (methylmalonic aciduria).

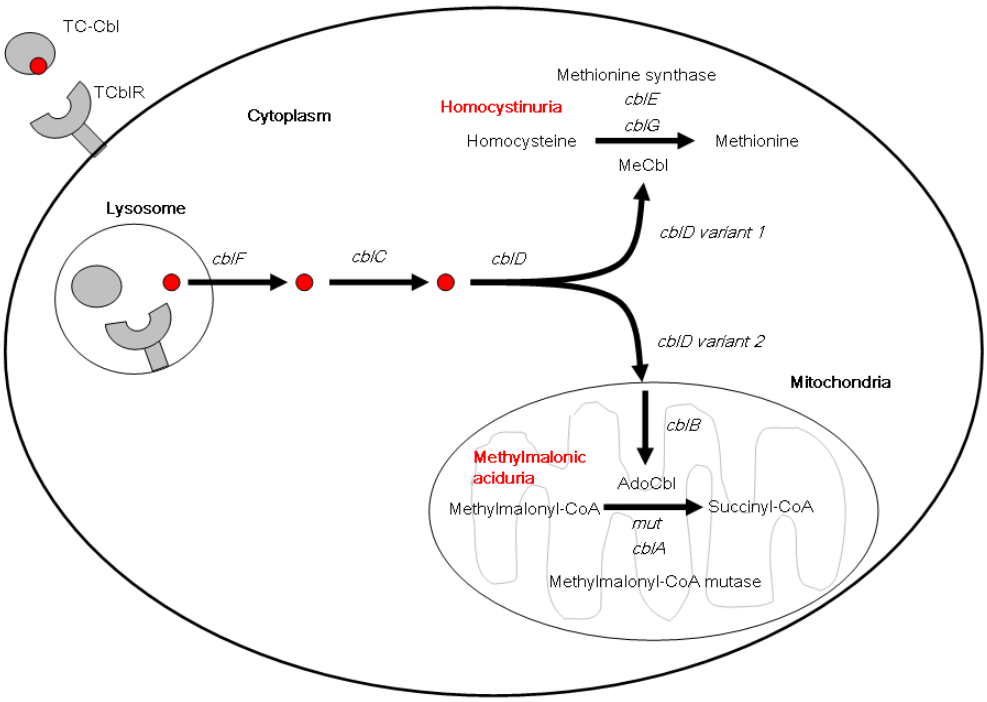

Figure 5: Intracellular cobalamin metabolism

1.7 Complementation Groups

1.7.1 Disorders affecting methionine synthase

cblG (MIM #250940)

Presentation

cblG is the complementation group corresponding to a deficiency in the methionine synthase enzyme [220]. Patients have elevated levels of homocysteine without MMA in blood and urine and their fibroblasts show a decreased incorporation of label from radioactive MeTHF, the other cofactor in the methionine synthase reaction, into cellular macromolecules. Symptoms include macrocytosis, developmental delay, ataxia, cerebral atrophy, seizures and blindness.

MTR, the gene responsible for *cblG*

The enzyme is encoded by the gene *MTR* [37, 92], and contains four functional domains [221]. The homocysteine-binding domain associates with the pterin binding domain to catalyze the methylation of cob(I)alamin from MeTHF. The pterin-binding domain catalyses the transfer of the methyl group to homocysteine. The cobalamin-binding domain is

responsible for binding the vitamin. Finally, the activation domain binds S-adenosylmethionine. Methionine synthase is essential in the folate cycle to regenerate tetrahydrofolate from MeTHF. In methionine synthase functional deficiency, the folate pool in the cell becomes biased towards MeTHF. Folate-dependant reactions such as purine synthesis and methylation are impaired. This situation has been referred as the "methylfolate trap" hypothesis, and is covered in more details in section 1.4.2. Homozygous *mtr* knockout mice die shortly after implantation, and are not recued by nutritional supplementation. Heterozygotes have normal or slightly elevated homocysteine levels, depending on the genetic background, and display signs of endothelial dysfunction [43, 222].

cblE (MIM #236270)

Presentation

There are about 30 known *cblE* cases in the world. It corresponds to a deficiency in the enzyme methionine synthase reductase. The presentation is undistinguishable from *cblG*.

MTRR, the gene responsible for *cblE*

The enzyme methionine synthase reductase is encoded by the gene *MTRR* [36]. Periodically, the cob(I)alamin molecule associated with the enzyme methionine synthase is oxidized to cob(II)alamin, inactivating the enzyme. Methionine synthase reductase performs a reductive methylation of the cofactor back to its 1+ state. S-adenosylmethionine is used as a methyl donor in this reaction to regenerate MeCbl [223, 224]. Interestingly, the most frequent mutation in *cblE* patient is a mutation deep in intron 6, c.903+469T>C. This change forms a new exon splice enhancer and leads to the inclusion of a pseudo-exon [225]. *Mtrr*-deficient mice are reproductively impaired. *Mtrr*-deficient mothers develop smaller placentae and the embryos are developmentally delayed and small. *Mtrr*-deficient embryos had a higher rate of ventricular septal defects than their littermates [44].

1.7.2 Disorders affecting methylmalonyl-CoA mutase

cblB (MIM #251110)

Presentation

cblB patients often present in the first year of life due to an acidotic crisis. These patients have an elevation of MMA without homocystinuria. Hospitalization typically results from vomiting, tachypnea, hypotonia and

dehydration, sometimes precipitated by diet, exercise or infection. Associated symptoms include failure to thrive, developmental delay, lethargy, and encephalopathy. The age of onset varies, with about one third presenting in the first week of life, and one quarter after one year of age [184, 226]. Some patients have presented during adolescence. Patients that present later in life are frequently reported have a self-selected low-protein diet. Less than half of the *cblB* patients respond to cobalamin therapy (decrease in MMA levels). In a cohort of ten *cblB* patients, three patients died from the disease and four were impaired (mental or developmental retardation, multiple hospitalizations for recurrent acidosis or other medical problems) [184].

MMAB, the gene responsible for *cblB*

The *cblB* type of cobalamin disorder is caused by a defect in the enzyme cob(I)alamin adenosyltransferase encoded by the *MMAB* gene [41]. It is located on 12q24. Identification of the gene was possible through the identification of clusters of cobalamin-dependant metabolic pathways in several microorganisms and comparison with human genes. The gene product, MMAB, localizes to the mitochondria. It catalyzes the transfer of adenosine from ATP to cobalamin. MMAB forms a trimer with ATP-binding

sites located at the junction between adjacent monomers. However, only two of the three sites are occupied by ATP at any specific time. Binding of ATP is presume to lead to cobalamin binding [227]. The *MMAB* gene has recently come under scrutiny when whole genome association studies on HDL-levels in human have identified a region upstream of the gene [228-230]. *MMAB* shares its promoter region with the gene *MVK* encoding mevalonate kinase, encoded in the opposite direction. Mevalonate kinase plays a role in sterol synthesis and was thought to be the cause of the association seen at this locus until it was demonstrated that expression levels of *MMAB* and not *MVK* correlate with HDL levels [231].

cblA (MIM #251100)

Presentation

The presentation in *cblA* patients is very similar to *cblB*. However, patients generally have milder symptoms and present later in life. A study of 14 *cblA* patients reported a response rate to cobalamin therapy over 90%. In that group, only one patient was reported to have died of the disease, most being alive and well [184]. Results were similar in an independent cohort of 20 *cblA* cases, where one single patient died at 14 days of age [185]. In a study of 37 *cblA* cases, only seven patients presented within

the first week of life [232]. Cognitive dysfunction was however present in about half of the patients assessed [185].

MMAA, the gene responsible for *cblA*

The gene responsible for the *cblA* type of cobalamin disorder was identified through prokaryotic gene arrangement [40]. The human *MMAA* gene is located at 4q31 and shares homology with the bacterial gene MeaB, encoding a G-protein chaperone located in the mutase gene operon. MeaB has a low intrinsic GTPase activity that is increased 100-fold in presence of MUT[233]. In the case of the human protein, one group observed a 8-fold increase in GTPase activity in the presence of human MUT [234] while another group did not detect a difference in activity [235]. MMAA and MUT form a stable complex. Complex formation is enhanced by the presence of GMPPNP, a non-hydrolysable analog of GTP, and inhibited by GTP and AdoCbl [234]. The structure of the human MMAA protein has been solved [234]. It is a homodimer. Its structure is generally very similar to the bacterial MeaB, the notable difference being a relative displacement of the dimerization arms causing the nucleotide-binding sites to be closer together in MMAA than MeaB. MMAA is postulated to reduce the AdoCbl molecule [55, 236]. The model predicts that periodically,

AdoCbl associated with the methylmalonyl-CoA enzyme is oxidized, inhibiting the reaction. The role of MMAA would be to reduce and reactivate the molecule. Like MMAB and MUT, MMAA is a mitochondrial protein.

mut (MIM #251000)

Presentation

The *mut* group corresponds to a defect in the methylmalonyl-CoA mutase enzyme. All *mut* patients display symptoms similar to *cblB* and *cblA* patients. Some patients have a complete absence of enzyme function, leading to a severe phenotype, while others have a residual enzyme activity and a milder phenotype. The severe phenotype, *mut*^{0}, has a phenotype more severe than *cblB* and over half of the patients die [184]. They present very early in life, with 80% in the first week of life. The milder form, *mut*$^{-}$, is associated with a phenotype similar to *cblA* [185]. Cultured fibroblasts from these patients display an increased enzymatic activity upon addition of cobalamin to the medium, contrarily to cells from *mut*^{0} patients [237]. The *mut*^{0} subgroup represent nearly half of the patients in the *cblA-cblB-mut* cohort.

MUT, the gene responsible for *mut*

A mutase is an enzyme that catalyses the transfer of a functional group from one position to another within a molecule.MUT, the enzyme encoded by the *MUT* gene, performs the transfer of a carbonyl-CoA group to the adjacent carbon in the backbone of MUTto produce succinyl-CoA. The gene is located at 6p21.2-p12. The substrate of the reaction, methylmalonyl-CoA, is produced from propionyl-CoA, a product of amino acid and odd-chain fatty acid catabolism. The product of the reaction, succinyl-CoA, is utilized as a substrate in the tricarboxylic acid cycle for energy production in the mitochondria. MUTfrom *Propionibacterium shermanii* is a heterodimer with one catalytic subunit [238]. The substrate binding site is located in a triosephosphateisomerase (TIM) barrel in the N-terminal domain of the protein. The AdoCbl-binding domain is located in the C-terminal domain. The N-terminal and C-terminal domains are connected by a linker [239]. Human MUTis a homodimer with two catalytic subunits [35]. The remainder of the structure is similar to the homologous *P. shermanii* enzyme. It is not known if the presence of two catalytic sites in the human MUThomodimer results in the presence of two MMAA homodimers, although the molecular weight of the complex detected with size exclusion chromatography favors the 2 MMAA dimers: 1 MUTdimer

hypothesis [234]. Addition of MMAA increased MUTactivity by 70%, presumably due to cofactor reactivation [235]. When MMAA was added at time 0, GMPPNP and GTP performed equally well at increasing MUTactivity. However, when MMAA was added after one hour, only GTP could produce an increase in MUTactivity [235].

1.7.3 Disorders affecting methionine synthase and methylmalonyl-CoA mutase

This thesis focuses on steps of the cobalamin metabolism that are common to the synthesis of both MeCbl and AdoCbl. These correspond to the *cblF*, *cblC* and *cblD* types of disorders that compose the initial steps of the intracellular cobalamin metabolism.

cblF (MIM #277380)

Presentation

Patients with the *cblF* type of cobalamin metabolism disorder typically present early in life with failure to thrive, feeding difficulties, and lethargy. Of fifteen patients diagnosed worldwide, four had congenital septal defects of the heart: One had a complex cardiac defect described as right

dominant atrioventricular septal defect with common atrium and double outlet right ventricle, transposition of the great vessels, hypoplastic left ventricle and common atrioventricular valve. A second had an atrial septal defect with patent ductus arteriosus and right ventricular hypertrophy. The two other patients had ventricular septal defects. Other congenital malformations were noted in *cblF* patients: tooth abnormalities were noted in three patients and one case presented dextrocardia. About half of the patients presented symptoms of inflammation such as glossitis, stomatitis, gastritis, arthritis or skin rashes. Six patients presented with low serum levels of cobalamin, which is unexpected in a disorder of intracellular metabolism. Five patients were diagnosed with macrocytosis. Convulsions were noted in two patients. Patients responded well to treatment with 1 mg intramuscular cobalamin once every week or two weeks. Two patients died from complications following corrective surgery for a congenital heart defect [157]. One patient died of sudden infant death syndrome [240]. Four patients are asymptomatic and the remaining present a mild psychological or growth delay. Half of the surviving patients are reported to have short stature. Biochemically, patients have elevations of homocysteine and MMA, although homocysteine was not detected in the index case [241]. Incorporation of label from propionate and MeTHF in

cellular macromolecules is decreased in all patients reported. Radiolabeled CNCbl added to cultured fibroblasts from *cblF* patients is minimally converted into the active coenzymes AdoCbl and MeCbl and mainly accumulates as CNCbl [241].

Impaired lysosomal transport

The first step of the intracellular cobalamin metabolism consists in the release of cobalamin from lysosome into the cytoplasm. The acidic pH inside the lysosome favors the dissociation of the TC-Cbl complex and TC is degraded [242, 243]. Very characteristic of the *cblF* group, cobalamin is almost entirely found associated with lysosomes, as demonstrated by radioautography [244]. In control cells, most of the silver grains tracking label from [^{57}Co] CNCbl was detected in the cytoplasm (47%) and mitochondria (23.4%), and only a small portion in the lysosome (4.7%). In cblF patients, 60% of the silver grains overlapped with lysosomes, with only 12.6% in the cytoplasm and 1.2% in the mitochondria. Lysosomal entrapment of cobalamin can be partially recapitulated by treating normal cells with chloroquine [245]. Chloroquine inhibits acidification of the lysosome. Similarly to *cblF* cells, chloroquine-treated cells retain cobalamin inside the lysosome. However, in chloroquine-treated cells, the

molecule remains associated with its carrier protein transcobalamin. In *cblF* patients, lysosomal acidification is intact and the complex dissociates. Most cobalamin is found in the free rather than the protein-bound form [245]. The disorder results from a failure in the transport of cobalamin across the lysosomal membrane rather than in the dissociation from transcobalamin. As a result, [^{57}Co] CNCbl added to cultured fibroblasts from *cblF* patients is largely recovered unmetabolized as CNCbl, with little synthesis of either MeCbl or AdoCbl. The total uptake of [^{57}Co] CNCbl in *cblF* cells is higher than in control cells or other groups of mutant cells [241].

cblC (MIM #277400)

Presentation

cblC is the most common class of inborn error of intracellular cobalamin metabolism, with over 500 cases reported. Synthesis of both AdoCbl and MeCbl is impaired, and unmetabolized CNCbl is not retained inside the cell. The function of methylmalonyl-CoA mutase and methionine synthase is decreased. Presentation is variable, with a majority patients presenting in early life. A late-onset, milder form of the disorder is also observed. Rosenblatt *et al.* published a summary of the clinical and laboratory

findings in 50 cblC cases, 44 early-onset and 6 late-onset [246]. Common symptoms include developmental delay, failure to thrive, poor feeding, and hypotonia. Hematological abnormalities were part of the findings in 34 of the 50 patients, manifesting most often as megaloblastosis and macrocytosis, and more rarely as hypersegmented polymorphonuclear leukocytes and thrombocytopenia. Seizures were present in 23 patients. Microcephaly was noted in 19 out of 44 early-onset patients. There are reports of hemolytic uremic syndrome in patients with the *cblC* disease, associated with a high mortality rate [247-255]. A progressive retinopathy is a frequent finding, particularly in early-onset patients [256-258]. There is an increased frequency of mild cardiac defects [156]. Symptoms are significantly milder in the late-onset form where neurological findings (dementia, psychosis, learning disability, neuropathy, etc.) are predominant [259]. As in cytathionine-ß-synthase patients, *cblC* patients develop early-onset arteriosclerosis and thrombotic events. The current hypothesis proposes that the long-term exposure to high levels of homocysteine in these patients causes arterial damage [96, 97, 260]. Prognostic is better in late-onset patient than in early-onset patients. There is a better response to hydroxycobalamin (OHCbl) than to the pharmacological preparation CNCbl [261, 262]. Despite treatment, most

early-onset patients have some degree of neurological impairment and nearly a third die [246]. Early diagnosis and initiation of treatment are currently the only tools to prevent long-term neurological sequelae.

MMACHC, the gene responsible for *cblC*

Mutations in the gene *MMACHC* are responsible for the disease [38]. The c.271dupA and c.331C>T mutations are associated with early-onset while the c.394C>T mutation is associated with late-onset of symptoms [263]. Mutations have variable frequencies in different populations. The c.609G>A mutation represents about half of the alleles in Northern Chinese and as much as three out of four alleles in Southern Chinese [264]. In patients of European ancestry, the c.207dupA mutation represents half of the disease-associated alleles [265]. The c.394C>T mutation is frequent in *cblC* cases from the Middle East, India, and Pakistan while the c.331C>T is a founder mutation in French-Canadian and Cajun populations [266]. The role of MMACHC is not fully understood although it has been reported that the protein can perform the decyanation of the CNCbl molecule, as well as the dealkylation of MeCbl and AdoCbl [267-269]. Both reactions involve the removal of the upper axial ligand but are predicted to act through different chemical processes. The

decyanation reaction is particularly surprising as this form of the vitamin does not exist in nature. However, it could explain the differential response seen with treatment with OHCbl versus CNCbl. The sequence of the protein MMACHC does not display the characteristic DXHXXG cobalamin-binding motif but experiments have shown binding with MeCbl and AdoCbl, and to a lesser degree with CNCbl and OHCbl [270]. MMACHC was also demonstrated to form an interaction *in vivo* and *in vitro* with the protein involved in the *cblD* disorder, MMADHC [270].

cblD (MIM #277410)

Presentation

The *cblD* type of inborn error of intracellular cobalamin metabolism is located at the point where the cobalamin pathway branches towards methionine synthase in the cytoplasm and methylmalonyl-CoA mutase in the mitochondria. Patients can present with an elevation of both homocysteine and MMA or with an isolated defect of one or the other [271]. For simplicity, the three forms are designated *classic* or combined, *cblD variant 1* for a defect in the synthesis of MeCbl and a deficiency in methionine synthase activity, and *cblD variant 2* for a defect in the synthesis of AdoCbl and a deficiency in methylmalonyl-CoA mutase

activity. Eleven patients are reported in the literature, with an additional patient not yet reported [39, 272]. Distribution is as follows: MMA only: three patients; combined: five patients; homocystinuria only: four patients. Clinical manifestations vary greatly, with a large spectrum of age of onset (first days of life to 14 years), type, and severity of symptoms. Developmental delay was reported in three out of four patients with homocystinuria only and one patient with combined homocystinuria and MMA. Poor feeding was reported in two patients with isolated MMA and one patient with combined homocystinuria and MMA. Seizures or convulsions were reported in four patients and was found in all three forms of the disease. Macrocytosis was reported in four out of five combined homocystinuria and MMA patients (the fifth patient was asymptomatic) and two out of four patients with isolated homocystinuria. Other symptoms reported in patients with MMA only include vomiting, ketoacidotic coma, lethargy, and necrotizing enterocolitis. Other reported presentations in patients with combined homocystinuria and MMA include mental retardation, marfanoid appearance, nygtagmus, respiratory infections, encephalopathy, and reduced myelination. Additional findings in patients with isolated homocystinuria include respiratory infection, hydrocephalus,

vena cava clot, spastic ataxia, delayed visual evoked potential, nystagmus, dystonia, and autistic features.

MMADHC, the gene responsible for *cblD*

The gene responsible, *MMADHC*, was identified by microcell-mediated chromosome transfer, a method consisting in introducing a normal copy of a chromosome or part of a chromosome to an affected cell and testing for correction of the biochemical phenotype [39]. The protein contains a putative mitochondrial leader sequence, and has a putative cobalamin binding motif covering residues 81 to 86 of the amino acid sequence. A region of homology to the ATPase component of a putative bacterial ATP-binding cassette (ABC) transporter has been detected. However, it lacks the three motifs critical for ATP-binding; Walker A, Walker B and ABC signature domain [273]. The sequence also contains a methionine codon in the context of a strong Kozak consensus sequence at position 62 of the amino acid sequence. It has been proposed that this codon could serve as an alternative start of translation, explaining the variant biochemical phenotypes seen in patients. Mutations associated with an isolated deficiency in the synthesis of AdoCbl are located at the N-terminus of the gene. It is speculated that translation in these patients re-starts at that

second ATG codon and maintains an active cytoplasmic part of the protein. Similarly, patients with an isolated defect in the synthesis of MeCbl have missense mutations clustered in the C-terminal region of the gene. In this case, the hypothesis is that a full-length protein is synthesized and active in the mitochondria, with a dysfunctional C-terminus [39]. As mentioned previously, MMADHC has been shown to interact with MMACHC [270].

1.8 Gene discovery in Mendelian disorders

The era of genetic mapping started in the mid-1980's. The genes responsible for Chronic Granulomatous Disease and Duchenne Muscular Dystrophy were discovered on the X chromosome as early as 1986 [274]. Since then, methods have evolved to identify genes involved in Mendelian disorders. Examples of approaches are localization based on homologies with known genes, linkage, exome capture and microcell-mediated chromosome transfer.

1.8.1 Homology with known genes

A traditional way to identify genes responsible for human disorders is to search for human homologs of genes involved in similar process in bacteria or animal models. The *MMAA* and *MMAB* genes were identified by analysis of the genes surrounding the methylmalonyl-CoA mutase gene in prokaryotes [40, 41]. In bacteria, genes in the same metabolic pathway are frequently found in close proximity in the genome, in a region under the control of a single promoter referred to as an operon. The human genes were identified by comparing genes around methylmalonyl-CoA mutase in bacteria and candidate human genes, and screening *cblA* and *cblB* patients for mutations in these candidates.

1.8.2 Linkage analysis

The most common method used in gene identification of Mendelian disorders is linkage analysis. The basis of linkage is that a disease-associated mutation in an affected family will be located on a single haplotype and markers present around the mutations will be in linkage disequilibrium (LD) with the condition. One large family with several affected and unaffected individuals is used, or multiple affected families. The result of the linkage is identification of a region of a chromosome that is larger or smaller depending on the density of informative markers at that

location. For example, *MMACHC*, the gene responsible for the *cblC* type of cobalamin disorder, was identified by linkage and homozygosity mapping. Homozygosity mapping is used in small families with few affected individuals. Affected individuals from different families are screened for consistent regions of homozygosity. Mutations can be different between families as long as individuals inherited the same mutation from both parents within a family. In *cblC*, the interval identified originally was 6.6 Mb in length [275]. Further haplotype analysis reduced the interval and a total of 15 genes were sequenced to identify causative mutations [38].

1.8.3 Exome capture

With recent developments in sequencing technologies, costs and times have been dramatically reduced. In addition to the traditional dye-terminator (Sanger) sequencing, a new array of what is collectively referred to as next generation sequencing has become available. These include pyrosequencing (454 Life Sciences), reversible dye-terminator (Solexa, Illumina) and sequencing by ligation (SOLiD, Applied Biosystems). These technologies have opened the possibility of sequencing entire genomes at ever-more affordable costs. In Mendelian

disorders, the majority of disease-causing mutations are located in the 1% of the genome that is protein-coding. Systematical sequencing of every protein-coding exon in the genome of one or a few patient thus is quickly becoming a rapid and affordable option to identify disease-causing genes. The first successful identification of a gene causing a Mendelian disorder by exome capture is the description of the role of the gene *DHODH* in Miller syndrome at the beginning of 2010 [276].

1.8.4 Microcell-mediated chromosome transfer

Introduction

Another approach that can be used to identify a gene based on its chromosomal location is microcell-mediated chromosome transfer (MMCT) [277]. This technique can be used when cultured cells from patients display a phenotype at the physical or biochemical level. MMCT consists in adding a normal copy of a chromosome to the patient's cells to see if that extra copy is able to correct the phenotype. Each of the 22 autosomes can be successively tested for correction. The gene responsible for the *cblD* type of cobalamin disorder, *MMADHC*, was identified in this manner.

Principle

Individual human chromosomes are isolated from donor murine-human hybrid cell lines containing one human chromosome labeled with a hygromycin resistance tag [278].Treatment of these donor cells with colcemid induces microtubule depolymerization resulting in the arrest of mitosis during metaphase. This process leads to the micronucleation of donor cells, in which condensed chromosomes are separated within vesicles constituted of nuclear and cell membrane. Cells are enucleated by treatment with cytochalasin B, which destabilizes the cell membrane. The microcells harvested in this way are fused to the recipient cells using polyethylene glycol. The recipient cells are then exposed to hygromycin, selecting for cells that have incorporated a tagged human chromosome. Clones formed in this manner are tested for correction of the phenotype (Fig. 6). Once one correcting chromosome has been identified, further refinement of the position of the gene can be performed in two ways. The first technique relies on spontaneous breaks happening in the transferred chromosome. Of the hygromycin-resistant clones, some will fail to correct the phenotype due to a chromosomal break causing a loss of the gene of interest. By comparing positive and negative clones with microsatellites or SNPs, it is possible to exclude regions (all regions present in negative

clones) and delimitate minimal intervals (regions common to all positive clones). Another approach to refine gene location in MMCT is the use of irradiated cell lines where chromosomal breaks are induced to increase their frequency. This technique is also referred to as irradiation-MMCT or XMMCT [279]. The increased number of breaks in the transferred human chromosome in XMMCT assists in the microsatellite/SNP analysis.

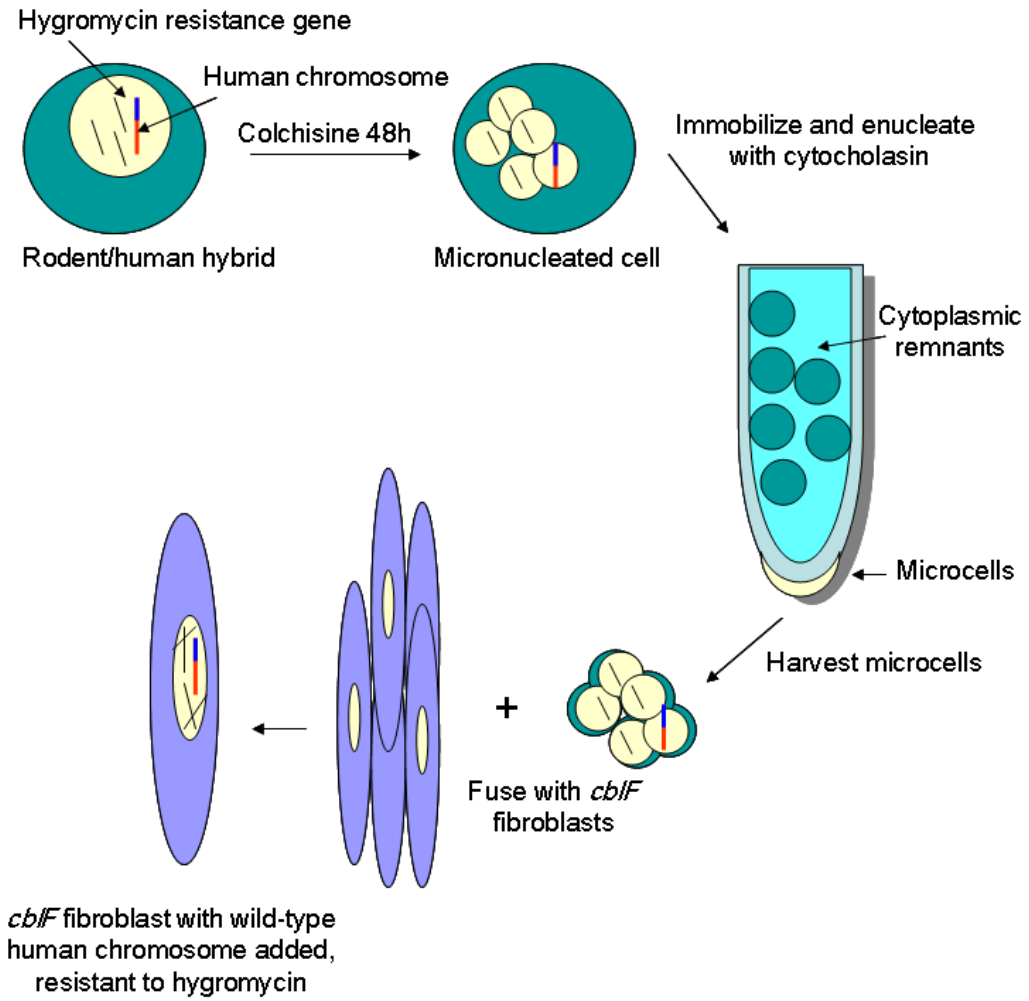

Figure 6: Microcell-mediated chromosome transfer

Application

In the cobalamin disorder *cblD*, patients' cells fused with chromosome 2-containing microcells resulted in an increase in the function of methionine synthase and methylmalonyl-CoA mutase, as indirectly measured by the incorporation of radiolabeled MeTHF (or formate) and propionate, respectively. Refinement of the position of the gene was achieved by exploiting spontaneous breaks in the chromosome transferred. Microsatellite analysis was performed on positive and negative clones from chromosome 2, delimiting a region containing 28 genes. These 28 genes were screened by cDNA sequencing to search for causative mutations [39].

MMCT is also applied to the identification of cancer suppressor genes. The phenotype observed in this case is the change from a neoplastic to a control phenotype. Doherty and Fisher [280] and Meaburn, Parris and Bridger [281] have reviewed the MMCT technique and its application to the search for cancer suppressor genes.

1.9 Protein-protein interactions

Protein-protein interactions are vital to many biochemical systems. For example, dozens of proteins have been described that participate in the mitochondrial respiratory chain. The mitochondrial respiratory chain is formed by large complexes of proteins, which are brought together by a series of assembly proteins. A deficiency in some of these assembly proteins is sufficient to produce life-threatening disorders, causing a failure of the complex formation. Recent data highlight the importance of protein-protein interactions in intracellular cobalamin metabolism. As presented in greater details in previous parts of this work, the interaction between MMAA and MUT led to an increase in enzymatic function [234, 235] and MMACHC and MMADHC have been demonstrated to interact [270].

1.9.1 Protein interactions in cobalamin metabolism

Four main facts lead us to believe that protein-protein interactions are necessary in intracellular cobalamin metabolism. The first fact is the low abundance of the vitamin inside cells. A classic study by Hsu and colleagues in 1966 has estimated the cobalamin concentration in human tissues to be as low as 30 ng per gram of wet healthy adult tissue in the brain, going up to 700 ng in the liver [282]. These amounts are further

separated into the different oxidation states (cob(I), (II) and (III)alamin), upper axial ligands (mainly OHCbl, MeCbl, and AdoCbl) and compartments (lysosomes, cytoplasm, mitochondria). The second fact is the state in which cobalamin is found. In control cultured fibroblasts, over 95% of the vitamin is found associated with proteins. This figure leaves very little free-floating vitamin available for chance interactions to occur. The third fact is the oxidation state of cobalamin. Cobalamin is stable in the cob(III)alamin form. However, it needs to be reduced to the cob(I)alamin state for the upper axial ligand to be substituted, creating the MeCbl and AdoCbl active forms of the vitamin. The cob(I) and cob(II)alamin are highly reactive and unstable in the cellular environment. The fourth fact is the base state of cobalamin. Studied cobalamin-binding proteins in the intracellular metabolism pathway bind the vitamin in its base-off state. The binding to a histidine residue in the protein structure lead to a base-off, his-on situation. However, the base-off form is not stable at neutral pH. At neutral pH, the base-on form is predominant. The base-off form is favored by low pH such as that found in the lysosome. Protein interactions are predicted to protect the base-off between metabolic stages. These four facts favor the hypothesis that the cobalamin molecule is constantly bound to proteins inside the cell. To process from

one step of the metabolism to the next in an efficient manner, cobalamin is proposed to go through a series of protein-protein interactions.

1.9.2 Proposed model

What is known about cobalamin is that it is rare, predominantly protein-bound, and very unstable in the forms required for cobalamin-dependant reactions to occur. These observations have led to a model where acidic pH in the lysosome favors the base-off, cob(III)alamin conformation. A series of protein-protein interactions would act to shield the vitamin against the cellular milieu. This would lead to a successful preservation in its base-off form and subsequent reduction to its cob(I)alamin oxidation state. Several approaches have been designed to observe and describe protein-protein interactions. The choice of one particular technique depends on the scientific question to address.

1.9.3 Phage display

Phage display predicts specific binding interfaces within proteins known to interact [283, 284]. It utilizes a library of bacteriophages displaying random peptides on their coat proteins. These phages are put into contact with the bait protein being studied and phages displaying sequences that have an

affinity for the bait are selected. The pool of affinity-selected phages can then be amplified in bacteria and used for further rounds of affinity-selection. DNA is isolated and sequenced from the phages and corresponding peptides translated (Fig. 7). By mapping these selected peptides against the sequence potential interactors, it is possible to obtain a prediction of the interacting surfaces. Phage display has been used to predict interaction sites in the bacterial cobalamin system [285, 286] and more recently in the human cobalamin metabolism pathway [270]. It has been used to screen protein partners in different human systems, often in combination with co-immunoprecipitation [287-290].

Figure 7: Phage display

Workflow of phage display experiment. 1: The phage library is incubated on a surface coated with the bait protein. 2: Phages with affinity for the target bind. 3: Unbound phages are washed away. 4: Affinity-selected phages are eluted. The clones are then either sent for sequencing or 5: amplified to be used in subsequent rounds of selection.

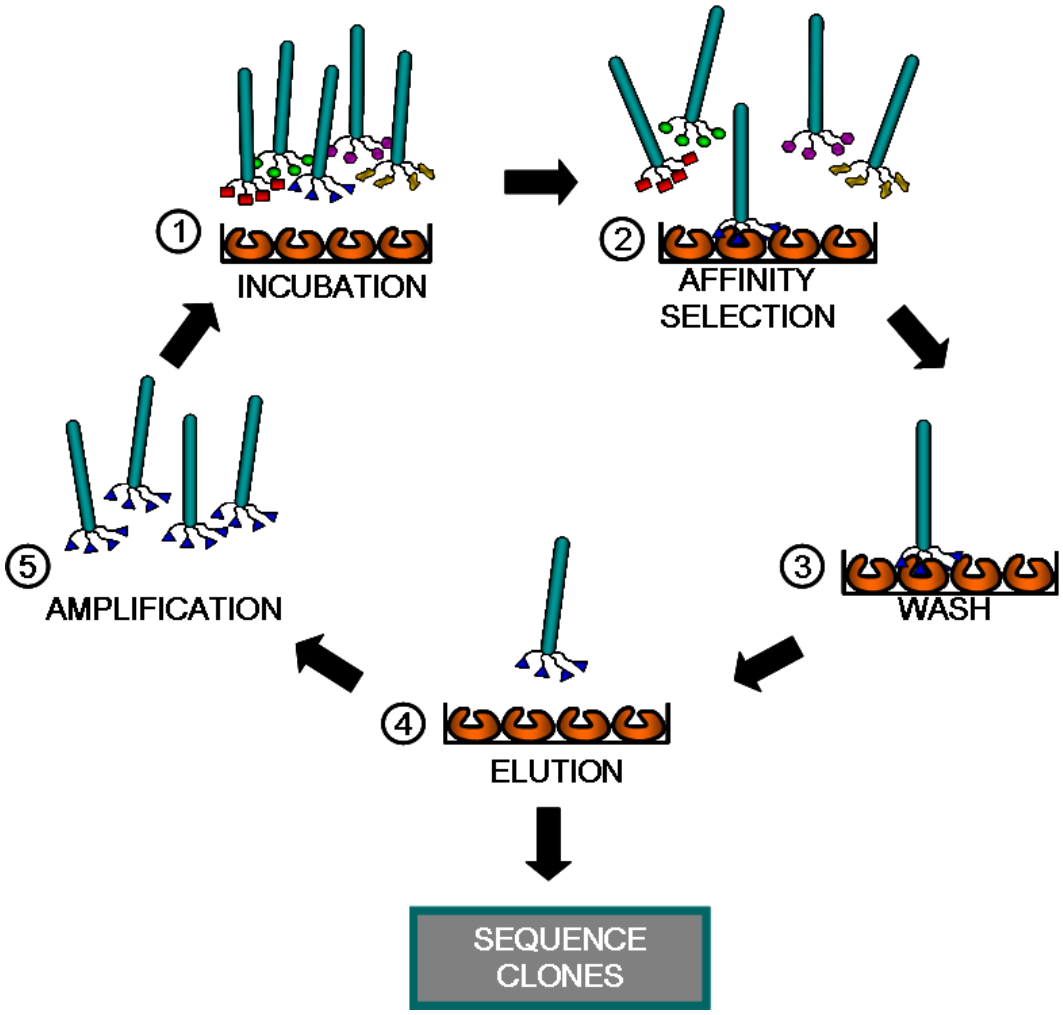

Figure 7: Phage display

1.9.4 Other approaches

Protein interactions can be detected using several other methods. The yeast two-hybrid method was developed to confirm or refute an interaction between two proteins [291]. A transcription factor is separated into two moieties, each cloned as a fusion with one of the candidate proteins. An interaction between the candidates brings in proximity the DNA-binding domain and transcription-activating domain, enabling transcription. The caveat of this approach is the high rate of false negatives created by the size and orientation of the proteins tested. Protein complexes present in cell lysates can be detected by co-immunoprecipitation. A candidate protein is immobilized using antibodies and proteins found associated with it are analyzed. Surface plasmon resonance (SPR) is a technique where interactions of molecules with an immobilized ligand induce measurable perturbations in electromagnetic waves parallel to the surface [292]. Precise measurements of association and dissociation constant can be obtained in this manner. A newer application of SPR includes micro-recovery, where eluted ligands can be recovered and analyzed [293, 294]. Isothermal titration calorimetry (ITC) measures very slight temperature variations resulting from the binding of two compounds. Binding affinity, enthalpy changes and stoichiometry can be measured in this fashion

[295]. Forster resonance energy transfer (FRET), also known as fluorescence energy transfer, involves the transfer of energy from an excited donor chromophore to an acceptor chromophore when two molecules are in close proximity (reviewed in [296]).

1.10 Rationale and objective

In this work, I have studied the first steps of intracellular cobalamin metabolism. These steps correspond to the *cblF*, *cblC* and *cblD* types of disorders. I first attempted to locate the gene responsible for the *cblF* type of cobalamin disorder. The method I chose was MMCT, due to the small number of patients and the absence of any known relationship between them. This work contributed to the discovery of the *LMBRD1* gene responsible for *cblF* and the description of the first mutations in *cblF* patients. I then described novel mutations in new *cblF* patients, as well as one previous *cblF* patient for which one mutation had not been identified. I also described novel mutations in three new *cblD* patients and compared them to other published mutations to identify correlations between the biochemical phenotype and the genotype for this disorder. Finally, in order to understand more about how the proteins involved in the first steps of intracellular cobalamin metabolism worked together, I analyzed protein-

protein interactions between the proteins underlying the *cblC* and *cblD* diseases by purifying the MMADHC protein and performing phage display. The thesis was assembled in the traditional style (non manuscript-based).

PREFACE TO CHAPTER 2

Publication:

Results from this chapter were published as a component of the paper:

Rutsch, F., Gailus, S., **Miousse, I. R.**, Suormala, T., Sagné, C., Toliat, M. R., Nurnberg, G., Wittkampf, T., Buers, I., Sharifi, A., Stucki, M., Becker, C., Baumgartner, M., Robenek, H., Marquardt, T., Höhne, W., Gasnier, B., Rosenblatt, D. S., Fowler, B., Nürnberg, P. *Identification of a putative lysosomal cobalamin exporter altered in the cblF defect of vitamin B_{12} metabolism.* Nat Genet, 2009. **41**(2): p. 234-9. [157]

Contribution of authors:

IR Miousse performed the MMCT experiment, as well as the [^{14}C] propionate incorporation assay. IR Miousse also performed the mutation analysis on cDNA and gDNA for the c.712-713delAC mutation.

Three *cblF* cell lines, PV013, PV014, and PV015, were immortalized by Timothy Johns from the laboratory of Dr. Eric Shoubridge.

The homozygosity mapping work, linkage, and mutation analysis was performed by Susan Gailus in Dr. Frank Rutsch's lab in Germany.

CHAPTER 2: IDENTIFICATION OF CHROMOSOME 6 AS THE LOCATION OF THE GENE RESPONSIBLE FOR THE *cblF* TYPE OF COBALAMIN DISORDER

2.1 Introduction

With the identification of the gene responsible for the *cblD* type of intracellular cobalamin disorder [39], only one complementation group remained for which the genetic basis was unknown: *cblF*. The identification of the gene defective in these patients would open up the field of molecular biology in the study of this disorder. Several approaches were available to accomplish this task, as summarized in chapter 1.

Based on the nature of the *cblF* defect, there was a high possibility that the gene altered in the patients encoded a lysosomal protein. One group had previously tried identifying the protein by preparing lysosomal extracts from control and patient cell lines and comparing them on two-dimensional protein electrophoresis gels (A. Pshezhetsky, Ste-Justine Hospital, personal communication). The goal was to identify a protein spot that would be present in controls and absent in *cblF* patients, and submit material extracted from that spot for mass spectrometry identification.

Although promising, the approach failed at identifying the protein. The cohort was one of small size (nine patients) composed of individuals unrelated to each other, which argued against the use of linkage studies.

Coincidentally with the start of this project, cobalamin deficiency was identified in a knockout mouse model for a multidrug resistance gene, *ABCC1* (S. Moestrup, personal communication) [79]. The mice exhibited a defect in cobalamin absorption from the gastro-intestinal tract. Because some of our patients exhibited such a defect in addition to the lysosomal phenotype, the *ABCC1* gene was sequenced in *cblF* patients. Although the gene was not reported to be located in the lysosome, lysosomal targeting is an incompletely understood process. Luminal lysosomal proteins possess signal sequences that target them to the lysosome, post-translational modifications with mannose-6-phosphate being the best understood pathway. However, other proteins use different and less understood pathways, particularly lysosomal membrane proteins (reviewed in [297]). The analysis of the *ABCC1* cDNA sequence in nine *cblF* patients did not reveal pathogenic variants.

The recent success at the identification of the gene responsible for the *cblD* type of intracellular cobalamin disorder directed our attention to an approach called microcell-mediated chromosome transfer (MMCT), reviewed in chapter 1 [39]. The *cblD* cohort, constituted of eight patients, is of comparable size to the *cblF* cohort. With the exception of two affected siblings, the *cblD* patients are unrelated. Addition of a normal copy of chromosome 2 to cultured fibroblasts from *cblD* patients corrected the incorporation of label from propionate and MeTHF into macromolecules. However, some clones (24/72) isolated after transfer of chromosome 2 failed to rescue the phenotype, and provided informative markers to narrow down the region of interest. The regions of the chromosome present in negative clones could be excluded, while regions common to all positive clones were selected for further inquiries. In the *cblD* case, the team used a panel of 38 microsatellite markers to refine the region of interest to 10.2 Mb. The region contained 28 genes, of which one, *C2orf25*, now *MMADHC*, was selected as a candidate and in which mutations were found in patients. We modeled our experimental plan to identify the gene underlying the *cblF* type of cobalamin disorder on this approach.

2.2. Materials and Methods

2.2.1 Cell lines used

A skin biopsy from *cblF* patient WG3377 was obtained with informed consent and fibroblasts were cultured and stored at the Montreal Children Hospital Cell Bank. The cells were immortalized using human telomerase and human papilloma virus type 16 protein E7 as previously described [298, 299]. The genes cloned into a retroviral vector were transfected into a packaging cell line (Phoenix helper-free retrovirus producer line, Nolan lab, Stanford, CA). Supernatant was collected from the packaging cell line and applied to the *cblF* fibroblasts. The increased cell cycle rate in transfected cells acted as a selection factor for presence of the two genes. The immortalized *cblF* fibroblast line was named PV014.

2.2.2 MMCT

Cell lines preparation

MMCT was performed on the cell line PV014 as previously described [300]. We used a mouse-human hybrid myoblasts containing a single human chromosome tagged with a hygromycin B resistance gene [278]. These cells were grown in minimum essential medium plus non-essential amino acids (MEM, Gibco, Invitrogen, Burlington, Canada) supplemented

with 5% fetal bovine serum and 5% iron enriched calf serum (Intergen, Burlington, MA) and containing 400 U/ml hygromycin B (Calbiochem, Gibbstown, NJ). Cells were plated on four 15 cm dishes to reach a confluency of 70 % after 24 hours. Demecolcine (Sigma-Aldrich, Oakville, Canada) 0.06 µg/mL was then added and cells were incubated for 48 hours. Sterile bullets made from the bottom surface of cell culture flasks and shaped to fit in centrifuge tubes were treated the day before transfer for cells to adhere to the surface. 21 bullets sterilized for 24 hours in ethanol and dried sterilely in the tissue culture hood were submerged in a filter-sterilized solution of 75 mg/ml 1-cyclohexyl-3-(2-morpholinoethyl) carbodiimide (CMC) (Sigma-Aldrich, Oakville, Canada) dissolved in a 0.9 % sodium chloride solution. The CMC solution was then replaced by a filter-sterilized solution of 15 mg/ml concanavalin A type IV (Sigma-Aldrich, Oakville, Canada) dissolved in 0.9 % sodium chloride solution. Excess concanavalin solution was removed and bullets were incubated three hours in the tissue culture hood and submerged in phosphate buffered saline (PBS) overnight at 4ºC.

Microcell harvesting

On the day of transfer, rodent cells were harvested by trypsinizing the cells and centrifuging the suspension at 250 g for 10 min. Cells were then resuspended in 12 ml MEM with serum and the cell suspension was carefully spread on the dry bullets in 15 cm dishes. Cells were allowed to attach for 15 minutes in the tissue culture hood then 36 ml of MEM with serum was added to the dishes. Cells were incubated on the bullets for three hours at 37ºC. After the incubation, bullets were placed in centrifuge tubes, two bullets per tube with cell-adhering side facing out. Each tube was filled with 25 ml of serum-free MEM containing 10 µg/ml cytochalasin B (Sigma-Aldrich, Oakville, Canada) and spun at 30 000 g at 30ºC for 30 minutes in a pre-warmed rotor. After spinning, the pelleted material was pooled and vigorously resuspended in 30 ml serum-free MEM. This solution was filtered two times through 8 µm filters and three times through 5 µm filters to separate microcells from cell remnants. The filtered microcell suspension was then spun at 1200 g for 10 minutes.

Fusion

Microcells were resuspended in 1.5 ml serum-free MEM and mixed with 1.5 ml phytohemmaglutinin P (Sigma-Aldrich, Oakville, Canada). Recipient

patient cells at 80 % confluency in a 10 cm dish were rinsed three times with 5 ml serum-free MEM. The microcell suspension was then spread and incubated 30 minutes at 37ºC to adhere to the rinsed recipient cells. Microcells and recipient cells were fused by exposure to 4 ml polyethylene glycol 1500 (Roche, Mississauga, Canada) in 10% dimethylsulfoxide (DMSO) (Sigma-Aldrich, Oakville, Canada) for 50 seconds. Cells were rinsed two times with 10 ml of serum-free MEM containing 10 % DMSO for one minute, then with 10 ml of serum-free MEM for one minute and 10 ml of serum-supplemented MEM for one minute. Cells were then incubated overnight in 10 ml serum-containing MEM with penicillin/streptomycin (50 U/mL penicillin, 50 µg/mL streptomycin) (Gibco, Invitrogen, Burlington, Canada).

Colony growth

The next day, cells were split into two 10 cm dishes. Cells were fed every two to three days with serum-supplemented MEM containing 100 U/mL of hygromycin B to select for resistant cells. Clones took about 30 days to develop. They were picked, transferred to separate dishes and grown to confluency in 175 cm^2 flasks for [^{14}C] propionate assay.

2.2.3 [^{14}C] propionate assay

Incorporation of [^{14}C] propionate into cellular macromolecules was measured in the immortalized and primary cells. Immortalization did not affect [^{14}C] propionate incorporation, which remains low in transformed patient fibroblasts compared to controls. Cells from the cell lines of interest were plated at a density of 400 000 cells in triplicate 35 mm tissue culture dishes and incubated for 24 hours. After the incubation, MEM was removed and replaced with Puck's F medium containing 15% fetal bovine serum and 100 µmol/l [^{14}C] propionate (Amersham Life Sciences, GE Healthcare, Chalfont St. Giles, United Kingdom) and unlabeled propionate (Sigma-Aldrich, Oakville, Canada) to give a final specific activity of 10 µCi/µmol. Cells were incubated with the radioactive serum-containing MEM for 18 hours. Macromolecules in the cells were then precipitated in three successive 15 minutes incubation at 4ºC in 5 % (w/v) trichloroacetic acid. Precipitate was dissolved by adding 0.2 N sodium hydroxide and incubating for 3 hours at 37ºC. Dissolved material was removed and radioactive propionate incorporated into proteins was measured by liquid scintillation counting of a 700 µL aliquot (Scintillation counter, Perkin Elmer Tri-Carb 2800TR). This value was divided by the concentration of protein in the sample, assessed by Lowry assay [301].

2.2.4 Mutation Analysis

gDNA and RNA were extracted from the PV014 cell line. gDNA was extracted using the Puregene kit (Qiagen, Mississauga, Canada) and RNA was extracted using TRIzol reagent. RNA was reverse-transcribed using poly dT universal primers (GE Healthcare Canada, Oakville). A mixture of 2 µL RNA, 2 µL primers and 8 µL RNA-free water was heated for 10 min at 75ºC. To this reaction was diluted into 1X MMLV RT buffer, 1 U/µL MMLV reverse transcriptase (USB, Cleveland, OH), 1 U/µL ribonuclease inhibitor (Invitrogen, Burlington, Canada), 0.5 mM dNTPs (Qiagen, Mississauga, Canada), and RNA-free water. The mix was then heated at 37ºC for 60 min and 75ºC for 10 min. PCR amplification was performed using primers listed in Table 2 (p.113). The reaction was performed as follows: 0.4-2 ng/µL template DNA was diluted into 1X PCR buffer, $MgCl_2$ at a final concentration of 3.5 mM, 200 µM dNTPs (Qiagen, Mississauga, Canada), 100 µM each forward and reverse primers, and 0.02 U/µL HotStar Taq polymerase (Qiagen, Mississauga, Canada). The mix was initially denatured at 96ºC, then cycled for 40 cycles at 96ºC (30 sec), the annealing temperature listed in Table 2 (60 sec) and 72ºC (60 sec per kb). A final elongation step was added at 72ºC for 10 min.

2.3. Results

2.3.1 MMCT

A total of nine hygromycin-tagged chromosomes were transferred in the PV014 immortalized *cblF* cell line and seven successfully produced clones to be tested (chromosomes 2, 4, 5, 7, 10, and 16) (Table 1). Of these, only the transfer of chromosome 6 produced clones in which the [^{14}C] propionate incorporation levels were corrected. Transfer of further chromosomes was halted after the correcting chromosome was identified and chromosomes that had failed to produce clones were not re-tested. Eleven clones from the transfer of chromosome 6 were tested for correction with [^{14}C] propionate. Of these, eight clones had markedly increased levels of incorporation, while three failed to show correction (Figure 8). Figures 9 and 10 show examples of chromosomes that did not produce clones with a correction of [^{14}C] propionate incorporation.

Table 1: Rescue observed in clones isolated from chromosome transfer, assayed by [^{14}C] propionate incorporation.

Chromosome	# clones	Rescuing	Non-rescuing
2	2	0	2
3	0	0	0
4	5	0	5
5	5	0	5
6	11	8	3
7	5	0	5
10	2	0	2
12	0	0	0
16	1	0	1

clones: number of clones isolated and tested with [^{14}C] propionate assay, Rescuing: number of clones for which the [^{14}C] propionate incorporated/mg protein/18hrs average of triplicate is significantly higher than baseline, Non-rescuing: number of clones for which the [^{14}C] propionate incorporated/mg protein/18hrs average of triplicate is not significantly different than baseline.

Figures 8-10: [^{14}C] propionate incorporation in clones isolated from chromosome transfer

Background; control fibroblasts incubated for 30 sec in [^{14}C] propionate for background radioactivity count. Control; fibroblasts from a healthy control. *cblF*; immortalized *cblF* patient fibroblasts. ChrX #1-14; number of the clone from immortalized *cblF* fibroblasts with transferred chromosome X. White bars; incorporation comparable to *cblF* line. Black bars; incorporation significantly higher than *cblF* baseline. Error bars indicate the standard deviation observed for the assays performed in triplicate.

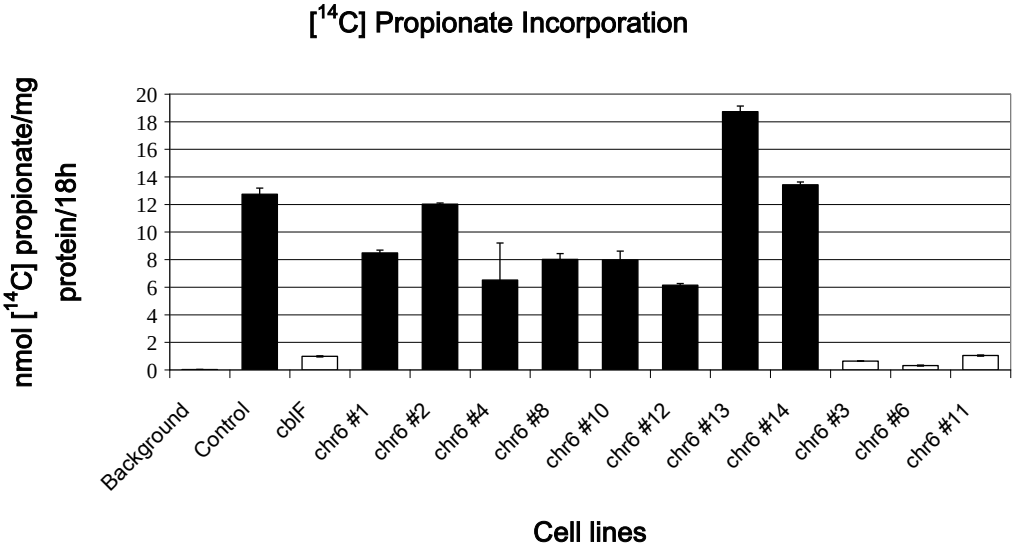

Figure 8: [^{14}C] propionate incorporation in clones from transfer of chromosome 6

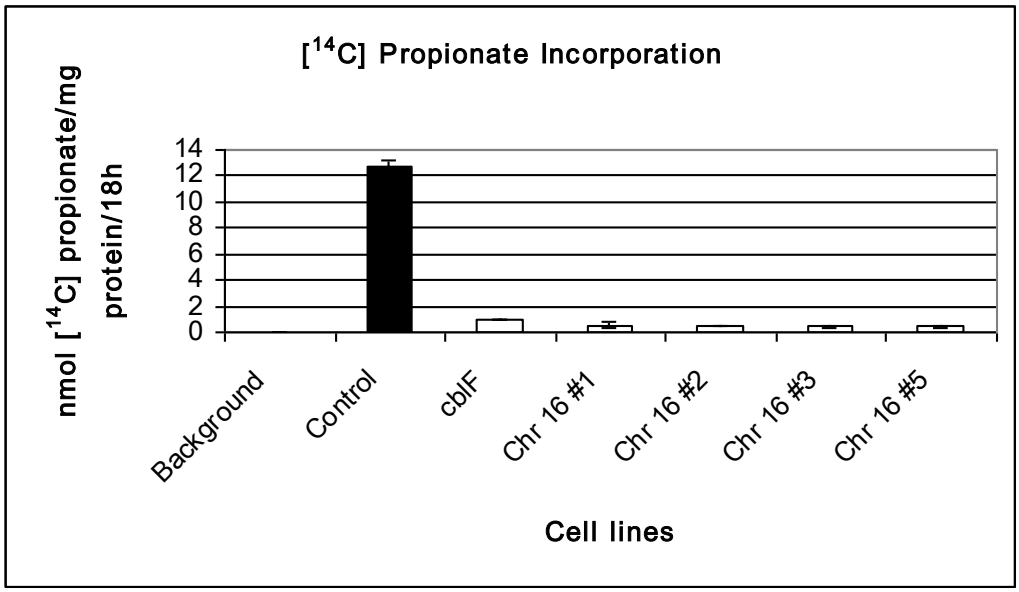

Figure 9: [14C] propionate incorporation in clones from transfer of chromosome 16

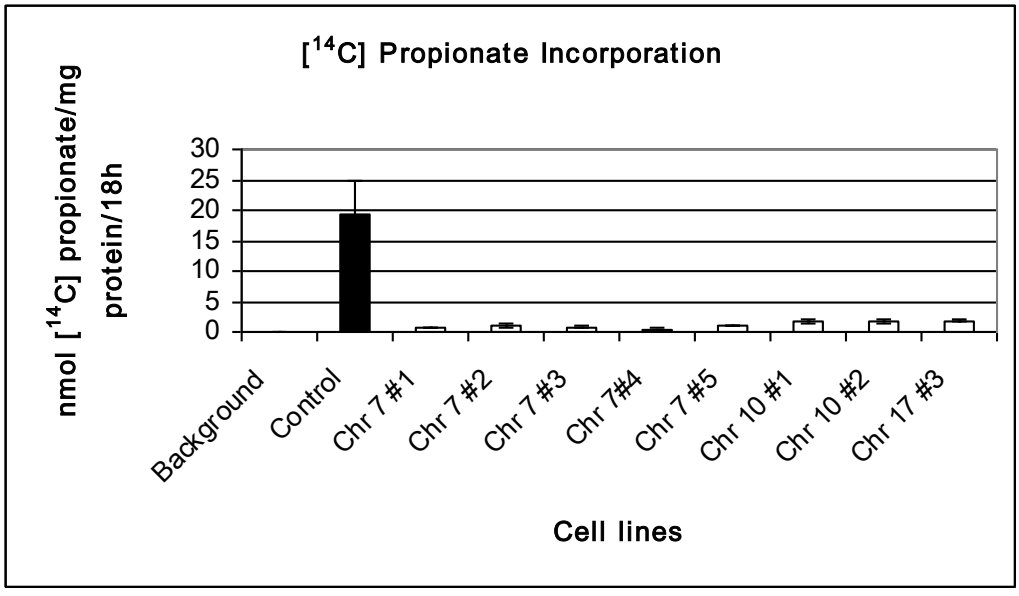

Figure 10: [14C] propionate incorporation in clones from transfer of chromosome 7, 10 and 17

2.3.2 Homozygosity mapping

Our collaborators Dr. Frank Rutsch and Susan Gailus in Muenster, Germany, performed homozygosity mapping on cell lines from nine *cblF* patients we provided to them and an additional three cell lines from European patients. To perform homozygosity mapping, multipoint linkage analysis was used to identify regions of homozygosity by descent in inbred affected individuals [302]. Here, parents of affected individuals were arbitrarily assigned as second-cousins. A single maximal HLOD score was identified on chromosome 6, confirming our MMCT results. Gene expression data revealed a decreased expression of the gene *LMBRD1* in this region. Transfection of the *LMBRD1* gene in a *cblF* cell line corrected the incorporation of labeled propionate. One mutation, c.1056delG -- p.L352fsX18, was identified in 17 of 24 alleles tested.

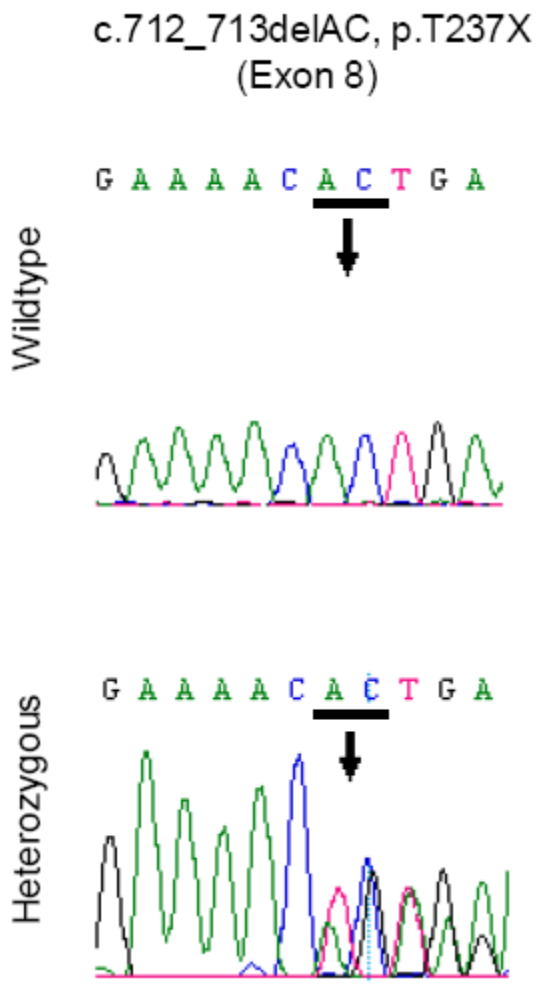

Figure 11: Mutation c.712_713delAC (p.T237X)

Legend:

c.712_713delAC (p.T237X) mutation on one allele of patient WG3377 (PV014) with the corresponding wild-type sequence.

2.3.3 Mutation Analysis

cDNA sequencing of the PV014 cell line used for MMCT confirmed the presence of the common c.1056delG mutation previously identified by the Rutsch group. The mutation was present on one allele. Additionally, we identified a second heterozygous frameshift mutation, c.712-713delAC – p.T237X, by cDNA sequencing. gDNA sequencing for exon 6 confirmed the mutation (Fig 11).

2.4. Discussion

The rationale for choosing MMCT to identify the gene responsible for the *cblF* type of intracellular cobalamin disorder was justified. Nothing in the patients' history could lead us to believe that they shared a common ancestry that would have directed us to the homozygosity mapping. It thus came as a surprise to identify a common mutation located on a shared haplotype in a large proportion of the patients (only one patient in this cohort did not have at least one copy of the c.1056delG allele). Retrospective analysis of the background of patients sharing the c.1056delG mutation leads us to believe that the mutation appeared in Europe, and then spread to America. Thus, although the homozygosity mapping approach found the causative gene in a faster and less labor-

intensive manner than MMCT, it was also an approach that had a lower chance of success a priori. On the other hand, in the presence of an observable cellular phenotype (such as here the decreased radioactive incorporation from a substrate), MMCT has a very high chance of success. MMCT is a technically challenging, slow, and labor-intensive approach that will succeed where other approaches fail. The result of chromosome transfer in this case provided a solid ground to go on with the investigation of the linkage peak on chromosome 6.

The gene identified, *LMBRD1*, has been localized to the lysosomal membrane by examining cryosections for colocalization of EGFP-tagged LMBD1, the protein encoded by *LMBRD1*, and the lysosomal marker LAMP1 [157]. It contains nine predicted transmembrane domains. LMBD1 shares homology with members of the PF04791 protein family. Homology is particularly significant between LMBD1 and LMBR1, a protein of unknown function, and LIMR, a membrane receptor for small secreted proteins: lipocalins. The membrane topology prediction places six putative N-glycosylation sites in the lysosomal lumen. This is consistent with the topology of other known lysosomal membrane proteins, among them

LAMP1 and LAMP2, which are among the most densely glycosylated proteins known (reviewed in [303]).

The co-localization of LMBD1 with the lysosome is consistent with a role of the protein in the export of cobalamin through the lysosomal membrane. However, several questions remain unanswered and require further experiments. The LMBD1 sequence does not reveal an identifiable vitamin B_{12}-binding motif. It is thus not known whether LMBD1 binds cobalamin directly. With nine putative transmembrane domains, LMBD1 has the potential to form a channel for the passage of the cobalamin molecule. Whether LMBD1 forms such a channel, as a monomer, as a dimer, or as part of a complex with accessory molecules, remains to be discovered. The mild phenotype seen in *cblF* patients as compared to the *cblC* cohort and their good response to therapy is not well understood. It has been proposed that about 1% of the cobalamin present in the gut can be passively absorbed. It remains to be tested if a similar passive absorption can be used by the cells to take up cobalamin from the blood. It is also interesting to observe that some *cblF* patients have abnormal Schilling test results, indicating a faulty absorption from the gastrointestinal tract. It is thus important to study the role of LMBD1 in enterocytes.

PREFACE TO CHAPTER 3

Publication:

This work was published as a brief communication as:

Miousse I.R., Watkins D and D.S. Rosenblatt. Novel splice site mutations and a large deletion in three patients with the *cblF* inborn error of vitamin B_{12} metabolism. Mol Gen Metab. 2011. 102(4): p.505-7

Contribution of authors:

Initial diagnosis work was performed by the clinical staff. Enzyme assays and complementation studies were performed by Jocelyne Lavallée, cobalamin distributions were assayed by Dr. David Watkins and the testing for the common mutation was performed by Maria Galvez.

The TspRI restriction enzyme assay was designed by IR Miousse and optimized by Lydia Vézina. All mutation analysis work on mutations c.404delC – p.T134fsX14, c.842_845delAGAG – p.K281fsX4, c.712_713delAC – p.T237X was performed by IR Miousse. Sequencing was done at the Genome Quebec Innovation Center.

CHAPTER 3: NOVEL MUTATIONS IN *cblF* PATIENTS

3.1. Introduction

In 2009, mutations in twelve *cblF* patients were published [157]. An important result from this analysis was the presence of one common mutation in the gene *LMBRD1*, c.1056delG – p.Leu352fsX18, on 17 out of 24 alleles tested. This mutation is a one base pair deletion leading to a frameshift and a premature stop codon. Seven patients were homozygous for the common mutation and four more were compound heterozygotes. A second mutation was identified in three patients (c.404delC – p.Thr134fsX14, c.842_845delAGAG – p.Lys281fsX4, c.712_713delAC – p.Thr237X), and could not be identified in the fourth patient. One patient was homozygous for a two base pair deletion, c.516-516delAC – p.Thr172fsX9. With the exception of c.712_713delAC which was a coincidental finding of the MMCT experiment, all the mutation analysis was performed in exonic genomic DNA by our collaborators Dr. Frank Rutsch and Susan Gailus in Münster, Germany. A thirteenth patient was published subsequently with a homozygous mutation, c.1405delG – p.Asp469fsX38 [304]. A summary of the mutations identified in *cblF* patients can be found in Table 3.

Two new *cblF* patients were referred to our clinical diagnosis laboratory. Diagnosis was made based on the absence of complementation of other *cblF* lines in the first patient. For the second patient, [^{14}C] propionate and [^{14}C] MeTHF incorporation in the cell was in the normal range, and thus complementation analysis was not attempted. However, the cobalamin distribution pattern was abnormal. Synthesis of MeCbl and AdoCbl was low, and CNCbl was high, a pattern characteristic of cells from *cblF* patients. Diagnosis was strengthened by the identification of one copy of the common mutation in both patients by clinical restriction digestion testing. We aimed to identify the second causative mutation in these two patients and at the same time analyzed an additional patient heterozygote for the common mutation for which a second mutation had not been identified (WG3365, patient 11 in Table 3 and ref. [157]). The objective of this study was to identify the second mutation in these three patients. All previously reported mutations led to a premature stop codon. An additional aim of this study was to observe if this trend is continued in more *cblF* patients.

3.2. Materials and Methods

3.2.1 Cell lines

Fibroblasts were obtained with informed consent from patients and sent to the Cell Bank of the Montreal Children Hospital (cellbank@mcgill.ca). Cells were cultured in minimum essential media (MEM, Gibco, Invitrogen, Burlington, Canada) supplemented with 5% fetal bovine serum and 5% iron enriched calf serum (Intergen, Burlington, MA). DNA was extracted using the Gentra Puregene kit (Qiagen, Mississauga, Canada) and RNA was extracted with TRIzol reagent (Molecular Research Center, Inc, Cincinnati, OH).

3.2.2 Mutation analysis

Primers were designed using the online tool Primer3 (http://frodo.wi.mit.edu/primer3/) [305]. The TspRI restriction site was identified using the online tool NEB cutter (http://tools.neb.com/NEBcutter2/, New England Biolabs, Ipswich, MA). RNA was reverse-transcribed using poly dT universal primers (GE Healthcare Canada, Oakville). A mixture of 2 µL RNA, 2 µL (50 units) of primers and 2 µL RNA-free water was heated for 10 min at 75ºC. To this reaction was added MMLV RT buffer, 1 U/µL M-MLV reverse transcriptase

(USB, Cleveland, OH), 1 U/μL ribonuclease inhibitor (Invitrogen, Burlington, Canada), 0.5 mM dNTPs (Qiagen, Mississauga, Canada), and RNA-free water. The mix was then heated at 37ºC for 60 min and 75ºC for 10 min. PCR amplification was performed using primers listed in Table 2. The reaction was performed as follows: 0.4-2 ng/μL DNA was diluted into 1X PCR buffer, $MgCl_2$ at a final concentration of 3.5 mM, 200 μM dNTPs (Qiagen, Mississauga, Canada), 100 μM each forward and reverse primers, and 0.02 U/μL Taq polymerase per (Qiagen, Mississauga, Canada). The mix was initially denatured at 94ºC for 3 min, then cycled for 40 cycles at 94ºC (30 sec), the annealing temperature listed in Table 2 (60 sec) and 72ºC (60 sec per kb). A final elongation step was added at 72ºC for 10 min. HotStar Taq was used for primers pairs giving a low amplification with regular Taq. In these cases, HotStar Taq was substituted to Taq in the preparation and the mix was initially denatured at 96ºC for 10 min, then cycled for 40 cycles at 96ºC (30 sec), the annealing temperature listed in Table 2 (30 sec) and 72ºC (60 sec per kb). A final elongation step was added at 72ºC for 10 min. Samples were run on a 1.2% agarose gel with ethidium bromide for quality control. Samples were sent for sequencing to the Genome Quebec Innovation Center (Montreal,

Canada). Sequences were analyzed with the tool Mutation Surveyor (Softgenetics, State College, PA).

Table 2: Primers used in this study

gDNA primers

Name	Sequence	Annealing T
LMBRD1_01F	CCGGCCCCATTGCCCAAGTC	
LMBRD1_01R	GCTTGCAGGGAAGCCAGCGA	65
LMBRD1_02F	TTTGCACTGTGTTTAATGAGGAA	
LMBRD1_02R	TGTGCCAGAAATTTGAAAGG	58
LMBRD1_03F	TGTGGGTGGATAGATTTTGGA	
LMBRD1_03R	CCCCCTTCTTTCTTGCCTAC	62
LMBRD1_04F	GCTCGGTTTATTATTTATTTCCACA	
LMBRD1_04R	CAGTCATTCATTCTCTGAAAAAGC	62
LMBRD1_05F	CAAGGGCCTAACTATTGAAAAGA	
LMBRD1_05R	TGTTAACAGGCAGATTACCAAGAA	58
LMBRD1_06F	CTTTTCACTCCCCTCTGTGC	
LMBRD1_06R	GCCTCCCAAAGTGCTAGGAT	62
LMBRD1_07F	CATTGAGAAAGGCCATGTGA	
LMBRD1_07R	CAGCTAAAATGATGATGGCTAA	58
LMBRD1_08F	TCCCATATACCATGTTTTCAGTG	
LMBRD1_08R	TGTACCAGATATGCTGCAAAAA	62
LMBRD1_09F	AGATTAAACCCCCAAATCCA	
LMBRD1_09R	CCACATTTTTATGCTGACCTTG	58
LMBRD1_10F	GATCATTGTCATATTCTAGCAACTCA	
LMBRD1_10R	TTGGACGTTTTAGCCATTCTTT	62
LMBRD1_11F	CATCAATTGAACAATAGCTGTGA	
LMBRD1_11R	TGTCAAACTATTCATAGGTTTTTAGC	58
LMBRD1_12F	TGTAAACATTTGCCGGATGA	
LMBRD1_12R	CCCCATTTAAGAACCACTGC	58
LMBRD1_13F	TGAAATTCTGTGTGCTGTTTCA	
LMBRD1_13R	TCCATGAACTTCTAACAGATGCT	58
LMBRD1_14F	GTTCAACACAGGACCTAAAGGA	
LMBRD1_14R	TGCAAATCCTTTCATCAACAA	58
LMBRD1_15_16F	GCATTGGTGGCATTCATTTTT	65

cDNA primers

Name	Sequence	Annealing T
LMBRD1_cDNA_1-5F	GGTGCATATTTCGGCCTCTTA	
LMBRD1_cDNA_1-5R	TTGAGTGCCGTTTTAATTTGA	58
LMBRD1_cDNA_4-8F	TTATGAAGAAAAGGATGATGATGA	
LMBRD1_cDNA_4-8R	TAACGCAGACATGCCATAGG	58
LMBRD1_cDNA_7-14F	CATGGTTTAGCTGCATTGTCA	
LMBRD1_cDNA_7-14R	TGGCACAGAAAGGGTTGAAT	58
LMBRD1_cDNA_9-13F	AATTTTGTGGCGCTCTGC	
LMBRD1_cDNA_9-13R	GGGCCTGGTTCTACCTCTTC	58
LMBRD1_cDNA_13-16F	CCCAAGCACTCCTTTTTCTCT	
LMBRD1_cDNA_13-16R	GCAGAATAGACAGAGGGCTCA	58

qPCR primers

Name	Sequence	Annealing T
qPCR_1F	TCCAAGCGCCTCCCCTACCA	
qPCR_1R	AGATGGCGACTTCTGGCGCG	60
qPCR_2F	TCCACTGGTAGAAGTGCTGATGTGA	60

Long-range PCR primers

Name	Sequence
LMBRD1_11kbF	ACCCCTGCCATAAGAAGGCAGA
LMBRD1_11kbR	CAGGCCCTGCAGTTGGCCTC

3.2.3 Quantitative PCR

Real-time quantitative amplification was done using SYBR green reagent master mix (Invitrogen, Burlington, Canada) supplemented with 2.5 mM $MgCl_2$. The final concentration of DNA was 2 ng/μL, with an additional control at 1 ng/ μL. All samples were run in duplicate. The reaction was performed for 40 cycles on a Rotor Gene RG3000 (Corbett Research).

3.2.4 Long-range PCR

Long range PCR was performed with LA Taq with Mg^{2+} buffer (TaKaRa Bio, Shiga, Japan). The reaction mix was prepared as follows: buffer containing 300 μM $MgCl_2$, 200 μM dNTPs (Qiagen, Mississauga, Canada), 100 μM each of forward and reverse primer, 0.02 U/μL LA Taq and 2 ng/μ L template DNA. The template was initially melted at 94ºC for 3 min, and then cycled 30 times between 98ºC for 5 sec and 68ºC for 15 min. A final elongation step at 72ºC for 10 min was included.

3.3. Results

3.3.1 Restriction digestion test for the common c.1056delG mutation

Because of the high frequency of the common c.1056delG mutation in *cblF* patients, we designed a restriction digestion test to serve in the clinical diagnosis laboratory. A cut site for the restriction enzyme TspRI was identified in the wild-type sequence of exon 11 of *LMBRD1* that is abolished by the 1056delG mutation (primers LMBRD1_exon 11F and LMBRD1_exon11R, Table 2). In wild-type alleles, the 390 bp PCR product is completely digested in two fragments of 240 bp and 150 bp. In heterozygotes, the 390 bp band corresponding to uncut product is visible in addition to the 240 and 150 bp control bands. In c.1056delG homozygotes, only the 390 bp band is present. This test is used in the clinical lab to support *cblF* diagnosis.

3.3.2 Patient WG3365

Patient WG3365 was previously reported as heterozygous for the common mutation (Patient 11 in [157]). The second mutation was unknown. We designed primers to amplify the gDNA for every exon of the *LMBRD1* gene, including at least 100 bp upstream and downstream of the

coding sequence. We confirmed the presence of the c.1056delG mutation by sequencing of exon 11, where the mutation is located. Upon analysis of the sequencing results, we identified a heterozygous G>T change at the base directly upstream of exon 10 (c.916-1G>T). We designed primers to amplify the region around exon 10 on cDNA. Amplification of bases c.887-1221 led to the generation of two fragments: one full-length fragment of 335 bp and one shorter fragment of 270 bp (Figure 12). Exon 10 is 65 bp in length. We concluded that the c.916-1G>T change on one allele of the patient perturbs the splice accepting site of exon 10. This results in the failure to include exon 10 in the transcript from that allele. Because the number of bases in the exon (65 bp) is not a multiple of three, the mis-splicing causes a frameshift that creates a stop codon after two codons (p.Ile306fsX2).

3.3.3 Patient WG4008

Patient WG4008 was identified on the basis of an abnormal newborn screen and referred to our clinical diagnostic laboratory. Incorporation of label from propionate and MeTHF was within the control range but the synthesis of AdoCbl and MeCbl was low, while CNCbl was high. As this is a feature of *cblF* cell lines, restriction digestion testing for the common

c.1056delG mutation was performed and the patient was found to be heterozygous. The sample was transferred to us for research purposes. We amplified and sequenced gDNA for every exon of the *LMBRD1* gene. We confirmed the presence of the common mutation on one allele by gDNA sequencing. Upon analysis of the sequencing results, we identified a heterozygous G>T change at the base directly upstream of exon 14, c. 1339-1G>T. We designed primers to amplify the region around exon 14 on cDNA. Amplification of bases c.1220-1619 led to three bands: a wild-type amplification band corresponding to 400 bp, a smaller band corresponding to 321 bp, and an intermediate-size band (Figure 12). The smaller 321 bp band is consistent with the absence of the 79 bp of exon 14 in the transcript, as confirmed by sequencing. Sequencing of the intermediate band revealed that it is composed of a mixture of wild-type transcript and of transcript missing exon 14. Exon 14 has a number of bases that is not a multiple of three, so the absence of exon 14 in the transcript induces a frameshift predicted to cause a stop codon after 33 codons (p.Thr447fsX33).

3.3.4 Patient WG4042

Patient WG4042 was a child with a cardiac malformation and trigonocephaly. Clinical analysis revealed a decreased synthesis of Me- and AdoCbl and a low incorporation of label from propionate and MeTHF in cellular macromolecules. Somatic cell complementation identified this patient as belonging to the *cblF* group. TspRI digestion identified one copy of the c.1056delG mutation.

We amplified gDNA for all exons of the *LMBRD1* gene and sequencing confirmed the TspRI digestion results. All other changes were catalogued SNPs. We thus amplified complete cDNA, split into four overlapping segments. The first segment, c.44-425, revealed a band of abnormal size in the patient. In the control, the amplification gives rise to a band consistent with the expected length of the product: 382 bp. In the patient, very little of that control band can be seen but a strong band is present around 200 bp (Figure 12). This size difference suggested the absence of exon 2, which is 177 bp in length. Further analysis of the regions around exons 1 to 5 did not reveal changes that would be predicted to affect splicing. We thus considered the possibility of a gDNA deletion of the entire exon 2 on one allele, or the deletion of exons 3 and 4 (exon 3: 61bp

and exon 4: 98 bp, total 158 bp). Because of its length more closely resembling the size difference observed on agarose gel, exon 2 was our first candidate.

Figure 12: cDNA migration

Agarose gel electrophoresis of cDNA PCR products from cblF patients and controls. In patient WG3365 (c.887–1221), there were two products: one of control length (335 bp) and a shorter band lacking the residues of exon 10 (270 bp). Investigations on the faint band seen at 700 bp were inconclusive. In patient WG4008 (c.1220–1619), there were three products: one of control length (400 bp) and a shorter band (321 bp) lacking the residues of exon 14. A third band of intermediate size is composed of mutant and normal product. In patient WG4042 (c.44-425), there was a band of 205 bp, in addition to the control band of 382 bp. This is consistent with a deletion of exon 2. Only a small amount of control product was detected.

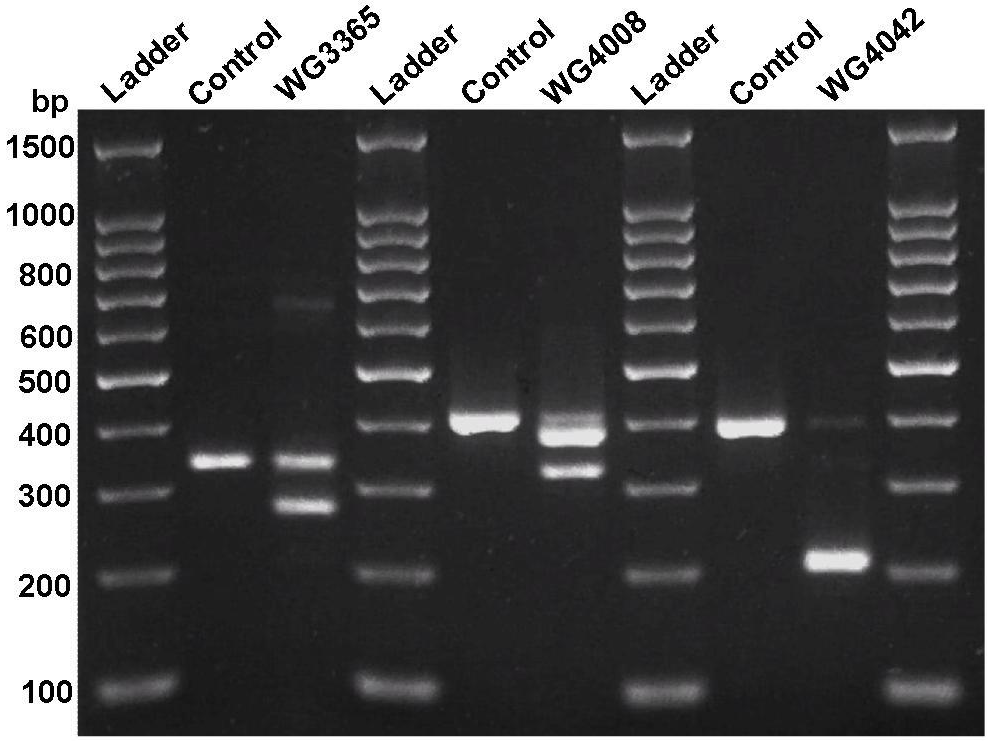

Figure 12: cDNA migration

To test this hypothesis, we performed quantitative PCR on gDNA for exon 2, using exon 1 as a control. In exon 1, fluorescence appeared after a similar number of cycles in the patient sample and in the control (ΔCT=-0.21). In exon 2, fluorescence in patient (ΔCT=3.0) was delayed compared to control (ΔCT=1.4). Diminishing by half the amount of DNA in the control resulted in values equivalent to patient (ΔCT=2.6) (Figure 13). This pattern suggested that there is half as much DNA template for exon 2 in the patient as in the control. These results supported the hypothesis of a deletion of one of the two alleles around exon 2 of *LMBRD1*.

To confirm a deletion and define its exact borders, we amplified the region between exons 1 and 3 by long range PCR. The whole region (intron 1, exon 2, and intron 2) is 17 kb in length. By sequencing regions rich in SNPs, we identified a heterozygous SNP in intron 2 (rs3799120 C/A). This proof of bi-allelism excluded the 6 kb region between this SNP and exon 3 from the putative deletion. Amplification of the 11 kb region between exon 1 and rs3799120 led to two species. The first species was about 11 kb in length while the second species was between 2.5 and 5 kb in length. There was preferential amplification of the shorter species. Sequencing of

the shorter product revealed a 6785 bp gap in the gDNA ranging from 4298 bp upstream to 2311 bp downstream of exon 2 (c.70-4298_246+2311del6785, p.Ala24_Lys82del). Exon 2 being 177 bp in length, the reading frame of the remaining transcript is conserved.

Figure 13: Quantitative real-time PCR on exon 2

Quantitative real-time PCR analysis of exon 2 in patient WG4042. a) 100 ng control gDNA(ΔCT=1.4) and b) 100 ng patient gDNA (ΔCT=3.0), superimposed with 50 ng (one half) control gDNA (ΔCT=2.6), delayed by 1.25 cycle compared to a), supporting evidence for the loss of one allele. All samples were run in duplicate. For exon 1, control gDNA showed a delay of 0.4 cycles compared to patient gDNA (data not shown).

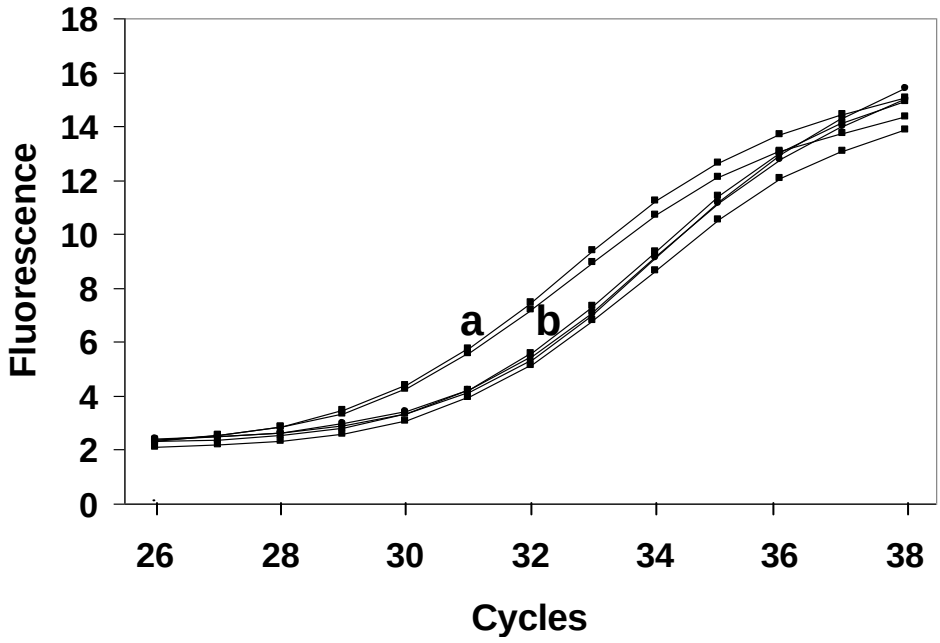

Figure 13: Quantitative real-time PCR on exon 2

3.3.5 Detection of the c.1056delG allele on cDNA

The weak intensity of the band of normal size on cDNA amplification of c.44-425 was unexpected (Fig. 12). We conducted a further study on two patients that were compound heterozygotes (WG1959 and WG3377) and two confirmed carriers for the common mutation (WG1174, mother of WG1087 and WG1977, mother of WG1976 (See segregation of mutations in *cblF* families, patients P5 and P3, in supplementary data of Rutsch et al, 2009 [157]). We amplified cDNA for the fragment c.887-1221 encompassing the common mutation and sent the samples for sequencing. Upon sequencing, the common mutation was detectable in one patient but was not seen in the other patient and the two obligate carriers. Amplification of the same region in one homozygote patient resulted in the detection of the c.1056delG allele. Because the common mutation is always found on the same haplotype, differential annealing of primers due to SNPs is unlikely. Non-sense mediated decay of that allele is plausible but more experiments are required to answer this question.

Table 3: Mutations in all known *cblF* patients

#	Patient code	DNA change	Protein change	Reference
1	WG3265	515_516delAC / 515_516delAC	T172fsX9 / T172fsX9	[157]
2	MM	1056delG / 1056delG	L352fsX18 / L352fsX18	[157]
3	WG1908	1056delG / 1056delG	L352fsX18 / L352fsX18	[157, 306]
4	WG2432	1056delG / 1056delG	L352fsX18 / L352fsX18	[157, 307]
5	WG1087	1056delG / 1056delG	L352fsX18 / L352fsX18	[157, 241, 245]
6	SJL	1056delG / 1056delG	L352fsX18 / L352fsX18	[157]
7	WG1903	1056delG / 1056delG	L352fsX18 / L352fsX18	[157, 308]
8	WG1350	1056delG / 1056delG	L352fsX18 / L352fsX18	[157, 240]
9	DME	404delC / 1056delG	T134fsX14 / L352fsX18	[157]
10	WG1959	842_845delAGAG / 1056delG	K281fsX4 / L352fsX18	[157, 308]
11	WG3365	916-1G>T / 1056delG	I306fsX2/ L352fsX18	[157, 309] (this study)
12	WG3377	712_713delAC / 1056delG	T237X / L352fsX18	[157]
13		1405delG / 1405delG	D469fsX38 / D469fsX38	[304]
14	WG4008	1339-1G>T / 1056delG	T447fsX33 / L352fsX18	[309] (this study)
15	WG4042	70-4298_246+2311del6785 / 1056delG	A24_K82del / L352fsX18	[309] (this study)

3.3.6 Non-synonymous SNPs in *LMBRD1*

Using the UCSC genome browser, we identified seven SNPs in the coding sequence of *LMBRD1*; one synonymous (rs34327883) and six non-synonymous SNPs (rs12214456 Thr>Ala, rs11555881 Leu>Pro, rs73477459 Phe>Ser, rs17854411 Ile>Val, rs9354880 Asp>Glu, rs76870386 Lys>Glu). An excess of non-synonymous to synonymous changes in the human exome has previously been reported [310]. Of these six non-synonymous SNPs, the population frequency is estimated for two, rs9354880 Asp>Glu (0.474±0.110) and rs76870386 Lys>Glu (0.044±0.142). Four changes were predicted to be benign by the web-based PolyPhen tool (http://genetics.bwh.harvard.edu/pph/), but two changes, rs73477459 Phe>Ser and rs11555881 Leu>Pro, were identified as possibly damaging. Except for rs17854411 Ile>Val, the changes affected amino acids that were conserved in placental mammals. Non-synonymous changes can potentially modulate *LMBRD1* expression or stability, as it is the case with the thermolabile 677C>T *MTHFR* variant. SNPs in *LMBRD1* are susceptible to influence the rate of birth defects in the general population, particularly cardiac malformations. With the known association between homocysteine levels and common conditions such as

heart disease, rates in the general population might also be influenced by such SNPs in cobalamin-related genes.

3.4. Discussion

We described here the first splice site mutations and long deletion in *cblF* patients. In all three cases, the novel mutation was found in compound heterozygosity with the common c.1056delG mutation. These three mutations brought to nine the total number of mutations reported in this disease. There was one common point in these nine mutations: they all lead to a shorter transcript. One mutation caused a premature stop codon. Seven, including mutations in patients WG3365 and WG4008 described here, caused a frameshift. Finally, the mutation in patient WG4042 deleted 59 of the 541 amino acids of the protein. Nevertheless, the phenotype in *cblF* patients was remarkably mild for this class of disorders. Although symptoms were often severe before initiation of therapy, patients in general responded very well to treatment with intramuscular injections of CNCbl or OHCbl. One patient died of sudden infant death syndrome (patient 8, Table 3) and two other patients did not survive a cardiac surgery (patient 1 and 6, Table 3). Interestingly, an example of variable phenotype was provided by patients WG4008 and WG4042 presented

here. Patient WG4008 was completely asymptomatic with normal apparent methionine synthase and methylmalonyl-CoA mutase activity on the propionate and MeTHF incorporation tests. It was tempting to presume that the location of the second mutation at the end of the gene, starting at amino acid 447 of 541, affected the protein at a lesser level. However, the mutation in patient 13 was located even closer to the C-terminal end of the protein, affecting amino acid 469, and yet caused a severe phenotype with seizures and intraventricular hemorrhage [304]. Patient WG4042 displayed important malformations of the head and heart. However, the nature of the mutation is similar in all cases, with no missense mutation having been identified yet.

The presence of the common c.1056delG mutation in all three patients analyzed here underlines the relevance of testing for this mutation in a suspected case of *cblF* disorder. The TspRI restriction digestion test on patient gDNA has proven to be a useful tool in the diagnosis of *cblF*. However, we presented evidence that the level of detection of the allele bearing the common mutation is variable in cDNA. Caution should therefore be taken when cDNA is used for mutation analysis.

Previous mutation analysis in *cblF* patients had relied solely on exonic sequencing of gDNA. By using a combination of gDNA and cDNA sequencing, we identified the first splice sites and long deletion mutations in *cblF* patients.

PREFACE TO CHAPTER 4

Publication:

This work was published as:

Miousse, I.R., Watkins, D., Coelho, D., Rupar, T., Crombez, E. A., Vilain, E., Bernstein, J. A., Cowan, T., Lee-Messer, C., Enns, G. M., Fowler, B., Rosenblatt, D. S. *Clinical and molecular heterogeneity in patients with the cblD inborn error of cobalamin metabolism.* J Pediatr, 2009. **154**(4): p. 551-6. [272]

Contribution of authors:

Patients were referred for clinical diagnosis by the treating physicians Drs. Rupar, Crombez, Vilain, Lee-Messer, Enns, Bernstein and Cowan.

Enzyme assays and complementation studies were performed by Jocelyne Lavallée, and cobalamin distributions were assayed by Dr. David Watkins.

David Coelho in the laboratory of Dr. Brian Fowler in Basel, Switzerland, performed the mutation analysis work on the three patients.

All data analysis was performed by IR Miousse.

CHAPTER 4: CLINICAL AND MOLECULAR HETEROGENEITY IN PATIENTS WITH THE *cblD* INBORN ERROR OF COBALAMIN METABOLISM

4.1 Introduction

Although we identified no phenotype-genotype correlations in *cblF* patients, patients belonging to the *cblD* group of cobalamin disorder show an association between the location of mutations in the *MMADHC* gene and their biochemical profile. In their 2008 article describing the discovery of the gene responsible for the *cblD* type of cobalamin disorder, Coelho et al. reported their observations about the clustering of the mutations with biochemical phenotype [39]. Out of the eight patients, two had isolated homocystinuria, two had isolated methylmalonic aciduria and four had combined homocystinuria and methylmalonic aciduria (Coelho et al. report on only one of two affected siblings with combined homocystinuria and methylmalonic aciduria, for a total of seven patients). The occurrence of three different phenotypes in a single complementation group was described four years before by the same group [271]. In spite of the small number of patients, nine different mutations were identified. Three missense mutations located near the C-terminus of the gene were found in patients with isolated homocystinuria. These missense mutations

occurred in conserved residues. Three mutations, one nonsense mutation, one in-frame duplication and frameshift deletion, were identified near the N-terminus of the gene in patients with isolated methylmalonic aciduria. Finally, three mutations located between the center and the C-terminus of the gene were identified. However, these mutations were very different from mutations found in isolated homocystinuria patients. Mutations in patients with the combined phenotype included one nonsense, one splice site deletion and one frame-shift duplication.

In their report, the authors speculated about the cause of the segregation of mutations in the *MMADHC* gene. They proposed that amino acid Met62 could act as an alternative start codon in patients with N-terminal mutations, allowing the synthesis of the C-terminal end of the protein and functional methionine synthase branch of the pathway. The missense mutations found in patients with isolated homocystinuria are proposed to be permissive for the N-terminal end of the protein to properly function in the methylmalonyl-CoA mutase branch of the pathway. Finally, the mutations identified in patients with the combined phenotype are proposed to damage the protein so that it can not perform in either branch of the pathway.

Our diagnostic lab was referred three new patients. One suffers from isolated homocystinuria, one from isolated methylmalonic aciduria and one from combined homocystinuria and methylmalonic aciduria. In addition to reporting the clinical and biochemical phenotype, we contacted the Fowler group to perform mutation analysis on these additional patients. Our goal was to assess if the findings in these new patients would weaken or strengthen the correlation seen in the first eight patients.

4.2 Materials and Methods

4.2.1 Cell lines

Fibroblast were obtained from patients and sent to the Cell Bank at the Montreal Children Hospital. Cells were maintained at 37ºC in minimum essential medium plus non-essential amino acids (MEM, Gibco, Invitrogen, Burlington, Canada) supplemented with 5% fetal bovine serum and 5% iron-enriched calf serum (Intergen, Burlington, MA)

4.2.2 Incorporation of [^{14}C] propionate

Incorporation of [^{14}C] propionate (Perkin Elmer, Waltham, Massachusetts, or MP Biomedicals, Solon, Ohio) into cellular macromolecules was measured. Fibroblasts from the patients of interest were plated at a

density of 400 000 cells in 35 mm tissue culture dishes in triplicate and incubated for 24 hours. After the incubation, MEM was removed and replaced with Puck's F medium containing 15% fetal bovine serum and 100 µmol/l [^{14}C] propionate and unlabeled propionate to give a final specific activity of 10 µCi/µmol. Fibroblasts were incubated with the radioactive Puck's medium for 18 hours. Macromolecules in the cells were then precipitated in three successive 15 minutes incubation at 4ºC in 5% (w/v) trichloroacetic acid. Precipitate was dissolved by adding 0.2 N sodium hydroxide and incubating for 3 hours at 37ºC. Radioactive propionate incorporated into proteins was measured by liquid scintillation counting (Scintillation counter, Perkin Elmer Tri-Carb 2800TR) and this value was divided by the concentration of protein in the sample, assessed by Lowry assay [301].

4.2.3 Incorporation of [^{14}C] 5-methyltetrahydrofolate

Incorporation of [^{14}C] MeTHF (Amersham Life Sciences, GE Healthcare, Chalfont St. Giles, United Kingdom) into cellular macromolecules was performed as [^{14}C] propionate incorporation by replacing the [^{14}C] propionate by [^{14}C] MeTHF, 1:100.

4.2.4 Complementation

Fibroblasts from the patients of interest were plated at a density of 400 000 cells in six 35 mm tissue culture dishes, 200 000 cells from the patient's cell line and 200 000 cells from a cell line to be tested against in each dish, and incubated for 24 hours. The next day, the Puck's medium was removed from the dishes and the dishes were washed with phosphate buffered saline (PBS). A solution of 40% polyethylene glycol was added to half of the dishes for 60 seconds and removed. All fused dishes were washed one time with PBS and seven times with MEM without serum. Dishes were refilled with MEM with serum and incubated at 37ºC for one hour. All dishes, fused and unfused, were re-fed with MEM containing serum and incubated 24 hours. The next day, [^{14}C] propionate and/or [^{14}C] MeTHF incorporation was measured in the cultures.

4.2.5 Cobalamin distribution

One confluent T175 tissue culture flask of primary fibroblasts was grown for each cell line to assess cobalamin uptake and coenzyme synthesis. The MEM was replaced by a filter-sterilized mix of 23 mL of serum-free MEM supplemented with 2 mL serum that had been incubated one hour at 37ºC with 20 µL ^{57}Co-CNCbl for a total of 0.21 µCi, 8.5 nCi/mL (MP

Biomedicals, Solon, OH) to allow binding to serum TC. The cells were incubated in the radioactive medium at 37ºC for 96 hours. The cells were harvested by trypsinisation at the end of the incubation (0.25% trypsin plus EDTA, Invitrogen, Mississauga, Canada). The fibroblasts were resuspended in 40 mL PBS, counted (Isoton II diluent and Z1 Coulter counter, Beckman-Coulter Canada, Mississauga), spun down and resuspended in 10 mL PBS, pelleted a second time and resuspended in 11 mL PBS. The cell suspension was divided into two aliquots of 5.5 mL each and 500 µL was taken from the two aliquots for gamma counts (Perkin Elmer Wizard 1470). The rest of the cell suspension was pelleted and the cell pellets kept at -80ºC until extraction. Under a dim red light, the cell pellet was resuspended in 8 mL of ethanol and the tube was incubated at 80ºC, for 20 min. The cell suspension in ethanol was centrifuged for 30 min. The supernatant was transferred to a new 50 mL tube. The supernatant was evaporated completely under nitrogen and the tube placed at -80ºC until ready to apply to HPLC. In a dark room, the dry sample was resuspended in 500 µL of ethanol, then with 1.5 mL of 0.05 M phosphoric acid buffer, pH 3.0. The suspension was filtered at 0.2 µM, loaded in a syringe and applied to an equilibrated HPLC column. (protocol adapted from [311] and [312])

4.2.6 Sequencing studies

DNA was extracted from cultured fibroblasts with the QIAamp DNA mini kit (Qiagen AG, Basel, Switzerland) and RNA was extracted with the RNeasy kit (Qiagen AG, Basel, Switzerland). RNA was reverse-transcribed to cDNA with the 1-step RT-PCR kit (Qiagen AG, Basel, Switzerland). gDNA and cDNA were amplified by PCR using conditions and primers described before [39]. PCR products were purified with the NucleoSEQ kit (Macherey-Nagel, Düren, Germany). Sequencing was performed on a ABI Prism 3100 sequencer (Applied Biosystems, Foster City, CA). Sequences were processed with the Sequence Analysis and Autoassembler v.2.1.1 software (Applied Biosystems, Foster City, CA).

4.3 Results

4.3.1 Patient WG3280

Case report

Patient WG3280 was born in Beirut from healthy non-consanguineous Lebanese parents. The mother was 32 and the father 39 years old. A cousin of the father died at age 28 with a myelopathic process, otherwise the parents did not report any relevant family history. The pregnancy was

uneventful and the child was born at term. The birth weight was the only measurement available, 3.2 kg. An older sibling is healthy. The patient was released from the hospital and developed poor feeding and lethargy during the first days of life that caused his readmission. The child was believed to suffer from an infection but cultures were negative. He developed profound metabolic acidosis for which he was treated and released after one week. The child was generally well after being released. Muscle weakness was the only symptom noted, with occasional wheezing associated with respiratory infections treated with bronchodilators.

He presented again at 4.5 years with a two-month history of weakness and complaints of poor weight gain. Examination found the patient with a weight between the 90th and the 95th percentile and a height at the 50th percentile. Metabolic acidosis was again noted. Renal tubular acidosis was considered. The patient came back to medical attention at 5 years and 10 months after repeated episodes of vomiting induced by physical activity. Metabolic acidosis was noted and there was report of weakness and a self-selected diet low in protein. Follow-up on the metabolic acidosis led to a diagnosis of methylmalonic acidosis based on the plasma acyl

carnitine profile and urine organic acids. MMA in plasma (0.45-0.8 mmol/L; not detected in controls) and urine (5.4-7.5 mg per mg creatinine; not detected in controls) was detected, but homocysteine levels were within normal range. The patient was started on a regiment of 1 mg intramuscular CNCbl every second day, 900 mg carnitine twice a day, and Polycitra 20 mL three times a day. Injections were later replaced with 5 mg of oral CNCbl daily.

The treatment resulted in a marked diminution of urine MMA to 0.45 mg per mg of creatinine. The patient was re-evaluated at six years of age. His development was normal and he was within appropriate milestones. Physical and neurological examinations were normal. However, he reportedly displayed poor social skills and behavioral problems.

Biochemical and mutation analysis

Cells from patient WG3280 were sent to our clinical diagnosis laboratory. The cultured fibroblasts showed a decreased incorporation of label from [^{14}C] propionate into cellular macromolecules. The value increased upon addition of 3.75 µmol/L OHCbl. Incorporation of label from [^{14}C] MeTHF was within normal range and did not increase with addition of OHCbl.

There was a decreased synthesis of AdoCbl from [^{57}Co] CNCbl. Only 1.6% of the label was found as AdoCbl as compared to 15.3±4.2% in controls. The proportion of label found as MeCbl was accordingly increased to 81% (normal 58±7%) (Table 4). These results pointed to the *mut*, *cblA*, or *cblB* type of disorder, or to the very rare *cblD variant 2*. Somatic cell complementation analysis was performed in cell lines known to belong to these groups (Table 5). There was a consistent increase in incorporation of label from propionate after fusion with *mut* and *cblB* cell lines. Four *cblA* cell lines showed an increase in propionate incorporation after fusion while one failed to show such an increase. The only available *cblD variant 2* cell line (originally *cblH*, see [313]) did not show complementation with the cell line from patient WG3280. Because most *cblA* cell lines showed complementation, a diagnosis of *cblD variant 2* was made.

DNA was sent to the Fowler laboratory in Switzerland where David Coelho performed mutation analysis of the *MMADHC* gene on the sample. The patient was a compound heterozygote for two novel mutations, a two bases insertion in exon 3 causing a frameshift, c.60insAT (p.Leu21fsX1) and a one base duplication in exon 5, also causing a frameshift,

c.455dupC (p.Thr152fsX10) (Fig. 14). Both mutations are predicted to cause a truncation of the protein product.

Table 4: Biochemical parameters for three *cblD* patients

	Propionate Uptake (nmol/mg protein/18h)		MeTHF uptake (pmol/mg protein/18h)		Cbl distribution (%)	
	w/t OHCbl	with OHCbl	w/t OHCbl	with OHCbl	AdoCbl	MeCbl
Control	10.8 ± 3.7	10.9 ± 3.5	225 ± 165	305 ± 125	15 ± 4	58 ± 7
WG3280	1.0 ± 0.5	3.2 ± 0.3	118 ± 7	119 ± 5	2	81
WG3583	1.5 ± 0.1	4.5 ± 0.4	24 ± 1	45 ± 1	7	3
WG3745	11.5 ± 0.3	11.1 ± 0.5	30 ± 1	43 ± 1	50	1

Table 5: Complementation analysis, patient WG3280

		Propionate Uptake (nmol/mg protein/18h) Fusion with WG3280		Fold increase with fusion
Cell lines	Type	No fusion	Fusion	
WG3280		1.1		
WG2951	*cblA*	1.0	3.6	3.6
WG3185	*cblB*	1.4	6.8	4.9
WG3200	*mut*	1.0	4.9	4.9
WG3205	*mut*	1.4	3.1	2.2
WG1437	*cblD*	1.1	1.0	0.9

4.3.2 Patient WG3583

Case report

Patient WG3583 was a girl born of Mexican parents. The mother was 34 years old, born in the same city as the father but consanguinity was denied. There are two healthy older brothers. Gestational diabetes was treated by diet alone. The decision was made to induce labor due to poor fetal growth. Induction failed and delivery was made by caesarean section. The only measurement available was the birth weight, 2.5 kg. The first weeks of life were unremarkable. The first hospital admission happened at three months of age for respiratory syncytial virus bronchiolitis with secondary bacterial pneumonia. Evaluation also identified right hip dysplasia and poor weight gain. One month later, physical and neurological examinations were normal but hypotonia and poor head control gave concerns about developmental delay.

The patient was missed on newborn screening. A posteriori, careful analysis of the newborn screen results show that the C3 levels were below the established cutoff at the time of birth. However, criteria were later modified to rather use a C3/C2 ratio and the patient would have been picked up according to the new guidelines. Biochemical measurements

taken later in life revealed macrocytosis. Homocysteine and MMA were elevated in plasma (157.8 μmol/L; normal under 20 μmol/L and 26 μmol/L; normal under 0.41 μmol/L, respectively). Treatment included a low-protein diet, 0.5 mg intramuscular OHCbl four times a day, oral betaine 250 mg per kg of weight per day, half a tablet of baby aspirin per day and 2 mg folic acid four times a day.

The patient was re-evaluated at two years of age. There was still developmental delay with improvement in cognitive and motor skills. Macrocytosis had disappeared. The treatment regimen has been reportedly difficult to follow.

Biochemical and mutation analysis

Cultured fibroblasts from patients WG3583 were analyzed in our clinical diagnosis laboratory. There was a decreased incorporation of label from both [^{14}C] propionate and [^{14}C] MeTHF into cellular macromolecules. The percentage of added ^{57}Co from CNCbl found as AdoCbl and MeCbl was decreased (7% and 3%, respectively) (Table 4). Complementation analysis was performed with two *cblC* cell lines (the most common disorder of combined methylmalonic aciduria and homocystinuria), one

cblD cell line and one *cblF* cell line. Cells from patient WG3583 complemented *cblC* and *cblF* lines but showed no complementation with cells from the *cblD* group (Table 6). This allowed classifying patient WG3583 as belonging to the *classical cblD* group. Mutation analysis in the Fowler group identified a novel homozygous nonsense mutation in exon 7, c.683C>G (p.Ser228X) (Fig. 14).

Table 6: Complementation analysis, patient WG3583

		Propionate Uptake (nmol/mg protein/18h) Fusion with WG3583		Fold increase with fusion
Cell lines	Type	No fusion	Fusion	
WG3583		1.0		
WG3480	*cblC*	1.2	4.7	3.9
WG3560	*cblC*	0.8	3.2	4.0
WG2025	*cblD*	2.0	2.1	1.1
WG3377	*cblF*	3.5	9.0	2.6

4.3.3 Patient WG3745

Case Report

Patient WG3745 was also a girl of Mexican origin. The parents are first cousins. An older sister is well. The parents did not report any contributory family history. The child was born at 38 weeks of pregnancy. The birth weight was 3.1 kg, length was 45.5 cm and the occipitofrontal circumference was 33 cm. An anteriorly displaced anus was noted. The first weeks of life were unremarkable. The patient was admitted at 4 months of age for respiratory distress and altered mental status. The child was diagnosed with respiratory syncytial virus causing the respiratory distress. Further investigation identified that the development was delayed and there was a significant head lag. The child was not rolling over yet. She reportedly fed well at the breast. Other symptoms were noted; visual tracking was inconsistent and the child was not well responding to voice. A non-obstructive, 4-ventricule hydrocephalus was observed on computed tomography scan of the head. Significant hair loss was noted after two weeks of hospitalization. Total plasma homocysteine was elevated at 52.2 μmol/L, with a normal value of under 14 μmol/L. MMA was normal. Plasma methionine was not detected and cysteine was low at 8 μmol/L (normal 16

to 84 μmol/L). Cobalamin and folate levels, as well as mean corpuscular volume, were normal (MCV 97.5 fL; normal 74-108 fL).

Treatment with OHCbl, folate, and betaine was initiated. Although biochemical parameters improved, this did not translate into a clinical improvement. A nearly obstructive inferior vena cava clot developed. The hydrocephalus progression and prolonged respirator dependency led to the decision to withdraw medical support. Retrospective analysis of a newborn screening bloodspot identified decreased methionine (5.5 μmol/L; abnormal under 10 μmol/L) and elevated total homocysteine (64.4 μmol/L, abnormal over 15 μmol/L). Both parents had normal homocysteine levels.

Biochemical and Mutation Analysis

Cells from patient WG3745 were sent to our clinical diagnosis laboratory. Incorporation of label from [^{14}C] propionate and [^{14}C] MeTHF was performed on cultured fibroblasts. Incorporation from propionate was within normal range but incorporation from MeTHF was decreased. There was also a deficit in synthesis of MeCbl from [^{57}Co] CNCbl. Only 1.4% of the recovered radioactivity was associated with MeCbl. The percentage of label associated with AdoCbl was accordingly increased (Table 4).

Complementation with cell lines from the *cblE*, *cblG* group was performed. The analysis also included the cell line derived from patient WG3583 to represent the *cblD* group. One *cblC* cell line was added as an extra control. Cells from patient WG3745 complemented two *cblE* cell lines, two *cblG* cell lines as well as the *cblC* cell line. MeTHF incorporation was not corrected in cells from patient WG3745 by fusion with cells from patient WG3583 (Table 7). Patient WG3745 belongs to the *cblD* group, variant 1. Mutation analysis identified a novel homozygous missense mutation in exon 8. The change leads to the replacement of a conserved aspartate residue to a glycine; c.737A>G (p.Asp246Gly) (Fig. 14).

Table 7: Complementation analysis, patient WG3745

		MeTHF Uptake (pmol/mg protein/18h) Fusion with WG3745		Fold increase with fusion
Cell lines	Type	No fusion	Fusion	
WG3745		63		
WG3728	*cblC*	68	196	2.9
WG3583	*cblD (Patient 2)*	60	61	**1.0**
WG3732	*cblE*	63	209	3.3
WG3589	*cblE*	57	134	2.4
WG3298	*cblG*	64	155	2.4
WG3412	*cblG*	68	218	3.2

Figure 14: Mutations in *MMADHC*

Mutations identified in this work are presented in blue, mutations published in Coelho et al. are presented in black. Exons are represented as boxes with the end cDNA position indicated. Adapted from Coelho et al.

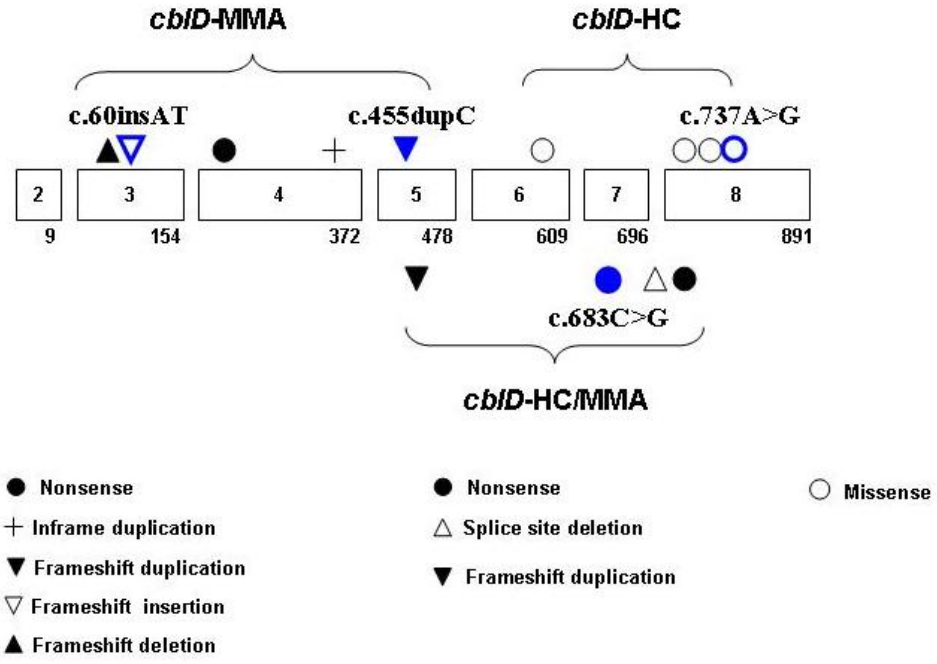

Figure 14: Mutations in *MMADHC*

4.4 Discussion

This work reported four novel mutations in three *cblD* patients. This brought from nine to thirteen the number of individual mutations known and added one new clinical description to each of the three different phenotypic subgroups of the *cblD* disorder, *classical* (or combined), *variant 1* (homocystinuria) and *variant 2* (methylmalonic aciduria). The *cblD* group however remains the rarest type of inborn disorder of intracellular cobalamin metabolism. Every patient description provides more information on disease presentation and progression. In general, symptoms in the *cblD* group are similar to the *cblC* group. The absence of description of hemolytic uremic syndrome and retinopathy in *cblD* patients is not significant at this point due to the small number of cases.

There was a striking difference between patient WG3745 and patients WG3280 and WG3582. While in patients WG3280 and WG3583 treatment resulted in major clinical improvement, patient WG3745 did not survive a progressive hydrocephalus. However, of the three cases presented, patient WG3745 also have the mutation that could have been predicted to have the least effect on the protein, being a missense. This case

exemplifies very well the challenge posed by the *cblD* disorder: there are only eleven patients in the world, but these patients are further sub-classified into three phenotypic groups based on whether one or two branches of the cobalamin pathway are affected. It would thus be premature to attempt to predict symptoms based on the complementation group. However, with the exception of patient WG3745, response to therapy is generally good. In patients for which we have follow-up data, biochemical parameters generally normalize and some degree of developmental or mental retardation is usually the main finding.

The mutations that we described in these three patients fall in agreement with the observations made by Coelho et al. It is particularly interesting that the mutation identified in patient WG3745 is a missense mutation, just like the three other mutations described in *cblD variant 1* patients. In *cblD variant 2*, patient WG3280 described here has one mutation before and the second one after the proposed alternative start of transcription, similarly to patient 4 in Coelho et al. Finally, patient WG3583 has a homozygous mutation causing a predicted truncation of the protein product, located after amino acid 62. Our results are thus in line with the observations made by Coelho et al. If we assume the Met62 alternative

start of transcription, our observations on the effect of the mutations are the following: when missense mutations are located in the second half of the gene, the associated phenotype is isolated homocystinuria; when the patient has at least one truncating mutation located before Met62 (c.184), the associated phenotype is isolated methylmalonic aciduria; when both mutations are truncating and located after Met62, the associated phenotype is combined homocystinuria and methylmalonic aciduria. It is thus unknown what would be the phenotype associated with a missense mutations early in the gene or the combination of a missense and an early truncating mutation.

PREFACE TO CHAPTER 5

Publication:

As of the time of writing, the data presented in chapter 5 have not been published but are part of current ongoing experiments.

Contribution of authors:

The purification protocol for MMADHC was optimized from a protocol originally designed by Stephane Paquette and Maria Plesa.

Protein cloning, expression and purification, as well as phage display experiments were performed by IR Miousse. Sequencing was performed at the Genome Quebec Innovation Center. Bioinformatic data analysis was performed by IR Miousse.

CHAPTER 5: PROTEIN INTERACTIONS IN THE COBALAMIN PATHWAY

5.1 Introduction

The *cblD* disorder is a complex and diverse entity. As was explained in more detail in chapter 4, mutations in the *MMADHC* gene can lead to three distinct phenotypes and the presentation varies greatly between patients [271]. The study of the *MMADHC* gene and of the twelve known affected patients highlighted several aspects of the normal function of MMADHC [39, 272]. It also raised several questions. Analysis of the *MMADHC* gene sequence first revealed a mitochondrial leader sequence encoded in the first 36 bases of the gene. Although mutations in *MMADHC* can manifest as a disorder of the mitochondrial branch of the pathway, it can also manifest as a disorder of the cytoplasmic branch of the pathway. This apparently cytoplasmic role for MMADHC is thus inconsistent with an exclusively mitochondrial location. Secondly, the MMADHC sequence displays a putative cobalamin binding motif. Further studies are required to establish if binding indeed occurs and if so, what are the affinities between different types of cobalamin and MMADHC. The gene also possesses a region of homology with the ATPase component of a bacterial ATP-binding cassette (ABC) transporter. However, it lacks the

three conserved motifs for ATP-binding of an ABC transporter: the Walker A and Walker B motifs (P-loop) and the ABC signature (C-loop). In a study of the cobalamin transport protein ABCC1, intact Walker A and signature domains were essential for nucleotide binding and ATP hydrolysis [273]. The absence of these essential motifs thus argues strongly against an ATPase role for MMADHC.

Our laboratory recently published results from experiments using the MMACHC and MMADHC protein, defective in *cblC* and *cblD* patients, respectively [270]. These experiments established that MMACHC and MMADHC interact. Using the purified MMACHC protein, they established five putative binding sites for MMACHC on the sequence of MMADHC. Dissociation constants were measured between MMACHC and four forms of cobalamin; the pharmacological form CNCbl and the three main physiological forms, OHCbl, MeCbl and AdoCbl. The interaction between MMADHC and MMACHC brought support in favor of the presence of MMADHC in the cytoplasm. Alternatively, the MMACHC protein could be present in the mitochondria. Some internal sequences in the MMACHC protein are consistent with a mitochondrial localization [314](CELLO subcellular localization predictor, http://cello.life.nctu.edu.tw/). However,

this is not consistent with the current view of the cobalamin pathway that requires MMACHC in the cytoplasm to accept cobalamin at its exit from the lysosome.

There exists a homology between MMACHC and the bacterial protein TonB. The C-terminal domain of MMACHC was modeled based on the C-terminal domain of TonB, for which a 3-dimensional structure has been determined. TonB is involved in cobalamin import in gram-negative bacteria. The protein is anchored in the inner (cytoplasmic) membrane through a transmembrane region located at the N-terminus. This region is followed by a proline-rich region believed to confer flexibility to the protein and finally, a globular C-terminal domain. The C-terminal domain has been purified and studied extensively. It folds into a globular domain that has been solved alone (PDB IDs: 1XX3, 1U07, 1QXX, 1IHR) and in complex with outer-membrane receptors BtuB (PDB ID: 2GSK) and FhuA (PDB ID: 2GRX). This domain binds to a region shared by several outer membrane receptors called the TonB box. This contact induces a conformational change that results in the import of substrates, including cobalamin, across the outer membrane. The C-terminus of TonB has also been reported to bind the periplasmic protein BtuF [286]. There are no

known functional domains in this region. The C-terminus of TonB is thus mainly known for its interactions with outer membrane receptors and the periplasmic protein BtuF. Because of the homology between TonB and MMACHC, our hypothesis is that the interaction between MMADHC and MMACHC will occur in the C-terminal region of MMACHC.

For the last part of this work, we aimed to deepen our understanding of the role of the *MMADHC* gene in the intracellular cobalamin pathway by studying the protein it encodes. Our approach was based on the previous successful experiments using purified MMACHC. The work presented here represents the first steps in a much wider project. We describe here the purification of human MMADHC from the bacterium *Escherichia coli* and the determination of putative binding sites for MMADHC on the sequence of MMACHC.

5.2 Materials and Methods

5.2.1 MMADHC construct

A construct was available for the purification of the full-length MMADHC protein [270]. However, the tag could not be removed and yields were low for this construct and purification protocol. We designed a new construct

using the pETM-41 vector (EMBL) with the mature MMADHC protein, excluding the first 12 amino acids encoding the mitochondrial leader sequence. The forward primer used to amplify *MMADHC* was 5'-ATATGCCATGGCATCCTATCTCCCAGG-3' and the reverse primer was identical to the one published in Plesa et al. [270], 5'-GCACCGGATCCCGCTGCTAATTTCCACTTAATTTC-3'. The insert was amplified with Taq Platinum HiFi (Invitrogen, Burlington, Canada). The PCR reaction was set up as follows: the reaction mix was composed of Platinum HiFi PCR buffer, 2 mM $MgSO_4$, 200 µM dNTPs, 0.2 µM each forward and reverse primers, 2 ng/µL template DNA and 1 unit Taq Platinum HiFi (Invitrogen, Burlington, Canada) per 50 µL of reaction. The cycling profile was: an initial denaturation at 94ºC for 2 min, 35 cycles of denaturation 94ºC for 30 sec, melting at 55ºC for 30 sec, amplification at 68ºC, and a final elongation step at 68ºC for 15 min. Insert and vector were digested with the restriction enzymes NcoI and BamHI (FastDigest, Fermentas, Burlington, Canada). 1 mg of DNA was double-digested with 1 unit of each enzyme. The reaction was performed at 37ºC for 7 min. The resulting digested products were applied to a 1.2% agarose gel and visualized with SYBR Safe DNA gel stain (Invitrogen, Burlington, Canada). Bands corresponding to the insert and vector were cut from the gel and

DNA was extracted (QIAquick gel extraction kit, Qiagen, Mississauga, Canada). Insert and vector were ligated overnight at room temperature with T4 DNA ligase (Fermentas, Burlington, Canada). The ligated vector was transformed into chemically competent DH5α cells. The construct was recovered from these cells by plasmid extraction (QIAprep spin Miniprep kit, Qiagen, Mississauga, Ontario).The MMADHC construct was sequenced using the T7 and T7 terminator primers (Genome Quebec Innovation Center, Montreal, Canada). The verified construct was then transformed into competent BL21(DE3) pLysS *E. coli* cells for protein expression.

5.2.2 Protein expression

E. coli BL21(DE3)pLysS cells transformed with the construct containing the mature MMADHC protein were grown overnight at 37ºC in LB media supplemented with kanamycin 30 µg/ml and chloramphenicol 34 µg/ml. The overnight culture was diluted 1:150 into 3 L of LB supplemented with 0.2% glucose and 30 µg/ml kanamycin. Cells were grown at 37ºC and allowed to reach an OD_{600} of at least 1.1.The cell culture was transferred to room temperature and MMADHC protein expression was induced with

0.25 mM isopropyl β-D-1-thiogalactopyranoside (IPTG) for 16 hours. In the morning, cells were harvested by centrifugation at 7300 g for 15 min.

5.2.3 Cold osmotic shock

The cell pellet was resuspended in 60 ml of TES buffer containing 0.2 M Tris-HCl pH 8.0, 0.5mM ethylenediaminetetraacetic acid (EDTA), and 0.5 M sucrose supplemented with one tablet of protease inhibitor cocktail, EDTA-free (Sigma-Aldrich, Oakville, Canada), 50 µg/mL each of RNase A and DNase, 1 mM phenylmethylsulfonyl fluoride (PMSF), and 5 mM $MgSO_4$.The cells were incubated with shaking at 4ºC for 30 min. The cell resuspension was diluted 1:4 by adding 240 ml of cold double-distilled water (ddH_2O) and incubated with shaking at 4ºC for 1 hr. Cell debris was collected by centrifugation in a cold SLA-1500 rotor at 10 000 g for 10 min at 4ºC. The clear supernatant was collected.

5.2.4 Purification

The supernatant from the cold osmotic shock was separated by fast protein liquid chromatography (FPLC). We used a Ni^{2+}-NTA Superflow column with a bed volume of 20 mL (Qiagen, Mississauga, Canada). The column was equilibrated with 6 column volumes (cv) of 20 mM Tris-HCl

pH 7.5, 200 mM NaCl, 5 mM imidazole and 10% glycerol. The column was washed with 3 cv of equilibration buffer followed by 3 cv equilibration buffer with 10% elution buffer (equilibration buffer with 400 mM imidazole). The 6xHis-MBP-MMADHC protein was eluted in 100% elution buffer. Fractions corresponding to the elution peak were pooled and the protein concentration estimated by a Bradford assay. A 1:10 ratio of hexahistidine-tagged tobacco etch virus (TEV) protease was added for removal of the hexahistidine/MBP tag and the reaction was allowed to process overnight at 4ºC. In the morning, the volume was halved with a centrifugal filter unit with a cutoff molecular weight of 10 kDa (Amicon Ultra-15, Millipore, Billerica, MA) at 3750 g for 10 min. The concentrated cleaved protein was brought up to 15 mL with equilibration buffer and re-spun in a filter unit. The process was repeated for a total of five spins. The 15 mL solution with a concentration of about 10 mM imidazole was applied to an equilibrated Ni^{2+}-NTA Superflow column. The column was washed as before. A linear gradient of imidazole was used for the elution step. Cleaved MMADHC was recovered in the flow through and in the washing steps. 6xHis-MBP and 6xHis-TEV were recovered in the elution gradient. Fractions from the flow-through and washing steps were pooled and applied to a centrifugal filter unit for concentration to about 10 mL. The

protein concentration was estimated by Bradford assay and further concentrated as required.

5.2.5 Phage Display- Panning one

Phage display was performed on MMADHC using two commercially available libraries: Ph.D.-12 and Ph.D.-C7C (New England Biolabs). The pure cleaved MMADHC protein was dialyzed against equilibration buffer to reduce the imidazole concentration. The protein was diluted to 100 µg/mL MMADHC in 0.1 M $NaHCO_3$, added to a microtiter plate well and incubated overnight at 4ºC. In the morning, the solution from the well coated with the MMADHC protein was poured off and the well was filled completely with a blocking solution of 5 mg/ml BSA in 0.1 M $NaHCO_3$ pH. 8.6 for 2 hr at 4ºC. The blocking solution was poured off and the well was washed vigorously 6 times with a solution of 50 mM Tris-HCl pH 7.5, 150 mM NaCl and 0.1% v/v Tween-20 (TBST-0.1%). A solution of 10 µL of random phage library corresponding to 1.5×10^{11} plaque forming units (pfu) (Ph.D-12 and Ph.D-C7C librairies, New England Biolabs, Pickering, Canada) diluted in 90 µL of TBST-0.1% was added to the well. The plate was gently rocked for 1 hr at room temperature to allow the phages to bind to the coated protein. The well was then washed vigorously ten times with

TBST-0.1%. Bound phages were eluted with 100 µL 0.2M Glycine-HCl pH 2.2 containing 1 mg/mL BSA by rocking for 10 min at room temperature. The solution was neutralized with 15 µL Tris-HCl pH 9.1. The phage elution was titered. An overnight culture of ER2738 *E. coli* cells was diluted 1:1000 in 5 mL of fresh LB with 20 mg/mL tetracycline and grown to an OD_{600} of 0.5. Serial dilutions of the phage eluate from 10^1 to 10^4 were added to 200 µL aliquots of cell culture and incubated 5 min at room temperature. The phage-infected cells were then mixed with melted top agar at 45ºC and spread on four warm LB/tetracycline/IPTG/X-gal plates (one per dilution). The number of blue lytic plaques was multiplied by the dilution factor to obtain the number of plaque-forming units (pfu) per mL of eluate.

5.2.5 Phage Display- Amplification

The first round unamplified eluate was amplified by mixing 85 µL of the phage eluate with a 1:100 dilution of an overnight ER2738 culture in 20 mL LB with tetracycline. The cell culture was incubated at 37ºC with shaking for 4.5 hr and then centrifuged 10 min at 12 000 g at 4ºC. The supernatant was transferred to a fresh tube and the centrifugation was repeated. The upper 80% of the supernatant was collected. A solution of

20% polyethylene glycol (PEG) in 2.5 M NaCl was added to allow phage precipitation, at a volume corresponding to 1:6 of the collected supernatant. The mix was incubated overnight at 4ºC. The next day, the PEG-precipitate was centrifuged at 12 000 g for 15 min at 4ºC. The supernatant was carefully discarded and the pellet resuspended in 1 mL TBS. The phage solution was microcentrifuged at 15 000 g for 5 min at 4ºC. The supernatant was recovered and phages were once again precipitated by adding 1:6 volume of 20% PEG in 2.5 M NaCl. Phages were incubated on ice for 1 hr and microcentrifuged at 15 000 g for 10 min at 4ºC. Supernatant was discarded and the pellet containing phage particles was resuspended in 200 µL TBS. The amplified phage eluate was titered as before, using 10^8 to 10^{11} serial dilutions.

5.2.6 Phage Display- Pannings two and three

The amplified eluate from round 1 was used as an input for subsequent rounds of panning. A microtiter well was coated and blocked as before. The blocking solution was poured off and the well was washed with TBS containing 0.3% Tween-20 (TBST-0.3%). A solution containing 10 µL of amplified phages in TBS and 90 µL TBST-0.3% was added to the well and incubated 1 hr at room temperature with gentle rocking. The phage

solution was poured off and the well was washed 10 times with TBST-0.3%. The bound phages were eluted as before and the eluate was titered. The eluate #2 was amplified and used for a third round of panning using TBS with 0.5% Tween-20.

5.2.7 Phage Display- Peptide analysis

Unamplified phages from round 2 or 3 were submitted to peptide analysis. Titration plates containing between 100 and 200 blue lytic plaques were used for phage DNA extraction. Individual plaques were picked with a 1 mL micropipette tip and added to tubes containing 4 mL of a ER2738 culture in LB-tetracycline at OD_{600} 0.2. Cells were grown at 37ºC for 4.5h. The tubes were centrifuged at 7300 g for 20 min at 4ºC. The upper 3 mL of supernatant containing phages but no bacterial cells was transferred to fresh tubes. Phage DNA was extracted from each individual culture using the QIAprep Spin M13 kit (Qiagen, Mississauga, Ontario). The DNA region encoding the random peptide was amplified using primers located upstream and downstream: forward 5'-GTGACGATCCCGCAAAAGCGGCCT-3' and reverse 5'-CCCCTCATAGTTAGCGTAACG-3'. Each PCR reaction contained PCR buffer with KCl, 2 mM $MgCl_2$, 200 µM dNTPs, 200 µM each forward and

reverse primer, 2 ng/μL template DNA and 0.015 U/μL recombinant Taq DNA polymerase (Fermentas, Burlington, Canada). The mix was first heated at 95ºC for 2 min, then cycled 40 times 95ºC for 30 sec, 55ºC for 30 sec, 72ºC for 30 sec. The final elongation step was 72ºC for 7 min. The PCR products were sequenced at the Genome Quebec Innovation Center (Montreal, Canada) using the reverse primer mentioned above. Text sequences were reverse transcribed into peptides and all results were revised manually based on the sequencing chromatogram data. Repeated sequences were eliminated and the pool of unique affinity-selected peptides was aligned to the sequence of the MMACHC protein with the Faster_scan.py and Faster_clustal.py analysis tools (P.D. Pawelek, unpublished data). Scores were assigned to the peptides based on the similarities between the amino acids in the peptides and the MMACHC primary sequence. Exact matches were given a score of 4 points, conservative matches were given a score of 1 point, neutral matches were given a score of 0 and non-conservative matches were given a score of -1. Window size (the number of consecutive residues in the affinity-selected peptides considered in the score) varied from 4 to 6. A score threshold of 13 was used. MMACHC regions with significant clusters of peptides (over 5 peptides mapping to the same region) were selected.

Figure 15: MMADHC protein purification

12% acrylamide SDS-PAGE gel stained with silver stain showing the outcome of MMADHC purification. First lane (Ladder): PageRuler Prestained Protein ladder (Fermentas). Lane 2 (Fusion): fusion material after Ni-NTA. Lane 3 (Cleaved): material after cleavage, the upper band represents MBP, the middle band represents cleaved MMADHC and the lower band is the TEV protease. Lane 4 (MMADHC): Isolated cleaved MMADHC protein.

Figure 15: MMADHC protein purification

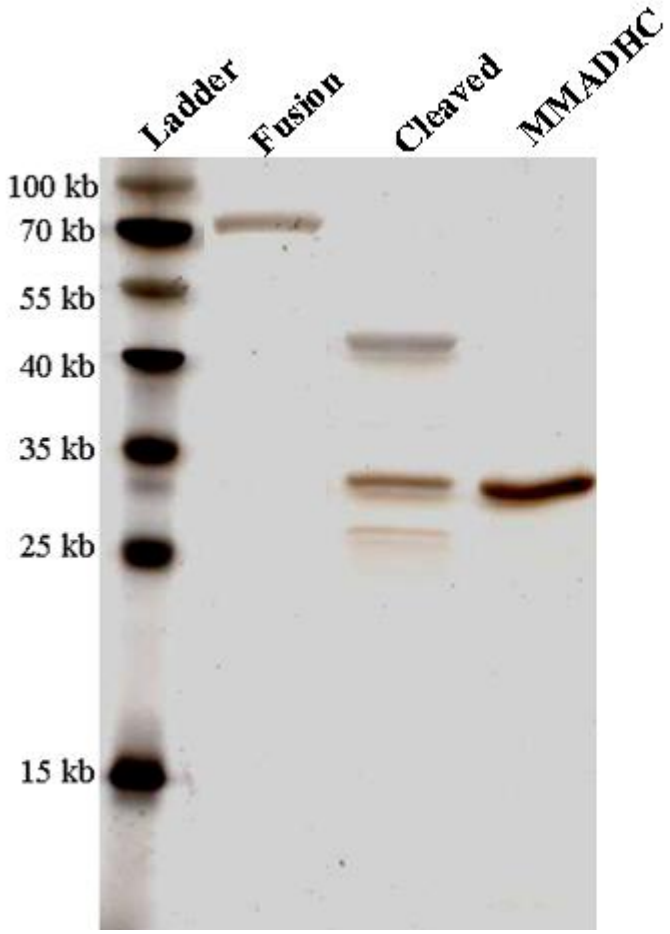

5.3 Results

5.3.1 Protein purification

The MMADHC protein was purified to homogeneity. Yields of 7 mg of fusion protein per liter were obtained after the first Ni^{2+}-NTA purification. The product migrated slightly above the 70 kDa marker on 12% SDS-PAGE gel treated with silver staining, the appropriate molecular weight calculated for 6xHis-MBP-MMADHC being 72 kDa (Fig. 15, second lane). Cleavage of the tag with TEV protease overnight at 4ºC was efficient (Fig. 15, third lane). A typical yield of 1.5 mg of pure, cleaved MMADHC protein per liter of cell culture was obtained after the second Ni^{2+}-NTA separation step. The product migrated at the appropriate molecular weight of 32 kDa (Fig. 15, fourth lane). The protein was stable in solution for a period of at least two weeks at 4ºC. This material was used for phage display experiments [283].

5.3.2 Phage Panning

Three rounds of panning were performed for each phage library. The M13 phage titers calculated for each round of panning are presented in Table 8. The phage library was not amplified after round 3 as no subsequent rounds of affinity selection were performed. We sequenced phages from

each of the Ph.D-12 and Ph.D-C7C libraries after the third round of panning, 24 from the second round unamplified and 24 from the third round unamplified. For Ph.D-12, one sequence was represented 13 times out of 23 sequences from round 3. There were no repeated sequences in round 2. For Ph.D.C7C, two sequences were repeated three times and one sequence was present twice in round 3. Two sequences were repeated twice in round 2. To limit duplication of sequences while conserving a selection pressure, 96 more clones were selected and sequenced from the second round of panning for each library. A total of 181 unique peptides were obtained, 102 from the Ph.D-12 library and 79 from the Ph.D-C7C library (Table 9). Redundancy was higher in the Ph.D-C7C library than in the Ph.D-12 library, explaining the lower number of unique phages identified.

Table 8: Phage titers, Ph.D.-12 and Ph.D.-C7C

Library		Round 1	Round 2	Round 3
Ph.D-12	Unamplified	$3.5x10^{6}$	$3.5x10^{6}$	$2.0x10^{6}$
	Amplified	$2.0x10^{13}$	$3.0x10^{12}$	
Ph.D-C7C	Unamplified	$5.0x10^{5}$	$6.0x10^{5}$	$2.0x10^{6}$
	Amplified	$1.5x10^{12}$	$2.5x10^{13}$	

Table 9: MMADHC affinity-selected peptides

Unique peptides from the Ph.D. 12 library

IVNSDSSNSIGM	KTDQSNAYTIWL	QYPALPLRVSHP
VILPSMGPHPAP	VKITTVLNPIVG	NAGPNAILPTAS
ELASVNSVYTTT	TWVPYNPGQRLP	RIFNHMMQFPDP
IQPSYHGSGYVR	DSLWLKLSNLHS	ARTASTNMIPNL
QYQMNHSPAVRP	SLPLNLTLWNQF	TSSPRSPQLQPY
LTPQGTFQAAPA	SLMSPTFTWSRA	YDLHQAFWYSSS
WHTSNGTLTSQV	HSMPSPPSNSIK	VNTSPPVKLKGM
TKLYPALPXASP	GFPLVTLASKPQ	QTAGTFEVQYDA
WVKSDNPWSTLK	AYFTSMSHDPRA	TTAAVDMPRSTP
LSYSTHQIPKPS	QPPSIYLESYQR	SQHRVLAVPSAN
TTYPHFPNRHDR	SSLNPRSLFPHT	VTPHLMQAMRHL
QLSPHPLWKTPH	SLTSFTTYYGHS	FPQRLETHMPHH
SPHILLTQMTSS	NTWHTFNTAYTR	TSPACASPRTLH
LPMLAGRPIVHK	KPSHNPQTVTSL	SVSVGMKPSPRP
HNYRASQDVDHD	LNTSQIKLHSTR	HDARPMAPYRVQ
QVLLLNPPSGRH	SETLHYPPRDDA	RPEPAVDRQSPV
SPLSMHRPYTPP	DSSPHVLIGTSR	GSMHMPSRMHTN
ALLELPRQIRTS	HPPFRWQSAMLY	QTFKANHSPDLV
QSTALLWTHQTL	TSAFPHPNRVTY	IWIAAATANAAV
SITFRTTFMSNG	AHALTRSADITP	YMSSPDRQPTLT
STVSLPVHDWTK	HPTRLSSSLPWT	HTGPEARGPAAR
HSAPPLTLEWAP	SWYSHGASPQPR	HYVPSMNGEGTS
DPLVYELNRILG	QPSGHNRTHTTP	DLLPLTHEKPSH
VHNWLYWSFPPR	DLTRVLPPNGPR	STAHPIGPNAHN
SPNSIPTLAAAR	NSTVLSSEYVSE	AATDSPFSLPIA
FHWTQYFSPWIR	NSVPHSTDLQMP	HHSGNPSRNNTG
FTPRHGYVPNHA	ALLQSHKMYSIT	TNTPPSQRVHLS
FTDTTSHLIRRN	YMTPKNPALMAR	SLPTNAPGLKFL
KCCFALQHQTFI	NSGSTNTILISA	DVFINAKWKFTT
ATWGHPRSSQGM	HDYQLRLGSLAH	TELTTRKLTLSV
FTLGQPHNSAAG	GIDQAAKTNDID	ALPIDYMLISTP
MPQTLVLPRSLL	VLALTAATHMTR	SRLQWEVNFSVR
HPRHWPPQINPH	DDPKLLLTRSQS	DYRSQHRIYLTS
VTVQMQRLVTIM	GLPPDGSSVTNR	YYTPQHQKQVGP

Unique peptides from the Ph.D.-C7C library

HGLRANL	SMTRYHT	TDRTQTS
VRGHLTE	PNMTPLH	TLPGTKL
DTIQAAG	LPTTSPS	SMATNFW
YTSGSLN	SPPEHLT	KTRPLSD
ELTHDRT	ENRGSLT	HPEAKHQ
KTKLETY	LQTAPGG	DNDNSSL
SNHAPPF	MRTGSSL	ELTHDRT
HPEHPRH	FPHPYSS	QAPRIEF
LYKPWHT	FYPDNHI	HDRADRQ
PPHASSR	SLQMTPW	IATGDTM
NSHNHHT	SKLHNPT	EQSHKAH
TMKSKMS	TSTQAAP	APWNHSL
QGIQTST	TLLSPAQ	PGPLKRT
STARNFW	LDLRANL	HSSKPFS
DSPHYTR	QMTLGST	SSMIPLD
LLTYGNG	GGPILPF	SSHLPAQ
SSLWPTT	DVMTQTT	PNVPTGD
PSTVPAV	TNLNYKF	QGQLTGY
LAPWELK	HAHNEHN	LTPTWPH
QGSQPYK	FNSATMP	VNTPKQT
QQLRQGF	AGKWKQQ	SSDTRHS
HEGPQYG	LTADIPS	PLCPQQR
QRATFYS	HSGQAFR	NWPTTQT
QQLRQGX	KASPARL	ELLMEQM

5.2.3 Analysis of the MMADHC affinity-selected peptides

The DNA sequences obtained were translated into peptides using the ExPASy Translate tool (http://ca.expasy.org/tools/dna.html). Peptides were aligned to the MMACHC sequence with a Python-based bioinformatic tool developed at the Argonne National Laboratory and optimized by Dr. Peter Pawelek [315]. Scores were verified by hand. Four clusters of sequences above the threshold of 13 aligning to the MMACHC sequenced were identified. The score is a quantitative representation of the degree of similarity between the peptide and the compared sequence, normally located between 12 and 20. The presence of multiple peptides above the threshold in a single region is more significant that the score of individual peptides. The first region mapped to the N-terminus of the protein and regions 2 to 4 mapped to the C-terminus of MMACHC.

Region 1 covered residues 34 to 57 of the MMACHC sequence (Fig. 16). The peptide cluster was composed of three peptides from the Ph.D-C7C library and eight peptides from the Ph.D-12 library. Nine peptides had a score of 14, one had a score of 15 and one had a score of 16 (Table 10). There is no known functional domain or motif in this portion of MMACHC.

Table 10: Peptides mapping to region 1

Peptide	Peptide match score	Scoring window	Region	Alignment position
TLLSPAQ	15	5	1	34
TLPGTKL	14	6	1	43
GGPILPF	14	6	1	45
QPPSIYLESYQR	14	6	1	36
DLTRVLPPNGPR	14	6	1	41
VILPSMGPHPAP	14	6	1	41
GFPLVTLASKPQ	14	6	1	44
SLPTNAPGLKFL	14	6	1	46
SPNSIPTLAAAR	16	4	1	46
ALPIDYMLISTP	14	5	1	52
SQHRVLAVPSAN	14	5	1	52

Figure 16: Matches to region 1

Residues 28 to 62 of the MMACHC protein (bold, center). Matching peptides from the Ph.D.-C7C libraries are displayed above, and peptides from the Ph.D.-12 under the sequence. Exact matches are highlighted in black and conservative matches are highlighted in grey.

Regions 2, 3, and 4 were located in the C-terminal region of MMACHC. Region 2, from residue 221 to 238, and region 3, from residue 232 to 250, overlapped and were presented as separate for clarity (Fig. 17). Region 2 was constituted of three peptides from the Ph.D-C7C library and eight peptides from the Ph.D-12 library. Two of these peptides overlapped with region 3. The average and median score was 15. Region 3 contained nine peptides, three from the Ph.D-C7C library and six from the Ph.D-12 library. The average and median score was 15. Region 4, ranging from residue 261 to 280, contained seven peptides from the Ph.D-12 library (Fig. 17). The average score was 15.5 and the median score was 15. All matching peptides are listed in Table 11 with the matching location on the MMACHC sequence as well as their score and the window size used. Together, the three regions mapping to MMACHC C-terminus covered 45.4% of the section that was modeled according to the structure of the C-terminal domain of TonB (TonB structural homology domain).

Table 11: Peptides mapping to region 2 to 4

Peptide	Peptide match score	Scoring window	Region	Alignment position
SSHLPAQ	14	6	2	223
PSTVPAV	15	5	2	223
TLLSPAQ	15	6	2,3	231
AYFTSMSHDPRA	14	5	2	221
YMSSPDRQPTLT	13	5	2	221
WHNWLYWSFPPR	16	6	2	221
AATDSPFSSPIA	16	6	2	222
TNTPPSQRVHLS	21	6	2	224
TWVPYNPGQRLP	16	5	2	226
QSTALLWTHQTL	14	6	2	228
ALLELPRQIRTS	15	5	2,3	232
HSSKPFS	15	6	3	240
LPTTSPS	13	4	3	244
SQHRVLAVPSAN	15	5	3	236
DLLPLTHEKPSH	16	4	3	241
HSMPSPPSNSIK	15	5	3	244
QTFKANHSPDLV	16	6	3	245
HSMPSPPSNSIK	15	5	3	243
HHSGNPSRNNTG	20	5	4	261
SSLNPRSLFPHT	16	6	4	268
QYQMNHSPAVRP	14	6	4	271
HPRHWPPQINPH	14	6	4	272
DLTRVLPPNGPR	15	5	4	272
QYPALPLRVSHP	15	5	4	273
TKLYPALPXASP	15	5	4	276

Figure 17: Matches to regions 2-4

Residues from the MMACHC protein are displayed in bold with the start and end residue between parentheses. Matching peptides from the Ph.D.-C7C libraries are displayed above, and peptides from the Ph.D.-12 under the sequence. Exact matches are highlighted in black and conservative matches are highlighted in grey.

Figure 17: Matches to regions 2 to 4

5.4 Discussion

Previous attempts at purifying the MMADHC protein had produced a protein that, although pure, could not be separated from the 40 kDa 6xHis-MBP tag. Plesa et al. [270] were able to use this fusion protein to provide evidence for MMACHC-MMADHC interaction by using purified free MBP as a control for the presence of the MBP tag. For phage display experiments, the presence of such a protein tag would create an important background of phages with affinity for the MBP tag. An option was to control for background by pre-incubating the phage library with free MBP to eliminate MBP-binding phages from the pool and use the pool of unbound phages to apply to the target. We considered this approach but the reduction in the background would not have completely prevented the presence of MBP-binding phages in the pool. We thus focused our effort in obtaining a construct where the MBP tag could be cleaved while retaining an acceptable yield of pure MMADHC.

Analysis of the MMADHC sequence identified the 12 first amino acids as part of a mitochondrial leader sequence. N-terminal leader sequences are cleaved after mitochondrial import to lead to the mature form of the

protein. We thus estimated that the mature form of the protein was preferable to the full-length form containing the leader sequence. The new construct we created containing the mature form of MMADHC was readily amenable to TEV cleavage of the 6xHis-MBP tag.

We also modified the type of purification column used with regard to the published protocol [270]. The use of a Ni^{2+}-NTA Superflow column in the place of an amylose resin column resulted in a ten-fold increase in yield with our specific construct. Technical issues with the amylose column used (e.g.: age of the resin, regeneration protocol, physical integrity of the column) might explain the scale of the difference observed. An advantage to the use of the Ni^{2+}-NTA resin was the absence of native MBP along with the fusion protein in the elution fraction. In general, the use of an amylose column leads to fewer contaminants due to high specificity for MBP. However, in spite of the addition of glucose in the growth media, some endogenous MBP is still produced by the bacterium and binds to the amylose column along with the MBP tag from the fusion protein. In addition to impeding an accurate measurement of the yield of fusion protein, contaminating endogenous MBP is problematic for the separation step after cleavage. Using an amylose column for both steps opf

purification, the his-tagged TEV protease required in the cleavage process is recovered in the flow-through along with cleaved MMADHC. Using a first amylose resin column followed by a Ni^{2+}-NTA column, it is endogenous MBP that is present in the flow through with MMADHC. Further purification steps such as ion exchange or size exclusion chromatography are required. On the other hand, the use of the Ni^{2+}-NTA resin typically leads to the presence of contaminants such as native proteins with containing clusters of histidine residues. This contamination was negligible in our case, presumably due to the use of cold osmotic shock rather than whole-cell lysis. The same column and buffers were used in both purification steps, facilitating the process.

These modifications to the MMADHC construct and purification process allowed us to obtain the starting material to perform protein-protein interaction experiments. Two phage libraries were used: the Ph.D-12 library is constituted of phages displaying a random linear 12-mer, while the Ph.D-C7C library is constituted of phages displaying a 7-mer bordered on either side by a cysteine residue, forming a disulfide bond. The two libraries were used on conjunction to obtain a wider variety of sequences. Diversity was lower in the third round of panning for both libraries as

compared to the second round of panning. This decrease in diversity is caused by the increase in the stringency of the selection between each round. Equilibrium between stringency of selection and diversity of the phage pool must be reached. We thus continued the analysis with phages from round 2 of panning. These phages were submitted to two rounds of selection but did not have the redundancy found in round 3. The lower number of individual phages selected from the Ph.D.-C7C library reflected a higher redundancy in this library than in the Ph.D-12 library, and not a higher proportion of uninterpretable sequences.

The use of a computer algorithm in the analysis of the data allows an unbiased alignment of peptides on the sequence. However, the selection of the clusters to display is done manually. For MMACHC, some peptides were mapped to regions outside of the clusters presented here, but these sequences were not supported by other peptides mapping to the same area, or a small number of low-scoring peptides were mapping to one area. This concern about the accuracy of our reporting led us to increase the scoring threshold from 12 to 13 to eliminate low scoring peptides which are the most likely to arise randomly. We were thus confident that the results we reported were the most significant.

The clusters of peptides identified on the sequence of MMACHC represent predicted sites of interaction, not proved sites of interaction. Phage display results cannot prove the interaction between two proteins. With the previous demonstration of the interaction between MMADHC and MMACHC by Plesa et al., these thus represent the most likely points of contact between the two proteins. Other teams have used site-directed mutagenesis to alter residues located in predicted sites of interaction and observe how these changes affect the binding between two molecules. However, it is not possible to know for sure whether the change in binding behavior is due to the absence of a residue essential in binding or to conformational changes induced by the change. The resolution of the three dimensional crystal structure of the complex between the two proteins can definitively address the binding events. The co-crystallization of MMADHC and MMACHC is one of the long-term objectives of this project.

Three of the four predicted regions were located in the region of MMACHC that has been modeled based on the structure of TonB (TonB predicted structural homology, residues 185 to 282). Regions 3 and 4 also

overlapped with the region of TonB sequence homology, spanning residues 242 to 280 [38]. There are no recognized functional motifs in this region of TonB. What we do know about the C-terminus of TonB is that it is involved in interactions with other proteins. It is thus interesting to find that this role appears also in its human counterpart. One might suggest that the C-terminal domain of MMACHC was conserved to perform protein-protein interactions involved in ligand import. Region 1 is located in the N-terminus of the protein. There is no known functional domain or motif in this section of MMACHC. Without a crystal structure available, it is not possible to determine the position of this segment with regard to the C-terminus of the protein. There is a possibility that region 1 forms a continuous accessible surface with regions 2, 3, and 4.

We hope that future experiments using the purified MMADHC protein will provide further information on its ability to bind to ligands such as different forms of cobalamin and ATP, and how the interaction between MMADHC and MMACHC is influenced by the presence of such ligands.

CHAPTER 6: DISCUSSION

The intracellular disorders of cobalamin metabolism are rare genetic disorders affecting the function of the enzymes methionine synthase and methylmalonyl-CoA mutase. They collectively represent around a thousand known patients worldwide. Despite this small number, these patients have set the foundation for most of the current knowledge about cobalamin intracellular metabolism.

cblF

Summary of findings

To date, over 15 genes responsible for cobalamin absorption, transport, and metabolism have been discovered, a body of work to which our advances to identify the gene underlying the *cblF* disorder contributed. We located the gene responsible for the *cblF* disorder to chromosome 6 and the exact gene was subsequently identified by our collaborators as *LMBRD1*. The properties of the protein it encodes, LMBD1, are in good accordance with the lysosomal entrapment of cobalamin observed in *cblF* patients. LMBD1 is a multipass transmembrane protein that colocalizes with the lysosomal marker LAMP1. These results supported the

hypothesis that efflux of cobalamin across the lysosomal membrane is defective in *cblF* patients. It remains to be determined if LMBD1 forms a channel as a monomer or multimer, alone or with other partner proteins, or functions under an alternative mechanism.

Only two types of mutations had been identified in the initial cohort of *cblF* patients: nonsense (1) and frameshift (5) mutations. We performed mutation analysis on two new patients and one patient for which one mutation had not been identified. We identifed three novel mutations in two new categories: two splice site mutations and a long, in-frame deletion of an entire exon. cDNA analysis, in addition to gDNA sequencing, was essential in confirming that exons were missing in the transcript in these patients.

Cardiac malformations in cblF patients

With homocysteine levels not higher than in *cblC*, *cblD*, *cblE* or *cblG* patients, it is difficult to explain the high frequencies of heart defects in *cblF* patients. This difference could be attributed to a defect in cobalamin absorption from the gastrointestinal tract in certain *cblF* patients, as demonstrated by abnormal Schilling test results. However, we observed

that heart malformations and decreased serum cobalamin/abnormal Schilling test results do not segregate together. One of the many consequences of the *LMBRD1* gene discovery is that expression levels can now be measured in different tissues and at different developmental stages and correlated with observed pathologies. These experiments are currently being performed in a mouse model.

cblD

Summary of findings

Contrarily to the *cblF* cohort, there are no common mutations in *cblD* patients. As our own study showed, the clinical presentation is very variable within this group. Our description of three new *cblD* patients was the first confirmation of results published by Coelho et al. about the correlation between localization and nature of mutations in *MMADHC* and the variant forms of *cblD*. The three biochemical presentations (MMA only, homocystinuria only and combined MMA and homocystinuria) show a distinct pattern of associated mutations.

Our approach to address questions surrounding the *cblD* type of cobalamin disorder involved producing the first tag-free purified MMADHC. We used this material to predict surfaces of interaction with MMACHC. Our results suggest an interaction of MMADHC largely with the C-terminus of MMACHC. These results are particularly interesting as this section of the protein shares homology with a bacterial protein known to interact with several proteins in cobalamin import.

Function MMACHC

Five years after the publication of the gene underlying the *cblC* defect and two years after the publication of the gene underlying the *cblD* defect, questions remain about the function of these proteins. Analysis of the MMACHC sequence revealed homology between the C-terminus of the human protein and the C-terminus of the bacterial cobalamin import protein TonB [38]. Biochemical analyses revealed an ability of the protein to bind cobalamin and to cleave alkyl groups (Me and Ado) at the upper axial position of the cobalamin molecule [267, 268]. An interaction has also been detected between the TonB structural homology domain of MMACHC and MMADHC [270]. Our findings are consistent with what is known of TonB. The C-terminus of TonB was shown to be involved in

protein-protein interactions with the periplasmic protein BtuF and with outer membrane receptors [285, 286]. The results of these experiments thus have contributed to shed light upon one of the roles of MMACHC; protein-protein interactions.

Function of MMADHC

The function of MMADHC is also unclear. It possesses a region of homology with the ATPase component of a bacterial ABC transporter but the three main ATPase functional parts, the Walker A, Walker B and signature domain, are missing. It possesses a cobalamin-binding motif, although our own preliminary data obtained with intrinsic fluorescence spectroscopy indicated minimal binding of four different cobalamin forms (Ado-, Me-, OH- and CNCbl) at neutral pH (unpublished data). The absence of the three ATPase critical motifs argues against it binding ATP. The mutation analysis in *MMADHC* provided further insights about the function of the protein [39, 272]. It was previously known that there are three biochemical phenotypes associated with the *cblD* defect: isolated homocystinuria, isolated methylmalonic aciduria and combined homocystinuria and methylmalonic aciduria [271]. As our own study confirmed, mutations causing isolated homocystinuria segregate in the C-

terminus of the protein and are missense, mutations causing isolated methylmalonic aciduria segregate at the N-terminal end of the protein and mutations causing a combined defect are truncating mutation in the C-terminal half of the gene. The protein thus seems to have two separate roles, one involved in the methylmalonyl-CoA mutase arm of the pathway and another in the methionine synthase arm of the pathway. Several questions remain to answer, such as the ability of MMADHC to bind cobalamin or ATP, and how pH and the interaction with MMACHC modulate these parameters. The availability of purified MMADHC allows for such questions to be addressed.

Localization of MMADHC

There exists an uncertainty about the subcellular localization of MMADHC. How can it perform its role in the cytoplasmic methionine synthase arm of the pathway and interact with the cytoplasmic MMACHC if it is indeed located inside the mitochondria as its leader sequence suggests? Because of the presence of a strong Kozak consensus sequence [316] around the amino acid methionine 62, there exists a possibility that translation is initiated at two different codons on the mRNA (reviewed in [317]). This is consistent with the presence of only one mRNA transcript

detected in cells [39]. This second, shorter protein product would lack a mitochondrial leader sequence and would have the potential to localize to the cytoplasm. Similar cases where a single mRNA gives rise to more than one protein product of different sizes localizing to different compartments have been reported before [318, 319]. This putative shorter isoform also corresponds to the fragment of MMADHC that is predicted to be involved more specifically in MeCbl synthesis, consistent with a cytoplasmic localization. Further studies are required to definitively address the subcellular localization of MMADHC and whether a single gene product or more are detected. An alternative explanation was provided by a report localizing the MMACHC protein to the mitochondria [320]. Both MMADHC and MMACHC could be mitochondrial proteins, with an intermediate form of cobalamin for MeCbl synthesis being exported from the mitochondria to the cytoplasm. Alternatively, both proteins could be found in both compartments.

Additional steps in the cobalamin pathway

Although *cblF* represents the last complementation group for which the gene was not known, we expect that more genes involved in the cobalamin metabolism are still to be discovered. An example of the

existence of additional genes in the cobalamin pathway was provided by two recent patients. One patient was referred to the European clinical diagnosis lab and the second was referred to Montreal. Both patients were biochemically undistinguishable from *cblF* but somatic cell complementation indicated that they did not belong to any known complementation group. Exome sequencing performed independently by the two groups identified an ATP-binding cassette (ABC) transporter. These recent results indicate that export of cobalamin from the lysosome is mediated by a second protein in addition to LMBD1.

The gene encoding the transcobalamin receptor was identified one year after the *LMBRD1* gene [42]. Children were eventually found to have mutations in the TCblR (*CD320*) gene. These cases were picked up on newborn screening with an elevation of MMA and are so far asymptomatic [90]. Incorporation of label from propionate and MeTHF are largely normal in these patients, explaining why this cohort was not identified before as a complementation group.

Other predicted metabolic steps in the pathway remain unaccounted for. It is not yet known by which mechanism cobalamin enters the mitochondria.

Also, it was originally thought that the gene underlying the *cblC* and *cblD* defects would encode reductases. The functional domains identified in the sequence of the *MMACHC* and *MMADHC* genes do not support a role as reductases for these proteins. Additional genes encoding reductases might therefore be discovered.

Exome sequencing

One major recent development in the field of genetics was the improvements in sequencing capabilities. It ultimately led to the possibility of sequencing every single coding exon of the genome for a few thousand dollars [321]. One application of exome sequencing that has changed the field of genetics is in the discovery of disease-causing genes [276]. Exome sequencing compares advantageously with whole genome scan and MMCT in terms of speed, cost and labor intensity for disorders with a small number of affected individuals. With the current technology, it would without a doubt be our first choice for the identification of the gene for the *cblF* disorder.

Protein science

Although there have been tremendous improvements in the accuracy of the gene function prediction algorithms based on sequence information, data is often scarce for newly identified genes. In order to understand gene function and relate it to the phenotype seen in patients, one needs to look at the gene product. Only then is it possible to address the localization, binding of partner proteins and substrates, and oligomeric form of a protein. Some of these questions can be answered in vivo, especially with the use of antibodies to target the gene product. Other questions require interrogating the isolated target protein. The success of protein purification is variable. In general, soluble proteins are more amenable to purification than membrane-associated protein. In our case, the soluble protein MMADHC was readily purified but only once it was associated with tag to increase its solubility. We also attempted the purification of the integral membrane protein LMBD1, but without success. Our experience was echoed by another group working independently. We hope that the challenges we faced in the purification of the protein LMBD1 will be overcome in the future.

Future directions

The next questions to be addressed in this project using the purified MMADHC protein will be assessing the binding with several forms of cobalamin, evaluating the dimerization potential of the protein, and confirming the binding parameters with MMACHC. Our group also aims to solve the three dimensional structure of MMACHC, MMADHC and the complex formed of MMACHC and MMACHC. We hope that these results will stimulate research for other teams and that these results will allow us to understand better the function of these proteins in both health and in disease.

The pool of MMADHC affinity-selected peptides obtained by phage display has been mapped against the sequence of the proposed partner MMACHC. An interesting aspect of the use of phage display is that the results can be used for more than one candidate gene. If future experiments detect an interaction with other proteins in the pathway, such as MMAB or MTR, the same pool of peptides can be used to predict the MMADHC-binding regions. Phage display thus is not restrained to the interaction between two given proteins. The answers obtained with this approach can be applied to any proven interactor.

Another project is the exome sequencing analysis on patients with elevation of homocysteine and/or MMA for which we have not been able to establish a diagnosis. We expect these patients to represent atypical phenotypic and biochemical profile for known disorders or to have mutations in genes not previously recognized as disease-causing. This approach combined with the increase in patients referred due to the spread of newborn screening tests across the world and better testing capacities in developing countries such as China and India is expected to lead to a steep increase in the rate of gene discovery. Along with the contribution from basic research, the future is promising for the better diagnosis and treatment of rare disorders, and for the application of research findings to common diseases.

LIST OF REFERENCES

1. Addison, T., *Anaemia-disease of the suprarenal capsules.* Med Gazette, 1849. **43**: p. 517-18.
2. Ehrlich, P., *Über regeneration und degeneration der rothen Blutschreiben bei Anäemien.* Berliner Klinische Wochenschrift, 1880. **117**: p. 405.
3. Cabot, R.C., *Pernicious Anemia (cryptogenic)*, in *A System of Medicine*, W.O.T. McCrae, Editor. 1908: Frowde, London. p. 612.
4. Russell, J.S.R., F.E. Batten, and J. Collier, *Subacute combined degeneration of the spinal cord.* Brain, 1900. **23**: p. 39-110.
5. Whipple, G.H., F.S. Robscheit, and C.W. Hooper, *Blood regeneration following simple anemia: IV. Influence of meat, liver and various extractives, alone or combined with standard diets.* Am J Physiol, 1920. **53**: p. 151-282.
6. Minot, G.R. and W.P. Murphy, *Treatment of pernicious anemia by a special diet.* Journal of the American Medical Association, 1926. **87**: p. 470-476.
7. Minot, G.R., E.J. Cohn, and W.P. Murphy, *Treatment of pernicious anemia with liver extract: effects upon the production of immature and mature red blood cells.* American Journal of the Medical Sciences, 1928. **175**(5): p. 599-621.
8. Castle, W.B., *Observations on the etiologic relationship of achylia gastrica to pernicious anemia: I. Effect of administration to patients with pernicious anemia of contents of normal human stomach recovered after the ingestion of beef muscle.* American Journal of the Medical Sciences, 1929. **178**(6): p. 748-763.
9. Castle, W.B. and W.C. Townsend, *Observations on the etiologic relationship of achylia gastrica to pernicious anemia: II. The effect of the administration to patients with pernicious anemia of beef muscle after*

incubation with normal human gastric juice. American Journal of the Medical Sciences, 1929. **178**(6): p. 764-776.

10. Mollin, D.L. and G.I. Ross, *Vitamin B_{12} deficiency in the megaloblastic anemias.* Proc R Soc Med, 1954. **47**(6): p. 428-31.
11. Glass, G.B., L.C. Lillick, and L.J. Boyd, *Metabolic interrelations between gastric intrinsic hematopoietic factor and vitamin B_{12}. II. Further assays of vitamin B_{12} in blood and urine of patients with pernicious anemia and following total gastrectomy by means of Escherichia coli mutant and Euglena gracilis technics.* Blood, 1954. **9**(12): p. 1127-40.
12. Markson, J.L., *Pernicious anaemia as an auto-immune disease and the significance of this.* Curr Med Drugs, 1963. **65**: p. 17-25.
13. Taylor, K.B., et al., *Autoimmune phenomena in pernicious anaemia: gastric antibodies.* Br Med J, 1962. **2**(5316): p. 1347-52.
14. Hoedemaeker, P.J., et al., *Investigations About the Site of Production of Castle's Gastric Intrinsic Factor.* Lab Invest, 1964. **13**: p. 1394-9.
15. Levine, S.A. and W.S. Ladd, *Pernicious anemia: a clinical study of one hundred and fifty consecutive cases with special reference to gastric acidity.* Johns Hopkins Hospital Bulletin, 1921. **32**: p. 254-266.
16. Edwards, L.J. and C.S. Constantinescu, *A prospective study of conditions associated with multiple sclerosis in a cohort of 658 consecutive outpatients attending a multiple sclerosis clinic.* Mult Scler, 2004. **10**(5): p. 575-81.
17. Arapakis, G., et al., *Diabetes mellitus and pernicious anaemia.* Br Med J, 1963. **1**(5324): p. 159-61.
18. Gräsbeck, R., K. Simons, and I. Sinkkonen, *Purification of intrinsic factor and vitamin B_{12} binders from human gastric juice.* Ann Med Exp Biol Fenn, 1962. **40(Suppl 6)**: p. 1-24.
19. Okuda, K., *Discovery of vitamin B_{12} in the liver and its absorption factor in the stomach: a historical review.* J Gastroenterol Hepatol, 1999. **14**(4): p. 301-8.

20. Hall, C.A. and A.E. Finkler, *In vivo plasma vitamin B12 binding in B12 deficient and nondeficient subjects.* J Lab Clin Med, 1962. **60**: p. 765-76.
21. Hall, C.A. and A.E. Finkler, *A Second Vitamin B12-Binding Substance in Human Plasma.* Biochim Biophys Acta, 1963. **78**: p. 234-6.
22. Schilling, R.F., *Intrinsic factor studies II. The effect of gastric juice on the urinary excretion of radioactivity after the oral administration of radioactive vitamin B12.* J Lab Clin Med, 1953. **42**(6): p. 860-6.
23. Gräsbeck, R., *[Familiar selective vitamin B_{12} malabsorption with proteinuria. A pernicious anemia-like syndrome.].* Nord Med, 1960. **63**: p. 322-3.
24. Imerslund, O., *Idiopathic chronic megaloblastic anemia in children.* Acta Paediatr Suppl, 1960. **49(Suppl 119)**: p. 1-115.
25. Seetharam, B., D.H. Alpers, and R.H. Allen, *Isolation and characterization of the ileal receptor for intrinsic factor-cobalamin.* J Biol Chem, 1981. **256**(8): p. 3785-90.
26. Tanner, S.M., et al., *Amnionless, essential for mouse gastrulation, is mutated in recessive hereditary megaloblastic anemia.* Nat Genet, 2003. **33**(3): p. 426-9.
27. Birn, H., et al., *Characterization of an epithelial approximately 460-kDa protein that facilitates endocytosis of intrinsic factor-vitamin B_{12} and binds receptor-associated protein.* J Biol Chem, 1997. **272**(42): p. 26497-504.
28. Rickes, E.L., et al., *Crystalline vitamin B_{12}.* Science (New York), 1948. **107**: p. 396-397.
29. Shorb, M.S., *Unidentified growth factors for Lactobacillus lactis in refined liver extracts.* J Biol Chem, 1947. **169**(2): p. 455.
30. Chaiet, L., C. Rosenblum, and D.T. Woodbury, *Biosynthesis of radioactive vitamin B12 containing cobalt 60.* Science, 1950. **111**(2892): p. 601-2.
31. Martens, J.H., et al., *Microbial production of vitamin B_{12}.* Appl Microbiol Biotechnol, 2002. **58**(3): p. 275-85.

32. Hodgkin, D.C., et al., *Structure of vitamin B_{12}.* Nature, 1956. **178**(4524): p. 64-6.
33. Hodgkin, D.G., et al., *The crystal structure of the hexacarboxylic acid derived from B_{12} and the molecular structure of the vitamin.* Nature, 1955. **176**(4477): p. 325-8.
34. Woodward, R.B., *The total synthesis of vitamin B_{12}.* Pure Appl Chem, 1973. **33**(1): p. 145-77.
35. Jansen, R., et al., *Cloning of full-length methylmalonyl-CoA mutase from a cDNA library using the polymerase chain reaction.* Genomics, 1989. **4**(2): p. 198-205.
36. Leclerc, D., et al., *Cloning and mapping of a cDNA for methionine synthase reductase, a flavoprotein defective in patients with homocystinuria.* Proc Natl Acad Sci U S A, 1998. **95**(6): p. 3059-64.
37. Gulati, S., et al., *Defects in human methionine synthase in cblG patients.* Hum Mol Genet, 1996. **5**(12): p. 1859-65.
38. Lerner-Ellis, J.P., et al., *Identification of the gene responsible for methylmalonic aciduria and homocystinuria, cblC type.* Nat Genet, 2006. **38**(1): p. 93-100.
39. Coelho, D., et al., *Gene identification for the cblD defect of vitamin B_{12} metabolism.* N Engl J Med, 2008. **358**(14): p. 1454-64.
40. Dobson, C.M., et al., *Identification of the gene responsible for the cblA complementation group of vitamin B_{12}-responsive methylmalonic acidemia based on analysis of prokaryotic gene arrangements.* Proc Natl Acad Sci U S A, 2002. **99**(24): p. 15554-9.
41. Dobson, C.M., et al., *Identification of the gene responsible for the cblB complementation group of vitamin B_{12}-dependent methylmalonic aciduria.* Hum Mol Genet, 2002. **11**(26): p. 3361-9.
42. Quadros, E.V., Y. Nakayama, and J.M. Sequeira, *The protein and the gene encoding the receptor for the cellular uptake of transcobalamin-bound cobalamin.* Blood, 2009. **113**(1): p. 186-92.

43. Swanson, D.A., et al., *Targeted disruption of the methionine synthase gene in mice.* Mol Cell Biol, 2001. **21**(4): p. 1058-65.
44. Deng, L., et al., *Methionine synthase reductase deficiency results in adverse reproductive outcomes and congenital heart defects in mice.* Mol Genet Metab, 2008. **94**(3): p. 336-42.
45. Peters, H., et al., *A knock-out mouse model for methylmalonic aciduria resulting in neonatal lethality.* J Biol Chem, 2003. **278**(52): p. 52909-13.
46. Smith, A.D. and H. Refsum, *Vitamin B_{12} and cognition in the elderly.* Am J Clin Nutr, 2009. **89**(2): p. 707S-11S.
47. Morris, M.C., et al., *Dietary folate and vitamin B_{12} intake and cognitive decline among community-dwelling older persons.* Arch Neurol, 2005. **62**(4): p. 641-5.
48. Quadros, E.V., Y. Nakayama, and J.M. Sequeira, *Targeted delivery of saporin toxin by monoclonal antibody to the transcobalamin receptor, TCblR/CD320.* Mol Cancer Ther, 2010. **9**(11): p. 3033-40.
49. Ruiz-Sanchez, P., et al., *Vitamin B_{12} as a carrier for targeted platinum delivery: in vitro cytotoxicity and mechanistic studies.* J Biol Inorg Chem, 2010.
50. Drennan, C.L., et al., *How a protein binds B_{12}: A 3.0 A X-ray structure of B_{12}-binding domains of methionine synthase.* Science, 1994. **266**(5191): p. 1669-74.
51. Marsh, E.N. and D.E. Holloway, *Cloning and sequencing of glutamate mutase component S from Clostridium tetanomorphum. Homologies with other cobalamin-dependent enzymes.* FEBS Lett, 1992. **310**(2): p. 167-70.
52. Watkins, D. and D.S. Rosenblatt, *Inborn errors of cobalamin absorption and metabolism.* Am J Med Genet C Semin Med Genet, 2011. **157**(1): p. 33-44.
53. Stich, T.A., et al., *Spectroscopic evidence for the formation of a four-coordinate Co2+ cobalamin species upon binding to the human*

ATP:cobalamin adenosyltransferase. J Am Chem Soc, 2005. **127**(21): p. 7660-1.

54. Ludwig, M.L. and R.G. Matthews, *Structure-based perspectives on B_{12}-dependent enzymes.* Annu Rev Biochem, 1997. **66**: p. 269-313.
55. Banerjee, R., C. Gherasim, and D. Padovani, *The tinker, tailor, soldier in intracellular B_{12} trafficking.* Curr Opin Chem Biol, 2009. **13**(4): p. 484-91.
56. Taga, M.E. and G.C. Walker, *Pseudo-B_{12} joins the cofactor family.* J Bacteriol, 2008. **190**(4): p. 1157-9.
57. Fedosov, S.N., et al., *Mechanisms of discrimination between cobalamins and their natural analogues during their binding to the specific B_{12}-transporting proteins.* Biochemistry, 2007. **46**(21): p. 6446-58.
58. Kadner, R.J. and G.L. Liggins, *Transport of vitamin B_{12} in Escherichia coli: genetic studies.* J Bacteriol, 1973. **115**(2): p. 514-21.
59. Fuller-Schaefer, C.A. and R.J. Kadner, *Multiple extracellular loops contribute to substrate binding and transport by the Escherichia coli cobalamin transporter BtuB.* J Bacteriol, 2005. **187**(5): p. 1732-9.
60. Gudmundsdottir, A., et al., *Point mutations in a conserved region (TonB box) of Escherichia coli outer membrane protein BtuB affect vitamin B_{12} transport.* J Bacteriol, 1989. **171**(12): p. 6526-33.
61. Locher, K.P., *Structure and mechanism of ABC transporters.* Curr Opin Struct Biol, 2004. **14**(4): p. 426-31.
62. Lewinson, O., et al., *A distinct mechanism for the ABC transporter BtuCD-BtuF revealed by the dynamics of complex formation.* Nat Struct Mol Biol, 2010. **17**(3): p. 332-8.
63. Yang, S.Y., P.S. Coleman, and B. Dupont, *The biochemical and genetic basis for the microheterogeneity of human R-type vitamin B_{12} binding proteins.* Blood, 1982. **59**(4): p. 747-55.
64. Andres, E., et al., *Food-cobalamin malabsorption in elderly patients: clinical manifestations and treatment.* Am J Med, 2005. **118**(10): p. 1154-9.

65. Carmel, R., *Malabsorption of food cobalamin.* Baillieres Clin Haematol, 1995. **8**(3): p. 639-55.
66. Yassin, F., et al., *Identification of a 4-base deletion in the gene in inherited intrinsic factor deficiency.* Blood, 2004. **103**(4): p. 1515-7.
67. Fyfe, J.C., et al., *The functional cobalamin (vitamin B_{12})-intrinsic factor receptor is a novel complex of cubilin and amnionless.* Blood, 2004. **103**(5): p. 1573-9.
68. Moestrup, S.K., et al., *Megalin-mediated endocytosis of transcobalamin-vitamin-B_{12} complexes suggests a role of the receptor in vitamin-B_{12} homeostasis.* Proc Natl Acad Sci U S A, 1996. **93**(16): p. 8612-7.
69. Strope, S., et al., *Mouse amnionless, which is required for primitive streak assembly, mediates cell-surface localization and endocytic function of cubilin on visceral endoderm and kidney proximal tubules.* Development, 2004. **131**(19): p. 4787-95.
70. Pedersen, G.A., et al., *AMN directs endocytosis of the intrinsic factor-vitamin B_{12} receptor cubam by engaging ARH or Dab2.* Traffic, 2010. **11**(5): p. 706-20.
71. Kalantry, S., et al., *The amnionless gene, essential for mouse gastrulation, encodes a visceral-endoderm-specific protein with an extracellular cysteine-rich domain.* Nat Genet, 2001. **27**(4): p. 412-6.
72. Czekay, R.P., et al., *The expression of megalin (gp330) and LRP diverges during F9 cell differentiation.* J Cell Sci, 1995. **108 (Pt 4)**: p. 1433-41.
73. Gburek, J., et al., *Megalin and cubilin are endocytic receptors involved in renal clearance of hemoglobin.* J Am Soc Nephrol, 2002. **13**(2): p. 423-30.
74. Gburek, J., et al., *Renal uptake of myoglobin is mediated by the endocytic receptors megalin and cubilin.* Am J Physiol Renal Physiol, 2003. **285**(3): p. F451-8.
75. Kozyraki, R., et al., *Megalin-dependent cubilin-mediated endocytosis is a major pathway for the apical uptake of transferrin in polarized epithelia.* Proc Natl Acad Sci U S A, 2001. **98**(22): p. 12491-6.

76. Cui, S., et al., *Megalin/gp330 mediates uptake of albumin in renal proximal tubule.* Am J Physiol, 1996. **271**(4 Pt 2): p. F900-7.
77. Orlando, R.A., et al., *Megalin is an endocytic receptor for insulin.* J Am Soc Nephrol, 1998. **9**(10): p. 1759-66.
78. Donnai, D. and M. Barrow, *Diaphragmatic hernia, exomphalos, absent corpus callosum, hypertelorism, myopia, and sensorineural deafness: a newly recognized autosomal recessive disorder?* Am J Med Genet, 1993. **47**(5): p. 679-82.
79. Beedholm-Ebsen, R., et al., *Identification of multidrug resistance protein 1 (MRP1/ABCC1) as a molecular gate for cellular export of cobalamin.* Blood, 2010. **115**(8): p. 1632-9.
80. Refsum, H., et al., *Holotranscobalamin and total transcobalamin in human plasma: determination, determinants, and reference values in healthy adults.* Clin Chem, 2006. **52**(1): p. 129-37.
81. Morkbak, A.L., S.S. Poulsen, and E. Nexo, *Haptocorrin in humans.* Clin Chem Lab Med, 2007. **45**(12): p. 1751-9.
82. Lindemans, J., et al., *The uptake of R-type cobalamin-binding protein by isolated rat liver cells.* Biochim Biophys Acta, 1982. **720**(2): p. 203-10.
83. Burger, R.L., et al., *Human plasma R-type vitamin B_{12}-binding proteins. II. The role of transcobalamin I, transcobalamin III, and the normal granulocyte vitamin B_{12}-binding protein in the plasma transport of vitamin B_{12}.* J Biol Chem, 1975. **250**(19): p. 7707-13.
84. Li, N., S. Seetharam, and B. Seetharam, *Genomic structure of human transcobalamin II: comparison to human intrinsic factor and transcobalamin I.* Biochem Biophys Res Commun, 1995. **208**(2): p. 756-64.
85. Nexo, B.A. and E. Nexo, *Structural homologies of cobalamin-binding proteins. Tryptic peptide mapping of intrinsic factor, transcobalamin and haptocorrin from man, hog and rabbit.* Biochim Biophys Acta, 1982. **708**(2): p. 178-84.

86. Nissen, P.H., et al., *Transcobalamin deficiency caused by compound heterozygosity for two novel mutations in the TCN2 gene: a study of two affected siblings, their brother, and their parents.* J Inherit Metab Dis.
87. Hakami, N., et al., *Neonatal megaloblastic anemia due to inherited transcobalamin II deficiency in two siblings.* N Engl J Med, 1971. **285**(21): p. 1163-70.
88. Hall, C.A. and J.A. Begley, *Congenital deficiency of human R-type binding proteins of cobalamin.* Am J Hum Genet, 1977. **29**(6): p. 619-26.
89. Carmel, R., J. Parker, and Z. Kelman, *Genomic mutations associated with mild and severe deficiencies of transcobalamin I (haptocorrin) that cause mildly and severely low serum cobalamin levels.* Br J Haematol, 2009. **147**(3): p. 386-91.
90. Anastasio, N., et al., *Mutations in TCblR, the gene for the transcobalamin receptor, result in decreased cellular uptake of vitamin B12 and methylmalonic aciduria.* 11th International Congress of Inborn Errors of Metabolism, Mol Genet Metab, 2010. **98**: p. 122 (Abstract 615).
91. Quadros, E.V., et al., *Positive newborn screen for methylmalonic aciduria identifies the first mutation in TCblR/CD320, the gene for cellular uptake of transcobalamin-bound vitamin B_{12}.* Hum Mutat, 2010. **31**(8): p. 924-9.
92. Leclerc, D., et al., *Human methionine synthase: cDNA cloning and identification of mutations in patients of the cblG complementation group of folate/cobalamin disorders.* Hum Mol Genet, 1996. **5**(12): p. 1867-74.
93. Van Tellingen, A., et al., *Long-term reduction of plasma homocysteine levels by super-flux dialyzers in hemodialysis patients.* Kidney Int, 2001. **59**(1): p. 342-7.
94. Quere, I., et al., *Spatial and temporal expression of the cystathionine beta-synthase gene during early human development.* Biochem Biophys Res Commun, 1999. **254**(1): p. 127-37.

95. Smulders, Y.M., et al., *Cellular folate vitamer distribution during and after correction of vitamin B_{12} deficiency: a case for the methylfolate trap.* Br J Haematol, 2006. **132**(5): p. 623-9.
96. McCully, K.S., *Vascular pathology of homocysteinemia: implications for the pathogenesis of arteriosclerosis.* Am J Pathol, 1969. **56**(1): p. 111-28.
97. McCully, K.S. and R.B. Wilson, *Homocysteine theory of arteriosclerosis.* Atherosclerosis, 1975. **22**(2): p. 215-27.
98. Humphrey, L.L., et al., *Homocysteine level and coronary heart disease incidence: a systematic review and meta-analysis.* Mayo Clin Proc, 2008. **83**(11): p. 1203-12.
99. Clarke, R., et al., *Hyperhomocysteinemia: an independent risk factor for vascular disease.* N Engl J Med, 1991. **324**(17): p. 1149-55.
100. Perry, I.J., et al., *Prospective study of serum total homocysteine concentration and risk of stroke in middle-aged British men.* Lancet, 1995. **346**(8987): p. 1395-8.
101. Nygard, O., et al., *Plasma homocysteine levels and mortality in patients with coronary artery disease.* N Engl J Med, 1997. **337**(4): p. 230-6.
102. Toole, J.F., et al., *Lowering homocysteine in patients with ischemic stroke to prevent recurrent stroke, myocardial infarction, and death: the Vitamin Intervention for Stroke Prevention (VISP) randomized controlled trial.* JAMA, 2004. **291**(5): p. 565-75.
103. Ebbing, M., et al., *Mortality and cardiovascular events in patients treated with homocysteine-lowering B vitamins after coronary angiography: a randomized controlled trial.* JAMA, 2008. **300**(7): p. 795-804.
104. Armitage, J.M., et al., *Effects of homocysteine-lowering with folic acid plus vitamin B_{12} vs placebo on mortality and major morbidity in myocardial infarction survivors: a randomized trial.* JAMA, 2010. **303**(24): p. 2486-94.
105. Albert, C.M., et al., *Effect of folic acid and B vitamins on risk of cardiovascular events and total mortality among women at high risk for*

cardiovascular disease: a randomized trial. JAMA, 2008. **299**(17): p. 2027-36.

106. Jamison, R.L., et al., *Effect of homocysteine lowering on mortality and vascular disease in advanced chronic kidney disease and end-stage renal disease: a randomized controlled trial.* JAMA, 2007. **298**(10): p. 1163-70.
107. Clarke, R., et al., *Effects of lowering homocysteine levels with B vitamins on cardiovascular disease, cancer, and cause-specific mortality: Meta-analysis of 8 randomized trials involving 37 485 individuals.* Arch Intern Med, 2010. **170**(18): p. 1622-31.
108. Miller, E.R., 3rd, et al., *Meta-analysis of folic acid supplementation trials on risk of cardiovascular disease and risk interaction with baseline homocysteine levels.* Am J Cardiol, 2010. **106**(4): p. 517-27.
109. Mei, W., et al., *Effect of homocysteine interventions on the risk of cardiocerebrovascular events: a meta-analysis of randomised controlled trials.* Int J Clin Pract, 2010. **64**(2): p. 208-15.
110. Smulders, Y.M. and H.J. Blom, *The homocysteine controversy.* J Inherit Metab Dis, 2010.
111. *Prevention of neural tube defects: results of the Medical Research Council Vitamin Study. MRC Vitamin Study Research Group.* Lancet, 1991. **338**(8760): p. 131-7.
112. Berry, R.J., et al., *Prevention of neural-tube defects with folic acid in China. China-U.S. Collaborative Project for Neural Tube Defect Prevention.* N Engl J Med, 1999. **341**(20): p. 1485-90.
113. CDC, *Spina bifida and anencephaly before and after folic acid mandate--United States, 1995-1996 and 1999-2000.* MMWR Morb Mortal Wkly Rep, 2004. **53**(17): p. 362-5.
114. De Wals, P., et al., *Spina bifida before and after folic acid fortification in Canada.* Birth Defects Res A Clin Mol Teratol, 2008. **82**(9): p. 622-6.

115. Williams, L.J., et al., *Decline in the prevalence of spina bifida and anencephaly by race/ethnicity: 1995-2002.* Pediatrics, 2005. **116**(3): p. 580-6.
116. Chen, B.H., et al., *NTD prevalences in central California before and after folic acid fortification.* Birth Defects Res A Clin Mol Teratol, 2008. **82**(8): p. 547-52.
117. Safdar, O.Y., et al., *Decline in the incidence of neural tube defects after the national fortification of flour (1997-2005).* Saudi Med J, 2007. **28**(8): p. 1227-9.
118. Alasfoor, D., M.K. Elsayed, and A.J. Mohammed, *Spina bifida and birth outcome before and after fortification of flour with iron and folic acid in Oman.* East Mediterr Health J, 2010. **16**(5): p. 533-8.
119. CDC, *Racial/ethnic differences in the birth prevalence of spina bifida - United States, 1995-2005.* MMWR Morb Mortal Wkly Rep, 2009. **57**(53): p. 1409-13.
120. Pangilinan, F., et al., *Transcobalamin II receptor polymorphisms are associated with increased risk for neural tube defects.* J Med Genet, 2010. **47**(10): p. 677-85.
121. Brody, L.C., et al., *A polymorphism, R653Q, in the trifunctional enzyme methylenetetrahydrofolate dehydrogenase/methenyltetrahydrofolate cyclohydrolase/formyltetrahydrofolate synthetase is a maternal genetic risk factor for neural tube defects: report of the Birth Defects Research Group.* Am J Hum Genet, 2002. **71**(5): p. 1207-15.
122. Harisha, P.N., et al., *Impact of 5,10-methylenetetrahydrofolate reductase gene polymorphism on neural tube defects.* J Neurosurg Pediatr, 2010. **6**(4): p. 364-7.
123. Houcher, B., et al., *Polymorphisms of 5,10-methylenetetrahydrofolate reductase and cystathionine beta-synthase genes as a risk factor for neural tube defects in Setif, Algeria.* Pediatr Neurosurg, 2009. **45**(6): p. 472-7.

124. Lucock, M., et al., *Altered folate metabolism and disposition in mothers affected by a spina bifida pregnancy: influence of 677c --> t methylenetetrahydrofolate reductase and 2756a --> g methionine synthase genotypes.* Mol Genet Metab, 2000. **70**(1): p. 27-44.
125. Blom, H.J., et al., *Neural tube defects and folate: case far from closed.* Nat Rev Neurosci, 2006. **7**(9): p. 724-31.
126. Okano, M., et al., *DNA methyltransferases Dnmt3a and Dnmt3b are essential for de novo methylation and mammalian development.* Cell, 1999. **99**(3): p. 247-57.
127. Wilson, A., et al., *A common variant in methionine synthase reductase combined with low cobalamin (vitamin B12) increases risk for spina bifida.* Mol Genet Metab, 1999. **67**(4): p. 317-23.
128. Gueant-Rodriguez, R.M., et al., *Transcobalamin and methionine synthase reductase mutated polymorphisms aggravate the risk of neural tube defects in humans.* Neurosci Lett, 2003. **344**(3): p. 189-92.
129. Brouns, R., et al., *Polymorphisms in genes related to folate and cobalamin metabolism and the associations with complex birth defects.* Prenat Diagn, 2008. **28**(6): p. 485-93.
130. van der Linden, I.J., et al., *The methionine synthase reductase 66A>G polymorphism is a maternal risk factor for spina bifida.* J Mol Med, 2006. **84**(12): p. 1047-54.
131. Gos, M., E. Sliwerska, and A. Szpecht-Potocka, *Mutation incidence in folate metabolism genes and regulatory genes in Polish families with neural tube defects.* J Appl Genet, 2004. **45**(3): p. 363-8.
132. Hobbs, C.A., et al., *Maternal folate-related gene environment interactions and congenital heart defects.* Obstet Gynecol, 2010. **116**(2 Pt 1): p. 316-22.
133. Candito, M., et al., *Nutritional and genetic determinants of vitamin B and homocysteine metabolisms in neural tube defects: a multicenter case-control study.* Am J Med Genet A, 2008. **146A**(9): p. 1128-33.

134. Relton, C.L., et al., *Low erythrocyte folate status and polymorphic variation in folate-related genes are associated with risk of neural tube defect pregnancy.* Mol Genet Metab, 2004. **81**(4): p. 273-81.
135. Rosenquist, T.H., S.A. Ratashak, and J. Selhub, *Homocysteine induces congenital defects of the heart and neural tube: effect of folic acid.* Proc Natl Acad Sci U S A, 1996. **93**(26): p. 15227-32.
136. Bennett, G.D., et al., *Failure of homocysteine to induce neural tube defects in a mouse model.* Birth Defects Res B Dev Reprod Toxicol, 2006. **77**(2): p. 89-94.
137. Molloy, A.M., et al., *Maternal vitamin B_{12} status and risk of neural tube defects in a population with high neural tube defect prevalence and no folic acid fortification.* Pediatrics, 2009. **123**(3): p. 917-23.
138. Ray, J.G., et al., *Vitamin B_{12} and the risk of neural tube defects in a folic-acid-fortified population.* Epidemiology, 2007. **18**(3): p. 362-6.
139. Thompson, M.D., D.E. Cole, and J.G. Ray, *Vitamin B_{12} and neural tube defects: the Canadian experience.* Am J Clin Nutr, 2009. **89**(2): p. 697S-701S.
140. Zhang, T., et al., *Maternal serum vitamin B_{12}, folate and homocysteine and the risk of neural tube defects in the offspring in a high-risk area of China.* Public Health Nutr, 2009. **12**(5): p. 680-6.
141. Gaber, K.R., et al., *Maternal vitamin B_{12} and the risk of fetal neural tube defects in Egyptian patients.* Clin Lab, 2007. **53**(1-2): p. 69-75.
142. Mills, J.L., et al., *Maternal vitamin levels during pregnancies producing infants with neural tube defects.* J Pediatr, 1992. **120**(6): p. 863-71.
143. Ceyhan, S.T., et al., *Serum vitamin B_{12} and homocysteine levels in pregnant women with neural tube defect.* Gynecol Endocrinol, 2010. **26**(8): p. 578-81.
144. Wild, J., et al., *Investigation of factors influencing folate status in women who have had a neural tube defect-affected infant.* Br J Obstet Gynaecol, 1993. **100**(6): p. 546-9.

145. van der Put, N.M., et al., *Altered folate and vitamin B12 metabolism in families with spina bifida offspring.* QJM, 1997. **90**(8): p. 505-10.
146. Ray, J.G. and H.J. Blom, *Vitamin B12 insufficiency and the risk of fetal neural tube defects.* QJM, 2003. **96**(4): p. 289-95.
147. Franke, B., et al., *An association study of 45 folate-related genes in spina bifida: Involvement of cubilin (CUBN) and tRNA aspartic acid methyltransferase 1 (TRDMT1).* Birth Defects Res A Clin Mol Teratol, 2009. **85**(3): p. 216-26.
148. Afman, L.A., et al., *Single nucleotide polymorphisms in the transcobalamin gene: relationship with transcobalamin concentrations and risk for neural tube defects.* Eur J Hum Genet, 2002. **10**(7): p. 433-8.
149. Swanson, D.A., et al., *Evaluation of transcobalamin II polymorphisms as neural tube defect risk factors in an Irish population.* Birth Defects Res A Clin Mol Teratol, 2005. **73**(4): p. 239-44.
150. Pietrzyk, J.J. and M. Bik-Multanowski, *776C>G polymorphism of the transcobalamin II gene as a risk factor for spina bifida.* Mol Genet Metab, 2003. **80**(3): p. 364.
151. Zhu, H., et al., *Homocysteine remethylation enzyme polymorphisms and increased risks for neural tube defects.* Mol Genet Metab, 2003. **78**(3): p. 216-21.
152. Pietrzyk, J.J., et al., *Polymorphisms of the 5,10-methylenetetrahydrofolate and the methionine synthase reductase genes as independent risk factors for spina bifida.* J Appl Genet, 2003. **44**(1): p. 111-3.
153. O'Leary, V.B., et al., *Analysis of methionine synthase reductase polymorphisms for neural tube defects risk association.* Mol Genet Metab, 2005. **85**(3): p. 220-7.
154. Li, D., et al., *Maternal methylenetetrahydrofolate reductase deficiency and low dietary folate lead to adverse reproductive outcomes and congenital heart defects in mice.* Am J Clin Nutr, 2005. **82**(1): p. 188-95.

155. Zhu, H., et al., *Cardiovascular abnormalities in Folr1 knockout mice and folate rescue.* Birth Defects Res A Clin Mol Teratol, 2007. **79**(4): p. 257-68.
156. Profitlich, L.E., et al., *High prevalence of structural heart disease in children with cblC-type methylmalonic aciduria and homocystinuria.* Mol Genet Metab, 2009. **98**(4): p. 344-8.
157. Rutsch, F., et al., *Identification of a putative lysosomal cobalamin exporter altered in the cblF defect of vitamin B_{12} metabolism.* Nat Genet, 2009. **41**(2): p. 234-9.
158. Scanlon, K.S., et al., *Preconceptional folate intake and malformations of the cardiac outflow tract. Baltimore-Washington Infant Study Group.* Epidemiology, 1998. **9**(1): p. 95-8.
159. Botto, L.D., et al., *Trends of selected malformations in relation to folic acid recommendations and fortification: an international assessment.* Birth Defects Res A Clin Mol Teratol, 2006. **76**(10): p. 693-705.
160. Shaw, G.M., et al., *Periconceptional nutrient intakes and risks of conotruncal heart defects.* Birth Defects Res A Clin Mol Teratol, 2010. **88**(3): p. 144-51.
161. Boot, M.J., et al., *Cardiac outflow tract malformations in chick embryos exposed to homocysteine.* Cardiovasc Res, 2004. **64**(2): p. 365-73.
162. Han, M., et al., *Folate rescues lithium-, homocysteine- and Wnt3A-induced vertebrate cardiac anomalies.* Dis Model Mech, 2009. **2**(9-10): p. 467-78.
163. Chan, J., et al., *Low dietary choline and low dietary riboflavin during pregnancy influence reproductive outcomes and heart development in mice.* Am J Clin Nutr, 2010. **91**(4): p. 1035-43.
164. Dionisi-Vici, C., et al., *Inborn errors of metabolism in the Italian pediatric population: a national retrospective survey.* J Pediatr, 2002. **140**(3): p. 321-7.

165. Klose, D.A., et al., *Incidence and short-term outcome of children with symptomatic presentation of organic acid and fatty acid oxidation disorders in Germany.* Pediatrics, 2002. **110**(6): p. 1204-11.
166. Horster, F. and G.F. Hoffmann, *Pathophysiology, diagnosis, and treatment of methylmalonic aciduria-recent advances and new challenges.* Pediatr Nephrol, 2004. **19**(10): p. 1071-4.
167. Deodato, F., et al., *Methylmalonic and propionic aciduria.* Am J Med Genet C Semin Med Genet, 2006. **142C**(2): p. 104-12.
168. Halenz, D.R. and M.D. Lane, *Net synthesis of methylmalonyl-CoA by ADP-, ATP-, and Mg-independent transcarboxylation catalyzed by propionyl carboxylase.* Biochem Biophys Res Commun, 1961. **5**: p. 27-9.
169. Chandler, R.J., et al., *Propionyl-CoA and adenosylcobalamin metabolism in Caenorhabditis elegans: evidence for a role of methylmalonyl-CoA epimerase in intermediary metabolism.* Mol Genet Metab, 2006. **89**(1-2): p. 64-73.
170. Bikker, H., et al., *A homozygous nonsense mutation in the methylmalonyl-CoA epimerase gene (MCEE) results in mild methylmalonic aciduria.* Hum Mutat, 2006. **27**(7): p. 640-643.
171. Gradinger, A.B., et al., *Atypical methylmalonic aciduria: frequency of mutations in the methylmalonyl CoA epimerase gene (MCEE).* Hum Mutat, 2007. **28**(10): p. 1045.
172. Dobson, C.M., et al., *Homozygous nonsense mutation in the MCEE gene and siRNA suppression of methylmalonyl-CoA epimerase expression: A novel cause of mild methylmalonic aciduria.* Mol Genet Metab, 2006.
173. Ostergaard, E., et al., *Deficiency of the alpha subunit of succinate-coenzyme A ligase causes fatal infantile lactic acidosis with mitochondrial DNA depletion.* Am J Hum Genet, 2007. **81**(2): p. 383-7.
174. Ostergaard, E., et al., *A novel missense mutation in SUCLG1 associated with mitochondrial DNA depletion, encephalomyopathic form, with methylmalonic aciduria.* Eur J Pediatr, 2010. **169**(2): p. 201-5.

175. Carrozzo, R., et al., *SUCLA2 mutations are associated with mild methylmalonic aciduria, Leigh-like encephalomyopathy, dystonia and deafness.* Brain, 2007.
176. Ostergaard, E., et al., *Mitochondrial encephalomyopathy with elevated methylmalonic acid is caused by SUCLA2 mutations.* Brain, 2007.
177. Brown, G.K., et al., *Malonyl coenzyme A decarboxylase deficiency.* J Inherit Metab Dis, 1984. **7**(1): p. 21-6.
178. Gregg, A.R., et al., *Combined malonic and methylmalonic aciduria with normal malonyl-coenzyme A decarboxylase activity: a case supporting multiple aetiologies.* J Inherit Metab Dis, 1998. **21**(4): p. 382-90.
179. Dionisi-Vici, C., et al., *'Classical' organic acidurias, propionic aciduria, methylmalonic aciduria and isovaleric aciduria: long-term outcome and effects of expanded newborn screening using tandem mass spectrometry.* J Inherit Metab Dis, 2006. **29**(2-3): p. 383-9.
180. Heidenreich, R., et al., *Acute extrapyramidal syndrome in methylmalonic acidemia: "metabolic stroke" involving the globus pallidus.* J Pediatr, 1988. **113**(6): p. 1022-7.
181. Harting, I., et al., *Looking beyond the basal ganglia: the spectrum of MRI changes in methylmalonic acidaemia.* J Inherit Metab Dis, 2008. **31**(3): p. 368-78.
182. Larnaout, A., et al., *Methylmalonic acidaemia with bilateral globus pallidus involvement: a neuropathological study.* J Inherit Metab Dis, 1998. **21**(6): p. 639-44.
183. Roodhooft, A.M., et al., *Symmetrical necrosis of the basal ganglia in methylmalonic acidaemia.* Eur J Pediatr, 1990. **149**(8): p. 582-4.
184. Matsui, S.M., M.J. Mahoney, and L.E. Rosenberg, *The natural history of the inherited methylmalonic acidemias.* N Engl J Med, 1983. **308**(15): p. 857-61.

185. Horster, F., et al., *Long-term outcome in methylmalonic acidurias is influenced by the underlying defect (mut0, mut-, cblA, cblB).* Pediatr Res, 2007. **62**(2): p. 225-30.
186. Rutledge, S.L., et al., *Tubulointerstitial nephritis in methylmalonic acidemia.* Pediatr Nephrol, 1993. **7**(1): p. 81-2.
187. Srinivas, K.V., et al., *Methylmalonic acidemia with renal involvement: a case report and review of literature.* Saudi J Kidney Dis Transpl, 2001. **12**(1): p. 49-53.
188. Lubrano, R., et al., *Kidney transplantation in a girl with methylmalonic acidemia and end stage renal failure.* Pediatr Nephrol, 2001. **16**(11): p. 848-51.
189. Coman, D., et al., *Renal transplantation in a 14-year-old girl with vitamin B_{12}-responsive cblA-type methylmalonic acidaemia.* Pediatr Nephrol, 2006. **21**(2): p. 270-3.
190. Cosson, M.A., et al., *Long-term outcome in methylmalonic aciduria: a series of 30 French patients.* Mol Genet Metab, 2009. **97**(3): p. 172-8.
191. Brusque, A.M., et al., *Inhibition of the mitochondrial respiratory chain complex activities in rat cerebral cortex by methylmalonic acid.* Neurochem Int, 2002. **40**(7): p. 593-601.
192. Calabresi, P., et al., *Inhibition of mitochondrial complex II induces a long-term potentiation of NMDA-mediated synaptic excitation in the striatum requiring endogenous dopamine.* J Neurosci, 2001. **21**(14): p. 5110-20.
193. Chandler, R.J., et al., *Mitochondrial dysfunction in mut methylmalonic acidemia.* FASEB J, 2009. **23**(4): p. 1252-61.
194. Okun, J.G., et al., *Neurodegeneration in methylmalonic aciduria involves inhibition of complex II and the tricarboxylic acid cycle, and synergistically acting excitotoxicity.* J Biol Chem, 2002. **277**(17): p. 14674-80.
195. Coude, F.X., L. Sweetman, and W.L. Nyhan, *Inhibition by propionyl-coenzyme A of N-acetylglutamate synthetase in rat liver mitochondria. A*

possible explanation for hyperammonemia in propionic and methylmalonic acidemia. J Clin Invest, 1979. **64**(6): p. 1544-51.

196. Bremer, J., *Pyruvate dehydrogenase, substrate specificity and product inhibition.* Eur J Biochem, 1969. **8**(4): p. 535-40.
197. Gregersen, N., *The specific inhibition of the pyruvate dehydrogenase complex from pig kidney by propionyl-CoA and isovaleryl-Co-A.* Biochem Med, 1981. **26**(1): p. 20-7.
198. Brock, M. and W. Buckel, *On the mechanism of action of the antifungal agent propionate.* Eur J Biochem, 2004. **271**(15): p. 3227-41.
199. Schwab, M.A., et al., *Secondary mitochondrial dysfunction in propionic aciduria: a pathogenic role for endogenous mitochondrial toxins.* Biochem J, 2006. **398**(1): p. 107-12.
200. Cheema-Dhadli, S., C.C. Leznoff, and M.L. Halperin, *Effect of 2-methylcitrate on citrate metabolism: implications for the management of patients with propionic acidemia and methylmalonic aciduria.* Pediatr Res, 1975. **9**(12): p. 905-8.
201. Dimmock, D., et al., *Quantitative evaluation of the mitochondrial DNA depletion syndrome.* Clin Chem, 2010. **56**(7): p. 1119-27.
202. Yano, S., et al., *Infantile mitochondrial DNA depletion syndrome associated with methylmalonic aciduria and 3-methylcrotonyl-CoA and propionyl-CoA carboxylase deficiencies in two unrelated patients: a new phenotype of mtDNA depletion syndrome.* J Inherit Metab Dis, 2003. **26**(5): p. 481-8.
203. Chakrapani, A., et al., *Metabolic stroke in methylmalonic acidemia five years after liver transplantation.* J Pediatr, 2002. **140**(2): p. 261-3.
204. McLaughlin, B.A., et al., *Methylmalonate toxicity in primary neuronal cultures.* Neuroscience, 1998. **86**(1): p. 279-90.
205. Kolker, S., et al., *Pathomechanisms of neurodegeneration in glutaryl-CoA dehydrogenase deficiency.* Ann Neurol, 2004. **55**(1): p. 7-12.

206. Kolker, S., et al., *NMDA receptor activation and respiratory chain complex V inhibition contribute to neurodegeneration in d-2-hydroxyglutaric aciduria.* Eur J Neurosci, 2002. **16**(1): p. 21-8.
207. de Baulny, H.O., et al., *Methylmalonic and propionic acidaemias: management and outcome.* J Inherit Metab Dis, 2005. **28**(3): p. 415-23.
208. Watson, M.S., et al., *Newborn screening: toward a uniform screening panel and system.* Genet Med, 2006. **8 Suppl 1**: p. 1S-252S.
209. Zwickler, T., et al., *Diagnostic work-up and management of patients with isolated methylmalonic acidurias in European metabolic centres.* J Inherit Metab Dis, 2008. **31**(3): p. 361-7.
210. Kasahara, M., et al., *Current role of liver transplantation for methylmalonic acidemia: a review of the literature.* Pediatr Transplant, 2006. **10**(8): p. 943-7.
211. Morioka, D., et al., *Efficacy of living donor liver transplantation for patients with methylmalonic acidemia.* Am J Transplant, 2007. **7**(12): p. 2782-7.
212. Chandler, R.J., et al., *Adenoviral-mediated correction of methylmalonyl-CoA mutase deficiency in murine fibroblasts and human hepatocytes.* BMC Med Genet, 2007. **8**: p. 24.
213. Chandler, R.J. and C.P. Venditti, *Adenovirus-mediated gene delivery rescues a neonatal lethal murine model of mut(0) methylmalonic acidemia.* Hum Gene Ther, 2008. **19**(1): p. 53-60.
214. Chang, C.C., et al., *Towards metabolic sink therapy for mut methylmalonic acidaemia: retrovirus-mediated transfer of the human methylmalonyl-CoA mutase cDNA into peripheral blood progenitor cells of a child with mut methylmalonic acidaemia.* J Inherit Metab Dis, 1999. **22**(8): p. 951-2.
215. Chandler, R.J. and C.P. Venditti, *Long-term rescue of a lethal murine model of methylmalonic acidemia using adeno-associated viral gene therapy.* Mol Ther, 2010. **18**(1): p. 11-6.

216. Hoffman, R.M. and R.W. Erbe, *High in vivo rates of methionine biosynthesis in transformed human and malignant rat cells auxotrophic for methionine.* Proc Natl Acad Sci U S A, 1976. **73**(5): p. 1523-7.
217. Willard, H.F., et al., *Rapid prenatal and postnatal detection of inborn errors of propionate, methylmalonate, and cobalamin metabolism: a sensitive assay using cultured cells.* Hum Genet, 1976. **34**(3): p. 277-83.
218. Silagi, S., G. Darlington, and S.A. Bruce, *Hybridization of two biochemically marked human cell lines.* Proc Natl Acad Sci U S A, 1969. **62**(4): p. 1085-92.
219. Siniscalco, M., et al., *Evidence for intergenic complementation in hybrid cells derived from two human diploid strains each carrying an X-linked mutation.* Proc Natl Acad Sci U S A, 1969. **62**(3): p. 793-9.
220. Watkins, D. and D.S. Rosenblatt, *Genetic heterogeneity among patients with methylcobalamin deficiency. Definition of two complementation groups, cblE and cblG.* J Clin Invest, 1988. **81**(6): p. 1690-4.
221. Drummond, J.T., et al., *Assignment of enzymatic function to specific protein regions of cobalamin-dependent methionine synthase from Escherichia coli.* Biochemistry, 1993. **32**(36): p. 9290-5.
222. Dayal, S., et al., *Cerebral vascular dysfunction in methionine synthase-deficient mice.* Circulation, 2005. **112**(5): p. 737-44.
223. Foster, M.A., M.J. Dilworth, and D.D. Woods, *Cobalamin and the Synthesis of Methionine by Escherichia Coli.* Nature, 1964. **201**: p. 39-42.
224. Kerwar, S.S., et al., *Interrelationship of adenosyl methionine and methyl-B12 in the biosynthesis of methionine.* Arch Biochem Biophys, 1966. **116**(1): p. 305-18.
225. Homolova, K., et al., *The deep intronic c.903+469T>C mutation in the MTRR gene creates an SF2/ASF binding exonic splicing enhancer, which leads to pseudoexon activation and causes the cblE type of homocystinuria.* Hum Mutat, 2010. **31**(4): p. 437-44.

226. Lerner-Ellis, J.P., et al., *Mutation and biochemical analysis of patients belonging to the cblB complementation class of vitamin B_{12}-dependent methylmalonic aciduria.* Mol Genet Metab, 2006. **87**(3): p. 219-25.
227. Schubert, H.L. and C.P. Hill, *Structure of ATP-bound human ATP:cobalamin adenosyltransferase.* Biochemistry, 2006. **45**(51): p. 15188-96.
228. Kathiresan, S., et al., *Common variants at 30 loci contribute to polygenic dyslipidemia.* Nat Genet, 2009. **41**(1): p. 56-65.
229. Waterworth, D.M., et al., *Genetic variants influencing circulating lipid levels and risk of coronary artery disease.* Arterioscler Thromb Vasc Biol, 2010. **30**(11): p. 2264-76.
230. Willer, C.J., et al., *Newly identified loci that influence lipid concentrations and risk of coronary artery disease.* Nat Genet, 2008. **40**(2): p. 161-9.
231. Fogarty, M.P., et al., *Allelic expression imbalance at high-density lipoprotein cholesterol locus MMAB-MVK.* Hum Mol Genet, 2010. **19**(10): p. 1921-9.
232. Lerner-Ellis, J.P., et al., *Mutations in the MMAA gene in patients with the cblA disorder of vitamin B_{12} metabolism.* Hum Mutat, 2004. **24**(6): p. 509-16.
233. Padovani, D., T. Labunska, and R. Banerjee, *Energetics of interaction between the G-protein chaperone, MeaB, and B_{12}-dependent methylmalonyl-CoA mutase.* J Biol Chem, 2006. **281**(26): p. 17838-44.
234. Froese, D.S., et al., *Structures of the human GTPase MMAA and vitamin B_{12}-dependent methylmalonyl-CoA mutase and insight into their complex formation.* J Biol Chem, 2010. **285**(49): p. 38204-13.
235. Takahashi-Iniguez, T., et al., *Protection and reactivation of human methylmalonyl-CoA mutase by MMAA protein.* Biochem Biophys Res Commun, 2010.

236. Padovani, D. and R. Banerjee, *A G-protein editor gates coenzyme B_{12} loading and is corrupted in methylmalonic aciduria.* Proc Natl Acad Sci U S A, 2009. **106**(51): p. 21567-72.
237. Willard, H.F. and L.E. Rosenberg, *Inherited methylmalonyl CoA mutase apoenzyme deficiency in human fibroblasts: evidence for allelic heterogeneity, genetic compounds, and codominant expression.* J Clin Invest, 1980. **65**(3): p. 690-8.
238. Marsh, E.N., S.E. Harding, and P.F. Leadlay, *Subunit interactions in Propionibacterium shermanii methylmalonyl-CoA mutase studied by analytical ultracentrifugation.* Biochem J, 1989. **260**(2): p. 353-8.
239. Mancia, F., et al., *How coenzyme B_{12} radicals are generated: the crystal structure of methylmalonyl-coenzyme A mutase at 2 A resolution.* Structure, 1996. **4**(3): p. 339-50.
240. Shih, V.E., et al., *Defective lysosomal release of vitamin B_{12} (cblF): a hereditary cobalamin metabolic disorder associated with sudden death.* Am J Med Genet, 1989. **33**(4): p. 555-63.
241. Rosenblatt, D.S., et al., *New disorder of vitamin B_{12} metabolism (cobalamin F) presenting as methylmalonic aciduria.* Pediatrics, 1986. **78**(1): p. 51-4.
242. Youngdahl-Turner, P., L.E. Rosenberg, and R.H. Allen, *Binding and uptake of transcobalamin II by human fibroblasts.* J Clin Invest, 1978. **61**(1): p. 133-41.
243. Youngdahl-Turner, P., et al., *Protein mediated vitamin uptake. Adsorptive endocytosis of the transcobalamin II-cobalamin complex by cultured human fibroblasts.* Exp Cell Res, 1979. **118**(1): p. 127-34.
244. Vassiliadis, A., et al., *Lysosomal cobalamin accumulation in fibroblasts from a patient with an inborn error of cobalamin metabolism (cblF complementation group): visualization by electron microscope radioautography.* Exp Cell Res, 1991. **195**(2): p. 295-302.

245. Rosenblatt, D.S., et al., *Defect in vitamin B_{12} release from lysosomes: newly described inborn error of vitamin B_{12} metabolism.* Science, 1985. **228**(4705): p. 1319-21.
246. Rosenblatt, D.S., et al., *Clinical heterogeneity and prognosis in combined methylmalonic aciduria and homocystinuria (cblC).* J Inherit Metab Dis, 1997. **20**(4): p. 528-38.
247. Russo, P., et al., *A congenital anomaly of vitamin B_{12} metabolism: a study of three cases.* Hum Pathol, 1992. **23**(5): p. 504-12.
248. Sharma, A.P., et al., *Hemolytic uremic syndrome (HUS) secondary to cobalamin C (cblC) disorder.* Pediatr Nephrol, 2007. **22**(12): p. 2097-103.
249. Roge Canales, M., et al., *[Neonatal hemolytic-uremic syndrome associated with methylmalonic aciduria and homocystinuria].* An Esp Pediatr, 1996. **45**(1): p. 97-8.
250. Kind, T., et al., *Cobalamin C disease presenting as hemolytic-uremic syndrome in the neonatal period.* J Pediatr Hematol Oncol, 2002. **24**(4): p. 327-9.
251. Guigonis, V., et al., *Late-onset thrombocytic microangiopathy caused by cblC disease: association with a factor H mutation.* Am J Kidney Dis, 2005. **45**(3): p. 588-95.
252. Geraghty, M.T., et al., *Cobalamin C defect associated with hemolytic-uremic syndrome.* J Pediatr, 1992. **120**(6): p. 934-7.
253. Chenel, C., et al., *[Neonatal hemolytic-uremic syndrome, methylmalonic aciduria and homocystinuria caused by intracellular vitamin B_{12} deficiency. Value of etiological diagnosis].* Arch Fr Pediatr, 1993. **50**(9): p. 749-54.
254. Cerone, R., et al., *[Neonatal hemolytic and uremic syndrome, methylmalonic aciduria and homocystinuria due to intracellular vitamin B_{12} deficiency].* Arch Pediatr, 1994. **1**(8): p. 762-3.
255. Bouts, A.H., et al., *CD46-associated atypical hemolytic uremic syndrome with uncommon course caused by cblC deficiency.* Pediatr Nephrol, 2010. **25**(12): p. 2547-8.

256. Gerth, C., et al., *Ocular phenotype in patients with methylmalonic aciduria and homocystinuria, cobalamin C type.* J AAPOS, 2008. **12**(6): p. 591-6.
257. Robb, R.M., et al., *Retinal degeneration in vitamin B12 disorder associated with methylmalonic aciduria and sulfur amino acid abnormalities.* Am J Ophthalmol, 1984. **97**(6): p. 691-6.
258. Traboulsi, E.I., et al., *Ocular histopathologic characteristics of cobalamin C type vitamin B12 defect with methylmalonic aciduria and homocystinuria.* Am J Ophthalmol, 1992. **113**(3): p. 269-80.
259. Ben-Omran, T.I., et al., *Late-onset cobalamin-C disorder: a challenging diagnosis.* Am J Med Genet A, 2007. **143A**(9): p. 979-84.
260. Carmel, R., et al., *Update on cobalamin, folate, and homocysteine.* Hematology (Am Soc Hematol Educ Program), 2003: p. 62-81.
261. Schuh, S., et al., *Homocystinuria and megaloblastic anemia responsive to vitamin B_{12} therapy. An inborn error of metabolism due to a defect in cobalamin metabolism.* N Engl J Med, 1984. **310**(11): p. 686-90.
262. Andersson, H.C. and E. Shapira, *Biochemical and clinical response to hydroxocobalamin versus cyanocobalamin treatment in patients with methylmalonic acidemia and homocystinuria (cblC).* J Pediatr, 1998. **132**(1): p. 121-4.
263. Lerner-Ellis, J.P., et al., *Spectrum of mutations in MMACHC, allelic expression, and evidence for genotype-phenotype correlations.* Hum Mutat, 2009. **30**(7): p. 1072-81.
264. Liu, M.Y., et al., *Mutation spectrum of MMACHC in Chinese patients with combined methylmalonic aciduria and homocystinuria.* J Hum Genet, 2010. **55**(9): p. 621-6.
265. Nogueira, C., et al., *Spectrum of MMACHC mutations in Italian and Portuguese patients with combined methylmalonic aciduria and homocystinuria, cblC type.* Mol Genet Metab, 2008. **93**(4): p. 475-80.

266. Morel, C.F., J.P. Lerner-Ellis, and D.S. Rosenblatt, *Combined methylmalonic aciduria and homocystinuria (cblC): Phenotype-genotype correlations and ethnic-specific observations.* Mol Genet Metab, 2006.
267. Kim, J., et al., *A human vitamin B12 trafficking protein uses glutathione transferase activity for processing alkylcobalamins.* J Biol Chem, 2009. **284**(48): p. 33418-24.
268. Kim, J., C. Gherasim, and R. Banerjee, *Decyanation of vitamin B_{12} by a trafficking chaperone.* Proc Natl Acad Sci U S A, 2008. **105**(38): p. 14551-4.
269. Hannibal, L., et al., *Processing of alkylcobalamins in mammalian cells: A role for the MMACHC (cblC) gene product.* Mol Genet Metab, 2009. **97**(4): p. 260-6.
270. Plesa, M., et al., *Interaction between MMACHC and MMADHC, two human proteins participating in intracellular vitamin B_{12} metabolism.* Mol Genet Metab, 2010.
271. Suormala, T., et al., *The cblD defect causes either isolated or combined deficiency of methylcobalamin and adenosylcobalamin synthesis.* J Biol Chem, 2004. **279**(41): p. 42742-9.
272. Miousse, I.R., et al., *Clinical and molecular heterogeneity in patients with the cblD inborn error of cobalamin metabolism.* J Pediatr, 2009. **154**(4): p. 551-6.
273. Ren, X.Q., et al., *Function of the ABC signature sequences in the human multidrug resistance protein 1.* Mol Pharmacol, 2004. **65**(6): p. 1536-42.
274. Monaco, A.P., et al., *Isolation of candidate cDNAs for portions of the Duchenne muscular dystrophy gene.* Nature, 1986. **323**(6089): p. 646-50.
275. Atkinson, J.L., *Genetic Mapping of Cobalamin C Deficiency: Linkage to Chromosome 1p32-34*. 2003, Univ. of Toronto: Toronto.
276. Ng, S.B., et al., *Exome sequencing identifies the cause of a mendelian disorder.* Nat Genet, 2010. **42**(1): p. 30-5.

277. Sanford, J.A. and E. Stubblefield, *General protocol for microcell-mediated chromosome transfer.* Somat Cell Mol Genet, 1987. **13**(3): p. 279-84.
278. Cuthbert, A.P., et al., *Construction and characterization of a highly stable human: rodent monochromosomal hybrid panel for genetic complementation and genome mapping studies.* Cytogenet Cell Genet, 1995. **71**(1): p. 68-76.
279. Dowdy, S.F., et al., *Irradiation microcell-mediated chromosome transfer (XMMCT): the generation of specific chromosomal arm deletions.* Genes Chromosomes Cancer, 1990. **2**(4): p. 318-27.
280. Doherty, A.M. and E.M. Fisher, *Microcell-mediated chromosome transfer (MMCT): small cells with huge potential.* Mamm Genome, 2003. **14**(9): p. 583-92.
281. Meaburn, K.J., C.N. Parris, and J.M. Bridger, *The manipulation of chromosomes by mankind: the uses of microcell-mediated chromosome transfer.* Chromosoma, 2005. **114**(4): p. 263-74.
282. Hsu, J.M. and B. Kawin, *Metabolic fate of 60Co-labeled cyanocobalamin in tryptophan-deficient rats.* J Nutr, 1966. **88**(1): p. 33-8.
283. Sidhu, S.S., et al., *Phage display for selection of novel binding peptides.* Methods Enzymol, 2000. **328**: p. 333-63.
284. Fuh, G. and S.S. Sidhu, *Efficient phage display of polypeptides fused to the carboxy-terminus of the M13 gene-3 minor coat protein.* FEBS Lett, 2000. **480**(2-3): p. 231-4.
285. Carter, D.M., et al., *Phage display reveals multiple contact sites between FhuA, an outer membrane receptor of Escherichia coli, and TonB.* J Mol Biol, 2006. **357**(1): p. 236-51.
286. James, K.J., et al., *TonB interacts with BtuF, the Escherichia coli periplasmic binding protein for cyanocobalamin.* Biochemistry, 2009. **48**(39): p. 9212-20.

287. Abram, C.L., et al., *The adaptor protein fish associates with members of the ADAMs family and localizes to podosomes of Src-transformed cells.* J Biol Chem, 2003. **278**(19): p. 16844-51.
288. Barker, T.H., et al., *SPARC regulates extracellular matrix organization through its modulation of integrin-linked kinase activity.* J Biol Chem, 2005. **280**(43): p. 36483-93.
289. Behrens, M., J.W. Margolis, and F.L. Margolis, *Identification of members of the Bex gene family as olfactory marker protein (OMP) binding partners.* J Neurochem, 2003. **86**(5): p. 1289-96.
290. Mohrluder, J., et al., *Identification of clathrin heavy chain as a direct interaction partner for the gamma-aminobutyric acid type A receptor associated protein.* Biochemistry, 2007. **46**(50): p. 14537-43.
291. Fields, S. and O. Song, *A novel genetic system to detect protein-protein interactions.* Nature, 1989. **340**(6230): p. 245-6.
292. Pollard-Knight, D., et al., *Immunoassays and nucleic acid detection with a biosensor based on surface plasmon resonance.* Ann Biol Clin (Paris), 1990. **48**(9): p. 642-6.
293. Lopez, F., et al., *Improved sensitivity of biomolecular interaction analysis mass spectrometry for the identification of interacting molecules.* Proteomics, 2003. **3**(4): p. 402-12.
294. Natsume, T., et al., *Combination of biomolecular interaction analysis and mass spectrometric amino acid sequencing.* Anal Chem, 2000. **72**(17): p. 4193-8.
295. Pierce, M.M., C.S. Raman, and B.T. Nall, *Isothermal titration calorimetry of protein-protein interactions.* Methods, 1999. **19**(2): p. 213-21.
296. Scharf, B.E., *Summary of useful methods for two-component system research.* Curr Opin Microbiol, 2010. **13**(2): p. 246-52.
297. Saftig, P. and J. Klumperman, *Lysosome biogenesis and lysosomal membrane proteins: trafficking meets function.* Nat Rev Mol Cell Biol, 2009. **10**(9): p. 623-35.

298. Compton, T., *An immortalized human fibroblast cell line is permissive for human cytomegalovirus infection.* J Virol, 1993. **67**(6): p. 3644-8.
299. Peters, D.M., et al., *Human papilloma virus E6/E7 genes can expand the lifespan of human corneal fibroblasts.* In Vitro Cell Dev Biol Anim, 1996. **32**(5): p. 279-84.
300. Zhu, Z., et al., *SURF1, encoding a factor involved in the biogenesis of cytochrome c oxidase, is mutated in Leigh syndrome.* Nat Genet, 1998. **20**(4): p. 337-43.
301. Lowry, O.H., et al., *Protein measurement with the Folin phenol reagent.* J Biol Chem, 1951. **193**(1): p. 265-75.
302. Kruglyak, L., M.J. Daly, and E.S. Lander, *Rapid multipoint linkage analysis of recessive traits in nuclear families, including homozygosity mapping.* Am J Hum Genet, 1995. **56**(2): p. 519-27.
303. Eskelinen, E.L., Y. Tanaka, and P. Saftig, *At the acidic edge: emerging functions for lysosomal membrane proteins.* Trends Cell Biol, 2003. **13**(3): p. 137-45.
304. Gailus, S., et al., *A novel mutation in LMBRD1 causes the cblF defect of vitamin B_{12} metabolism in a Turkish patient.* J Inherit Metab Dis, 2010. **33**(1): p. 17-24.
305. Rozen, S. and H.J. Skaletsky, *Primer3 on the WWW for general users and for biologist programmers*, in *Bioinformatics Methods and Protocols: Methods in Molecular Biology*, M.S. Krawetz S, Editor. 2000, Humana Press: Totowa, NJ. p. 365-386.
306. Wong, L.T.K., et al., *Diagnosis and treatment of a child with cblF disease.* Clin Invest Med, 1992. **15**: p. A111.
307. Waggoner, D.J., et al., *Methylmalonic aciduria (cblF): case report and response to therapy.* Am J Med Genet, 1998. **79**(5): p. 373-5.
308. MacDonald, M.R., et al., *Clinical heterogeneity in two patients with cblF disease.* Am J Hum Genet, 1992. **51**: p. A353.

309. Miousse, I.R., D. Watkins, and D.S. Rosenblatt, *Novel splice site mutations and a large deletion in three patients with the cblF inborn error of vitamin B_{12} metabolism.* Mol Genet Metab, 2011. **102**(4): p. 505-7.
310. Li, Y., et al., *Resequencing of 200 human exomes identifies an excess of low-frequency non-synonymous coding variants.* Nat Genet, 2010. **42**(11): p. 969-72.
311. Jacobsen, D.W., et al., *Rapid analysis of cobalamin coenzymes and related corrinoid analogs by high-performance liquid chromatography.* Anal Biochem, 1982. **120**(2): p. 394-403.
312. Rosenblatt, D.S., et al., *Altered vitamin B_{12} metabolism in fibroblasts from a patient with megaloblastic anemia and homocysteinuria due to a new defect in methionine biosynthesis.* J Clin Invest, 1984. **74**: p. 2149-2156.
313. Cooper, B.A., D.S. Rosenblatt, and D. Watkins, *Methylmalonic aciduria due to a new defect in adenosylcobalamin accumulation by cells.* American Journal of Hematology, 1990. **34**: p. 115-120.
314. Yu, C.S., et al., *Prediction of protein subcellular localization.* Proteins, 2006. **64**(3): p. 643-51.
315. Mandava, S., et al., *RELIC--a bioinformatics server for combinatorial peptide analysis and identification of protein-ligand interaction sites.* Proteomics, 2004. **4**(5): p. 1439-60.
316. Kozak, M., *Point mutations define a sequence flanking the AUG initiator codon that modulates translation by eukaryotic ribosomes.* Cell, 1986. **44**(2): p. 283-92.
317. Kozak, M., *Constraints on reinitiation of translation in mammals.* Nucleic Acids Res, 2001. **29**(24): p. 5226-32.
318. Packham, G., M. Brimmell, and J.L. Cleveland, *Mammalian cells express two differently localized Bag-1 isoforms generated by alternative translation initiation.* Biochem J, 1997. **328 (Pt 3)**: p. 807-13.

319. Vagner, S., et al., *Alternative translation of human fibroblast growth factor 2 mRNA occurs by internal entry of ribosomes.* Mol Cell Biol, 1995. **15**(1): p. 35-44.
320. Pagliarini, D.J., et al., *A mitochondrial protein compendium elucidates complex I disease biology.* Cell, 2008. **134**(1): p. 112-23.
321. Ng, S.B., et al., *Targeted capture and massively parallel sequencing of 12 human exomes.* Nature, 2009. **461**(7261): p. 272-6.

APPENDIX I : LIST OF *cblF* PATIENTS

Table legend:

Complex congenital heart defect in patient WG3265:

Right dominant atrioventricular septal defect with common atrium and double outlet right ventricle, transposition of the great vessels, hypoplastic left ventricle and common atriventricular valve.

SGA: small for gestational age

FTT: failure to thrive

IUGR: Intrauterine growth retardation

SIDS: sudden infant death syndrome

Patient	Origin	Sex	Age at presentation	Age at diagnosis	Symptoms	Clinical Course	B_{12}	DNA change
1 WG3265	Hispanic	M		3 weeks	SGA, tracheoesophageal fistula, complex congenital heart defect, left pes equinovarus, abnormal newborn screening	Short stature, died after cardiac surgery (Glenn procedure) at 9 months of age		515_516delAC/515_516delAC
2 MM	Netherland	F		2 months	FTT, anemia, neutropenia, septic shock	Mild developmental delay, special education at 14 years of age		1056delG/1056delG
3 WG1908	Native Indian-Carrier nation	F	6 months	8 months	FTT, developmental delay, hypotonia, recurrent infections, megaloblastic anemia	18 years of age, Asymptomatic after B12 therapy	116 pmol/L Schilling <1%	1056delG/1056delG
4 WG2432	Caucasian	F	4 weeks	4 months	Stomatitis, feeding difficulties, FTT, muscular apical VSD	Asymptomatic after B12 therapy Weight = 10th percentile and height < 1st percentile at 14 yo	221 pg/ml	1056delG/1056delG
5 WG1087 WG1173	French Canadian	F	48 h	3 weeks	Stomatitis, glossitis, seizures, hypotonia, developmental delay, feeding difficulties, dextrocardia, bifid incisors	Short stature, otherwise asymptomatic at 27 years of age	Schilling <1%	1056delG/1056delG
6 SJL	Germany	F		4 weeks	IUGR, SGA, fetal distress, ASD, patent ductus arteriosus, right ventricular hypertrophy	Death at 10 months of age after heart surgery for ASD		1056delG/1056delG
7 WG1903	Caucasian	M	11 years	11 years	Recurrent stomatitis, skin rashes, skin hyperpigmentation, arthritis, developmental delay, pancytopenia, encephalopathy, megaloblastic anemia, small thrombus in deep femoral vein	Impaired coordination, poor attention span, weakness in lower extremities, does well in school	20 pg/ml Schilling <0.2%	1056delG/1056delG
8 WG1350	El Salvador	F	18 days	44 days	SGA, FTT, developmental delay, hypotonia, stomatitis, intermittent fever, skin rashes, megaloblastic anemia, osteopenia	Feeding problems, SIDS at 5 months of age	250 pg/ml, 184pmol/L	1056delG/1056delG

9 DME	Germany	M		3 weeks	IUGR, SGA, glossitis, feeding difficulties, FTT, tooth abnormalities, anemia, abnormal newborn screening	Short stature, hepatomegaly on therapy	Decreased B12, Schilling abnormal	404delC/1056delG
10 WG1959	Caucasian	M	18 days	13 months	Aspiration pneumonia at birth, poor feeding, lethargy, hypotonia, hepatomegaly, temporary cholestasis, neutropenia, thrombocytopenia	Mild developmental delay, height below the 5th percentile at 4 years of age	318 pg/ml	842_845delAGAG/1056delG
11 WG3365	Germany/Sweden/Britain	M	3.5 months	10 months	Severe gastritis, FTT	Speech delay, pegged teeth	2100pg/ml	1056delG/916-1G>T
12 WG3377	Caucasian	M	NBS	1 month	Asymptomatic, abnormal newborn screening	Initial developmental delay, appropriate for age at 5 years of age		712_713delAC/1056delG
13	Turkish	M		8 days	SGA, microcephaly, cerebral seizures due to intraventricular hemorrhage, microcytic hypochromic anemia	Psychomotor development 3 SD < avg at 26 mo, weight and head circ. < 3rd percentile	118ng/L	1405delG/1405delG
14 WG4008	Caucasian	F	NBS		Asymptomatic, newborn screening	Asymptomatic after B12 therapy		1339-1G>T/1056delG
15 WG4042	Caucasian	F	NBS		Feeding difficulties, ridged metopic suture with trigonocephaly, asymmetric and cup shaped ears, micro/retrognathia, high arched palate, left torticollis, and upslanting palpebral fissures, systolic murmur, VSD	Mild general hypotonia and slight delay in fine and gross motor milestones	148 pg/ml	70-4298_246+2311del6785/1056delG

APPENDIX II : LIST OF *cblD* PATIENTS

Table legend:

IQ: Intellectual quotient

NBS: Newborn screen

M: Months

MCV: Mean corpuscular volume

RSV: Respiratory syncitial virus

Wk: Weeks

Y: Years

Patient	Sex	Origin	Age at presentation	Presentation	Outcome	Mutations
WG1437 (MMA)	M	Haitian	NBS	Vomiting and poor feeding followed by ketoacidotic coma, dehydration, hyperammonemia, leucopenia, thrombocytopenia	Can crawl and stand at 1 yo but does not walk	c.160C>T/307_324dup p.Arg54X/Leu103_Ser108 dup
WG3280 (MMA)	M	Arab	6 y	Poor feeding, lethargy in the newborn period, admitted for infection, cultures negative, seizure, acidosis. Respiratory tract infections, flu like illness with vomiting, anorexia and acidosis. Further episode of vomiting and lethargy at 6 yo	Appropriate milestones	c.60insAT/455dupC p.Leu21fsX1/Thr152fsX10
(MMA)	M	Indian	8 mo	Preterm birth at 32 wk of gestation, grade II respiratory distress syndrome, necrotizing enterocolitis, neonatal convulsions	Attends special school for mild learning problems at 12 yo	c.57_64delCTCTTTAG/57_64delCTCTTTAG p.Cys19fsX1/Cys19fsX1
WG1071 WG2022 (MMA+HCY)	M	Spanish-American	14 y	Acute psychotic episode, moderate mental retardation (IQ50), marfanoid appearance, horizontal nystagmus increased by lateral gaze, slightly hyperactive deep tendon reflexes, impaired finger to nose movement, increased MCV	Good mental and physical health, IQ remains low	c.748C>T/748C>T p.Arg250X/ Arg250X
WG2025 (MMA+HCY)	M	Spanish-American	2.5 y	Asymptomatic sibling picked up on testing	Asymptomatic	c.748C>T/748C>T p.Arg250X/ Arg250X
WG3583 (MMA+HCY)	F	Mexican	4 mo	RSV bronchiolitis with secondary bacterial pneumonia, right hip dysplasia and poor weight	Mild developmental delay at 2 yo	c.683C>G/683C>G p.Ser228X/Ser228X

				gain at 3 mo. At 4 mo, concerns of developmental delay because of hypotonia and poor head control, megaloblastic anemia		
(MMA+HCY)	F	Scandinavian	3 mo	Developmental delay, seizures, megaloblastic anemia		c.419dupA/419dupA p.Tyr140X/Tyr140X
(MMA+HCY)	M	Italian	22 days	Poor feeding, encephalopathy, seizures, increased mean corpuscular volume, reduced myelination, small cerebral vermis	Normal gross and fine motor skills, speech delay and low IQ at 4 y	c.696+1_4delGTGA/696+1_4delGTGA p.Phe204_Ala232del/Phe204_Ala232del
WG3745 (HCY)	F	Mexican	4 mo	Respiratory distress (RSV pneumonia), altered mental status, developmental delay, progressive 4-ventricle nonobstructive hydrocephalus, hair loss, nearly obstructive vena cava clot	No clinical improvement, patient died	c.737A>G/737A>G p.Asp246Gly/Asp246Gly
(HCY)	M	Irish	6 y	Global developmental delay, spastic ataxia, gait problems, delayed visual evoked potentials, increased mean corpuscular volume	16 yo, severely mentally retarded, nearly normal gait, speak single words, erratic behavior, hyperactivity and aggression	c.776T>C/776T>C p.Leu259Pro/Leu259Pro
(HCY)	M	Italian	3 mo	Hypotonia, nystagmus, dystonia, seizures, megaloblastic anemia		c.545C>A/746A>C p.Thr182Asn/Tyr249Cys
WG4035 (HCY)	F	East Indian	6 y	Developmental delay, autistic features, mental retardation		c.746A>G/746A>G p.Tyr249Cys/Tyr249Cys

APPENDIX III: REPRINTS

nature genetics

Identification of a putative lysosomal cobalamin exporter altered in the cblF defect of vitamin B_{12} metabolism

Frank Rutsch[1], Susann Gailus[1], Isabelle R Miousse[2], Terttu Suormala[3], Corinne Sagné[4], Mohammad Reza Toliat[5], Gudrun Nürnberg[5], Tanja Wittkampf[1], Insa Buers[6], Azita Sharifi[4], Martin Stucki[7,8], Christian Becker[5], Matthias Baumgartner[7], Horst Robenek[6], Thorsten Marquardt[1], Wolfgang Höhne[9], Bruno Gasnier[4], David S Rosenblatt[2], Brian Fowler[3] & Peter Nürnberg[5,10]

Vitamin B_{12} (cobalamin) is essential in animals for metabolism of branched chain amino acids and odd chain fatty acids, and for remethylation of homocysteine to methionine[1]. In the cblF inborn error of vitamin B_{12} metabolism, free vitamin accumulates in lysosomes, thus hindering its conversion to cofactors[2,3]. Using homozygosity mapping in 12 unrelated cblF individuals and microcell-mediated chromosome transfer, we identified a candidate gene on chromosome 6q13, *LMBRD1*, encoding LMBD1, a lysosomal membrane protein with homology to lipocalin membrane receptor LIMR. We identified five different frameshift mutations in *LMBRD1* resulting in loss of LMBD1 function, with 18 of the 24 disease chromosomes carrying the same mutation embedded in a common 1.34-Mb haplotype. Transfection of fibroblasts of individuals with cblF with wild-type LMBD1 rescued cobalamin coenzyme synthesis and function. This work identifies *LMBRD1* as the gene underlying the cblF defect of cobalamin metabolism and suggests that LMBD1 is a lysosomal membrane exporter for cobalamin.

To date, eight distinct defects of the intracellular cobalamin pathway have been defined by somatic cell complementation analysis: cblA, cblB, cblC, cblD, cblE, cblF, cblG and mut (Supplementary Fig. 1 online)[4]. Depending on their localization within the pathway, these complementation defects can cause either isolated hyperhomocysteinemia (cblD-homocystinuria, cblE and cblG), isolated methylmalonic aciduria (cblA, cblB, cblD-methylmalonic aciduria and mut) or both (cblC, combined cblD and cblF). Although the functions of some of the responsible proteins are not known, all of the genes underlying these defects have been identified except for the gene underlying cblF (MIM277380)[4]. Among the 12 unrelated children (6 males, 6 females) with the cblF disorder present in our cohort, clinical presentation was variable (Supplementary Table 1 online). Frequent findings included being small for gestational age, poor feeding, failure to thrive, developmental delay and persistent stomatitis. Two individuals had minor facial abnormalities, including pegged teeth and bifid incisors (individuals P5 and P11), and four had congenital heart defects (P1, P4, P5 and P6). Macrocytic anemia, neutropenia, thrombocytopenia and pancytopenia were observed frequently. Affected individuals were identified by elevated homocysteine and methylmalonic acid concentrations in blood or urine samples, and in some cases (P1, P9 and P12), increased propionylcarnitine concentrations detected by newborn screening initiated the diagnostic workup. Cobalamin absorption and serum cobalamin concentrations were decreased in some individuals (P3, P5, P7 and P9). The diagnosis of the cblF defect was established by fibroblast studies as described, including complementation analysis[5].

Whereas some affected individuals showed retarded growth and a mild developmental delay under parenteral hydroxocobalamin therapy, others became completely asymptomatic during the course of treatment. One individual died suddenly despite apparent clinical response to therapy (P8), and two died after cardiac surgery (P1 and P6).

There are several examples of founder mutations that are prevalent in individuals with an autosomal recessive disorder who originate from Europe[6–8]. Thus, a high rate of homozygous individuals may be observed even though consanguineous marriages are uncommon among Europeans. This prompted us to carry out a high-resolution genome scan to identify homozygous regions shared by individuals

[1]Department of General Pediatrics, Münster University Children's Hospital, Albert-Schweitzer-Strasse 33, D-48149 Münster, Germany. [2]Department of Human Genetics, Division of Medical Genetics/McGill University, McGill University Health Centre, Room N5-13, Ghosert Biology Building, 1205 Dr. Penfield Avenue, Montreal, Quebec H3A 1B1, Canada. [3]Metabolic Unit, University Children's Hospital, Römergasse 8, CH-4058 Basel, Switzerland. [4]Institut de Biologie Physico-Chimique, Centre National de la Recherche Scientifique - UPR 1929, Université Paris Descartes, 13 rue Pierre et Marie Curie, F-75005 Paris, France. [5]Cologne Center for Genomics and Institute for Genetics, Zülpicher Strasse 47, D-50674 Cologne, Germany. [6]Leibniz Institute for Arteriosclerosis Research, Münster University, Domagkstrasse 3, D-48149 Münster, Germany. [7]Division of Metabolism and Molecular Pediatrics, University Children's Hospital, Steinwiesstrasse 75, CH-8032 Zürich, Switzerland. [8]Zürich Center for Integrative Human Physiology (ZIHP), University of Zürich, Winterthurerstrasse 190, CH-8057 Zürich, Switzerland. [9]Institute of Biochemistry, Charité University Medicine, Monbijoustrasse 2, D-10117 Berlin, Germany. [10]Cologne Excellence Cluster on Cellular Stress Responses in Aging-associated Diseases (CECAD), University of Cologne, Zülpicher Strasse 47, D-50674 Cologne, Germany. Correspondence should be addressed to F.R. (rutschf@medizin.uni-muenster.de).

Received 13 August 2008; accepted 9 October 2008; published online 11 January 2009; doi:10.1038/ng.294

with chIF with the hope of finding the underlying disease-causing gene in one of these regions. We used the Affymetrix GeneChip Human Mapping 250K Sty Array and the program Merlin with the recently implemented linkage disequilibrium (LD) modeling option to avoid inflated lod scores[9]. We assigned arbitrarily second-cousin parents to all individuals of unknown consanguinity and carried out linkage analysis under the assumption of locus heterogeneity (HLOD calculation). We have used this approach successfully in previous mapping

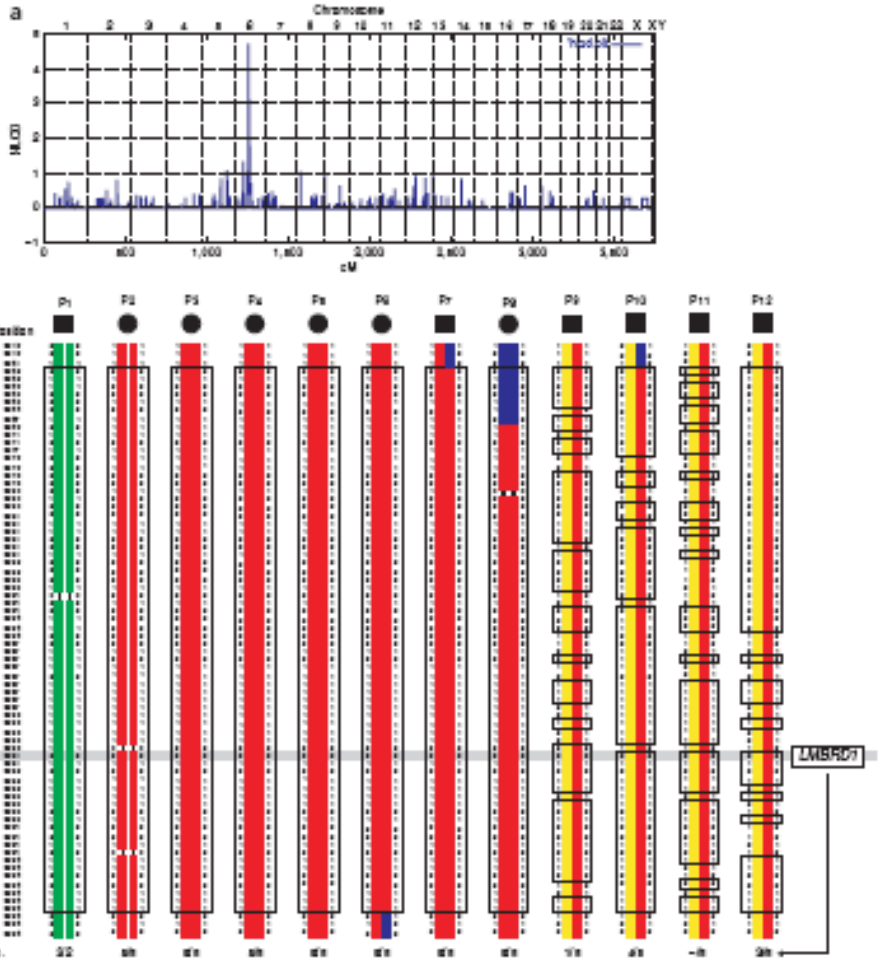

Figure 1 Mapping of a locus for chIF on chromosome 6q13. (a) Multipoint linkage analysis of the genome-wide scan using the Affymetrix GeneChip Human Mapping 250K Sty Array. The scan included all 12 affected individuals and 1 unaffected sibling. Scores are plotted over genetic distance across the genome, where chromosomes are concatenated from p-ter to q-ter from left to right. Under the assumption of locus heterogeneity (HLOD calculation), the highest scores were obtained for chromosome 6 markers with a maximum HLOD score of 4.7 at 83.65 cM according to the decode map. (b) Haplotype analyses of the 12 individuals with chIF for SNP markers within the linked region on chromosome 6q13. Different haplotypes are highlighted by different colors. The haplotype shown in red is present on 18 of a total of 24 disease chromosomes, suggesting a common founder mutation. Recombinations in individuals P6 and P7 define the distal and proximal borders, respectively, of a critical interval of 1.6.2 Mb (boxed). Individual P8, although homozygous throughout the whole region, has different alleles in the proximal part of her haplotype, revealing a further recombination and thereby reducing the critical interval to 1.3.4 Mb. This interval harbors *LMBRD1*, the position of which is highlighted by gray shading. Five different mutations were identified in this gene. The distribution of the different mutations (bottom line) is in accordance with the haplotype composition of the affected individuals. Yellow color indicates different haplotypes. Boxed haplotype segments of the compound heterozygous individuals P9–P12 indicate homozygous SNP alleles which are identical with the red haplotype. Mutation numbers refer to **Figure 3b**, **Supplementary Table 1** and **Supplementary Figure 3**.

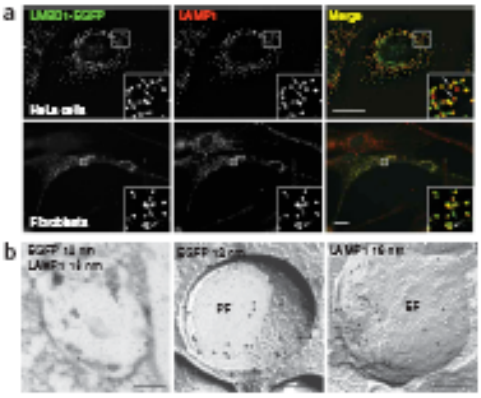

Figure 2 Colocalization of LMBD1 with the lysosomal membrane marker LAMP1. (**a**) Immunofluorescence analysis. LMBD1-EGFP (left column) transiently expressed in HeLa cells (upper row) or in human primary fibroblasts (lower row) colocalizes extensively with the endogenous late endosomal and lysosomal marker LAMP1 (middle column). Merged images of LMBD1-EGFP (green) and LAMP1 (red) distributions are shown on the right. Data were acquired by epifluorescence (lower lane) or deconvolution fluorescence microscopy (upper lane and insets). Insets are magnification of the indicated squares. Scale bars, 20 µm. (**b**) Immunogold double labeling. Simultaneous immunogold labeling for EGFP (12 nm, encircled) and LAMP1 (18 nm) in cryosections of lysosomes of transfected fibroblasts examined by electron microscopy shows prominent labeling at the surfaces of lysosomes (left panel), consistent with the immunofluorescence results. In freeze-fracture replica immunolabeling (middle and right panels), both fracture faces of the lysosomal membranes are labeled (fracture face of half-membrane leaflet adjacent to the cytoplasm is the P-face (PF); fracture face of half-membrane leaflet adjacent to the lysosomal matrix is the E-face (EF)). LMBD1-EGFP is detected exclusively on the PF (middle panel), and LAMP1 exclusively on the EF (right panel) of the lysosomal membranes. Scale bars, 0.2 µm.

projects in which a high proportion of consanguineous families was assumed but not proven a priori[10,11]. For cblF, this kind of linkage analysis yielded a single maximum HLOD score of 4.7 for the region 6q12–13 (Fig. 1a).

As a second strategy to identify the underlying gene defect, we carried out microcell-mediated chromosome transfer (Supplementary Methods online). For this, mouse-human hybrid fibroblasts carrying a single human chromosome tagged with a hygromycin resistance gene[12] were micronucleated with demecolchicine. Micronuclei were harvested by centrifugation, filtered and fused to PV014 cells. The resulting clones were selected with hygromycin to measure [^{14}C]propionate incorporation and to test for correction of the biochemical phenotype[13]. Fusion with normal human chromosomes 2, 4, 5, 7, 10 or 16 and immortalized fibroblasts of a subject with cblF (derived from individual P12) produced resistant clones that did not rescue the low incorporation of label from propionate. Transfer of chromosome 6 yielded 11 hygromycin-resistant clones (Supplementary Table 2 online), of which 8 corrected the incorporation of label from propionate (Supplementary Fig. 2 online).

According to the haplotype data from affected individuals with extended homozygosity, the interval on chromosome 6 is delimited by the SNP markers SNP_A-4269716 and SNP_A-4290582 and comprises 1.62 Mb of genomic DNA (Fig. 1b). The proximal border could be shifted further toward the telomere to SNP_A-2062606, as indicated by the partially different haplotype of individual P8, thereby reducing the critical interval to 1.34 Mb. Only four affected individuals (P9–P12) did not show a homozygous segment in this narrow interval, suggesting either compound heterozygosity or locus heterogeneity (Fig. 1b). Among the three genes annotated in this region on chromosome 6q13, we considered *LMBRD1* as the most promising positional candidate gene (Fig. 1b) because its gene product, LMBD1, was known to be a membrane protein expressed in the liver[14].

Direct genomic sequencing of the 16 coding exons and flanking intronic regions of *LMBRD1* identified homozygous and compound heterozygous deletion mutations in the *LMBRD1* gene in all affected individuals. Mutations were confirmed by Pyrosequencing. Five different mutations accounted for 22 of the 24 mutant alleles (Fig. 1b, Supplementary Table 1 and Supplementary Fig. 3 online); these were not present in 348 control chromosomes. By sequencing the mutated exons in all available family members, we confirmed that the mutations cosegregated with the disease trait (Supplementary Fig. 4 online). The 1056delG allele leading to a frameshift and premature termination codon in exon 11 was present on 18 of the 24 disease chromosomes, suggesting a common founder of European ancestry. We estimate that this mutation must have occurred at least eight to nine generations ago[9]. This single-base-pair deletion was also present on one allele of the four compound heterozygous individuals. In one of these individuals (P11), the second mutation was not detected. However, in a fibroblast cell line derived from this individual, significant downregulation of the *LMBRD1* transcript was evident, as in fibroblasts from individuals carrying mutations on both alleles (Supplementary Fig. 5 online). In our cohort of individuals with cblF, who all carried truncating *LMBRD1* mutations, no obvious genotype-phenotype correlation was observed. Instead, among individuals carrying the common 1056delG mutation on both alleles, a marked phenotypic variability was evident, including early death in infancy (P8) and asymptomatic long-term survival (P5).

LMBD1 is a protein of 61.4 kDa consisting of 540 amino acids. To examine the intracellular localization of LMBD1, we transiently expressed a construct tagged with EGFP at its C terminus (LMBD1-EGFP) in HeLa cells and human primary fibroblasts and examined its distribution by deconvolution fluorescence microscopy. In both cell types, LMBD1-EGFP showed a punctate distribution throughout the cytoplasm and the perinuclear region, which colocalized extensively with the late endosomal and lysosomal marker LAMP1 (Fig. 2a). Some puncta had a ring-shaped appearance, suggesting localization at the limiting membrane of lysosomes and late endosomes. We confirmed lysosomal membrane localization by cryothin-section electron microscopy and immunogold-labeling (Fig. 2b, left panel). To further characterize the localization of the C-terminally labeled LMBD1 construct within the lysosomal membrane, we carried out freeze-fracture replica immunolabeling. Where the fracture follows the outermost membrane of the lysosome to give a concave fracture, the outer phospholipid monolayer is seen (Fig. 2b, middle panel); convex fractures give mirror-image views (Fig. 2b, right panel). The LAMP1 label was seen exclusively on the endosomal leaflet (E-face) of the lysosomal membrane (Fig. 2b, right panel); no label was seen on the cytoplasmic leaflet (P-face). In contrast, the EGFP label was found exclusively on the P-face of the lysosomal membrane (Fig. 2b, middle panel), corresponding to a localization of the C terminus of LMBD1 at the cytoplasmic leaflet. No label with either antibody was apparent on the lysosomal or cytoplasmic matrix or the membranes of other cellular organelles.

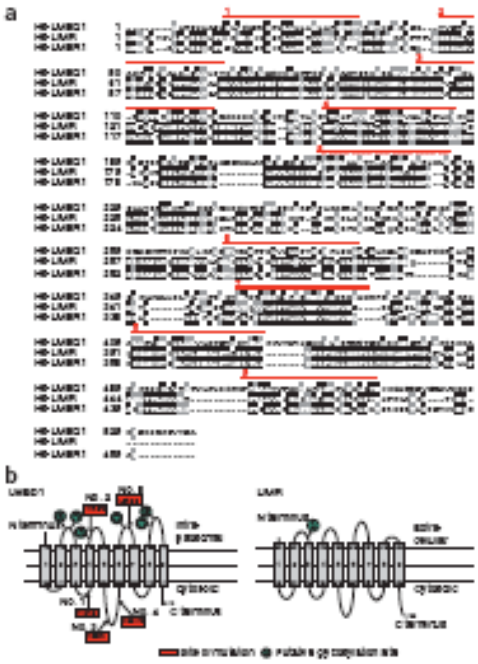

Figure 3 Multiple sequence alignment and structure prediction of LMBD1. (a) Phylogenetic relationships of LMBD1 with other LMBR1-related human proteins. The LMBD1 sequence was compared to that of LMBR1 and LMR using the multiple alignment software ClustalW2. Amino acid identities and similarities are highlighted in black and gray, respectively. Transmembrane domains, as predicted in panel b, are labeled by red lines above the LMBD1 sequence. (b) Schematic representation of the membrane spanning topology and putative glycosylation sites for LMBD1 (left panel) and LMR (right panel). The loci of the five frameshift mutations described in this paper for LMBD1 (T134fsX14; T237X; T172fsX3; K281fsX4; L352fsX18), as well as the putative glycosylation sites for LMBD1 and LMR, are indicated. Membrane spanning helices were predicted using TMHMM. fs, frameshift.

LMBD1 shares significant homology (*E* value = 0.00024) to a membrane protein family (PF04791), which includes the limb region 1 (LMBR1) protein[6] and the lipocalin-1 interacting membrane receptor (LIMR)[9] (Fig. 3). The *LMBR1* gene was initially linked to preaxial polydactyly, but subsequent studies revealed that this association is incidental to the phenotype[6,7]. Lipocalins are small, secreted proteins which bind and carry hydrophobic molecules in biological fluids[10]. LIMR is a cell-surface receptor which internalizes two lipocalins, tear lipocalin and β-lactoglobulin[9,11], a lipocalin which also binds protoporphyrin IX[12]. Multiple sequence alignment showed that LMBD1 shares 15.9% and 13.7% amino acid identity (31.5% and 27.8% similarity) with LMBR1 and LIMR, respectively (Fig. 3a).

Different membrane helix prediction programs resulted in a somewhat different membrane topology and orientation for LMBD1, namely a nine-transmembrane helix and a ten-transmembrane helix model. These models predicted different candidate N-glycosylation sites among the six Asn-X-Ser/Thr motifs of the primary sequence. These sites should be situated only at the intralysosomally exposed sequence parts of the membrane-spanning LMBD1. We transiently expressed LMBD1-EGFP in COS-7 cells and analyzed its glycosylation status by immunoblotting with antibody to EGFP (Supplementary Fig. 6 online). The results are consistent with a nine-transmembrane helix model with an N terminus in the lysosomal interior and a cytoplasmatic C terminus (Fig. 3b). This orientation was further proven by the localization of the C-terminal EGFP tag of LMBD1-EGFP on the cytoplasmic leaflet (P-face) of the lysosomal membrane by freeze-fracture replica immunolabeling (Fig. 2b).

The subcellular distribution, the homology to lipocalin receptors and the topological model of the LMBD1 protein were consistent with a lysosomal transporter function for cobalamin. To prove the functional relevance of the LMBD1 protein, we transfected immortalized fibroblasts of individuals P2 and P9 and controls with a LMBD1

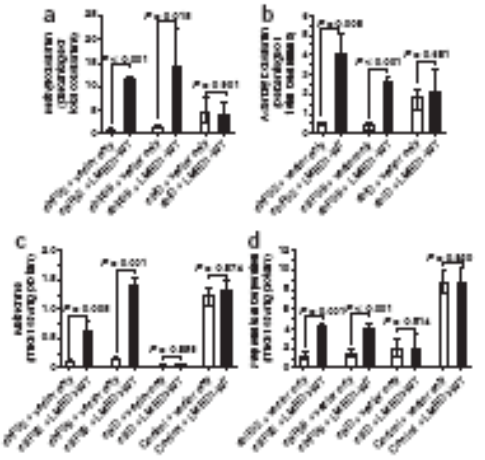

Figure 4 Complementation of the cblF defect by transfection with the wild-type human LMBD1 construct. Transfection experiments were done in immortalized fibroblasts of individual P2 (cblF02; homozygous for L352fsX18) and individual P9 (cblF09; compound heterozygous for L352fsX18 and T134fsX14) with the cblF defect. An immortalized cell line of an individual with combined cblD defect and of an unaffected individual (control) were used as controls (cblD subject 7 and control in ref. 8). Transient transfection was done by electroporation with pcDNA3 vector containing the LMBD1 wild-type (LMBD1-WT) construct. Background activity was measured in cells transfected with the pcDNA3 vector without insert (vector only). (a,b) Synthesis of methylcobalamin and adenosylcobalamin from [^{57}Co]cyanocobalamin bound to human transcobalamin. (c) Formation of methionine from [^{14}C]formate. (d) Incorporation of [^{14}C]propionate into cell proteins. Columns represent mean values; vertical lines indicate the range of results from four replicate experiments with single determinations. In the unaffected control, mean values of methylcobalamin and adenosylcobalamin synthesis were 50.7% (range 45.1–60.8%) and 15.8% (range 11.2–17.8%) of total cobalamin, respectively, when transfected with vector only (data not shown). When transfected with the LMBD1-WT construct, the mean values of methylcobalamin and adenosylcobalamin synthesis were 52.7% (range 46.1–58.5%) and 15.2% (range 11.1–17.5%), respectively.

wild-type cDNA construct and measured the synthesis of methylcobalamin and adenosylcobalamin, formation of methionine, and incorporation of propionate as described earlier[5]. There was a significant increase ($P < 0.05$) of methylcobalamin and adenosylcobalamin synthesis from less than 2% of the mean control value up to 18–29% (Fig. 4a,b), an increase of methionine formation from 9–13% up to 50–105% (Fig. 4c) and an increase of propionate incorporation from 14–16% up to 46–47% (Fig. 4d), thus showing rescue of the biochemical cblF phenotype with the LMBD1 wild-type construct. In contrast, transfection of fibroblasts of a subject with cblD[4] or an unaffected control with the LMBD1 wild-type cDNA construct had no effect on these activities. Similar results were obtained when fibroblasts of individual P9 were transfected with the LMBD1-EGFP construct: synthesis of methylcobalamin increased up to 26–42% (mean value 33%, four replicate experiments) of the mean control value, and that of adenosylcobalamin up to 20–28% (mean value 23%). These data suggest that the molecular and cellular functions of LMBD1 are not affected by the EGFP tag, which should also be the case in subcellular localization experiments.

The partial rescue of methyl- and adenosylcobalamin synthesis by transfection of the LMBD1 wild-type construct and the lysosomal membrane localization of LMBD1 are suggestive of a cobalamin receptor-transporter function for the protein, which should be tested by further studies. The homology of LMBD1 to the lipocalin receptor IIMR[16], including the nine-transmembrane topology and orientation of the N terminus inside the lysosome, moreover argues for the existence of a hypothetical binding protein within the lysosome that binds free cobalamin and transfers it to the LMBD1 protein. Future studies should also aim to identify and characterize such a ligand.

In summary, we have identified *LMBRD1* as the gene responsible for the cblF defect of intracellular vitamin B_{12} metabolism. This gene encodes LMBD1, a previously uncharacterized lysosomal membrane protein with significant homology to lipocalin receptors and which possibly acts as a lysosomal exporter for cobalamin, perhaps with the help of an as-yet-undefined binding protein.

METHODS

Subjects. Twelve individuals with the cblF defect of cobalamin metabolism participated in the study. Skin fibroblasts had been obtained from these individuals for diagnostic purposes. The cblF defect was defined as deficient synthesis of both adenosylcobalamin and methylcobalamin from [^{57}Co]cyanocobalamin bound to human transcobalamin together with high normal or elevated total uptake of cobalamin, deficient activity of the adenosylcobalamin-dependent methylmalonyl-coenzymeA mutase as shown by reduced incorporation of [^{14}C]propionate into cell proteins, and deficient activity of the methylcobalamin-dependent methionine synthase as shown by reduced synthesis of methionine from [^{14}C]formate or reduced incorporation of [^{14}C]methyltetrahydrofolate into cell proteins[5,22]. The cblF defect was confirmed in each cell line by somatic complementation analysis, as described earlier[5]. The study was approved by the institutional ethics committees of Münster University and the McGill University Health Centre. Subjects were included after informed consent.

Linkage analysis. We genotyped DNA samples from 12 affected individuals and 1 unaffected sibling using the Affymetrix GeneChip Human Mapping 250K Sty Array. This array uses the *Sty*I restriction enzyme for the initial fragmentation of the genomic DNA and allows one to interrogate ~238,000 SNPs distributed over the genome. Genotypes were called by the GeneChip DNA Analysis Software (GDAS v5.0, Affymetrix). We verified sample sexes by counting heterozygous SNPs on the X chromosome. Relationship errors were evaluated with the help of the program Graphical Relationship Representation[23]. Non-mendelian errors were identified by using the program MERLIN[24], and unlikely genotypes for related samples were deleted. For linkage analysis, we introduced consanguinity loops into the pedigree files of all 12 families with either one or two offspring. Parametric linkage analysis was done with the program ALLEGRO[25] and a new version of MERLIN that allows for marker clustering to compensate for linkage disequilibrium (LD) between adjacent markers[23]. Haplotypes were constructed using the program ALLEGRO and presented graphically with HaploPainter[26]. All data handling was done using the graphical user interface ALOHOMORA[26].

Mutation analysis. All exons of *LMBRD1*, including their flanking splice sites, were amplified from subject DNA by PCR using intronic primers designed with the Primer3 software (Supplementary Table 3 online). The PCR products were purified within an enzymatic reaction using the PCR Product Pre-sequencing Kit (USB) according to the manufacturer's instructions. Sequencing reactions were done on both strands using the BigDye Terminator Cycle Sequencing Kit V3 (Applied Biosystems) according to the manufacturer's instructions. After purification with filter plates Multiscreen HV (Millipore), the products were analyzed on an ABI Genetic Analyzer 3730 (Applied Biosystems) and the traces were evaluated using the SeqMan II software (DNAStar).

LMBRD1 indel genotyping was done by Pyrosequencing on the PSQ HS96A System (Biotage AB). We designed PCR primers using Primer SNP Design Version 1.01 software (Supplementary Table 3). All PCR were carried out in a reaction volume of 15 µl with 6 ng genomic DNA, 10 µM dNTP, 10 µM of each forward and reverse oligonucleotide PCR primers (one of which is biotinylated), Taq polymerase (5 U/µl), 1.5 mM $MgCl_2$. Protocols were standard as defined by the supplier (Biotage AB). Samples were sequenced by Pyrosequencing PSQ96 HS System with a proprietary pyrosequencing software (Biotage AB).

cDNA constructs used for transfection. cDNA constructs of full-length human LMBD1 were used with or without EGFP tag as indicated. For these constructs, the LMBD1 coding sequence was subcloned into pcDNA3 (Invitrogen) or, to create the C-tagged LMBD1-EGFP fusion protein, into a modified version of pEGFP-N1 (Clontech) with a valine in place of the EGFP initiation methionine. Furthermore, pcDNA3 vector without insert was used as negative control.

Transfection. For transfection studies, primary fibroblasts of affected individuals and controls were first immortalized with pWE8 vector[27] using electroporation. After this, immortalized fibroblasts as well as HeLa and COS-7 cells were transfected with the above described LMBD1 cDNA constructs using electroporation[4].

Immunofluorescence analysis. Fibroblasts or HeLa cells transfected with the above described EGFP-tagged LMBD1 cDNA construct were grown on glass coverslips. Cells were washed with PBS containing 100 µM $MgCl_2$ and 100 µM $CaCl_2$ (PBS/Ca/Mg), and fixed with 4% paraformaldehyde (PFA; Sigma) for 10 min. After washing and quenching PFA with 50 mM NH_4Cl for 15 min, cells were washed with PBS and permeabilized in blocking buffer (0.05% saponin/0.2% BSA in PBS/Ca/Mg) for 20 min. Coverslips were then incubated for at least 1 h with a mouse monoclonal antibody to LAMP1 (H4A3; Developmental Studies Hybridoma Bank, University of Iowa; 0.75 µg/ml) in blocking buffer, washed with PBS/Ca/Mg, incubated for 1 h with a Cy5-conjugated donkey antibody to mouse (Jackson ImmunoResearch; 1.4 µg/ml) in the blocking buffer and rinsed with PBS and water. Coverslips were mounted on glass slides with Fluoromount-G (Southern Biotechnology Associates). Epifluorescence micrographs were acquired under a ×40 (fibroblasts) or a ×100 (HeLa cells and insets) objective lens with a Nikon Eclipse TE-2000 microscope equipped with a charge-coupled device (CCD) camera (Coolsnap). To compare LMBD1 and LAMP1 distributions, we corrected out-of-focus signal in the selected focal plane by deconvolution microscopy: we collected at least five z-sections (0.2-µm spacing) on both sides of the selected plane, and deconvolved the stacked images using the PSF-based Iterative 3D Deconvolution module of Metamorph software (Universal Imaging Corporation).

Cryothin-section electron microscopy. Cells were fixed in 4% formaldehyde (freshly prepared from paraformaldehyde) in PB, scraped from the culture vessels, prepared further for cryoimmunoelectron microscopy basically as outlined by Tokuyasu[28] and immunogold-labeled for EGFP and LAMP1.

Freeze-fracture replica immunolabelling. The principle of the freeze-fracture replica immunolabeling technique used to localize the EGFP-tagged LMBD1 in

the transfected cells has been described elsewhere[29,30]. In brief, after rapid freezing, fracturing under high-vacuum and preparation of platinum-carbon replicas, the replicated samples are treated with sodium dodecyl sulfate to remove the bulk of the cellular material, leaving just a fine layer of directly adherent molecules. In this way, epitopes are retained for immunolabeling without compromising the visibility of structural detail in the replicas. Double immunolabeling was carried out by using mixtures of antibodies to EGFP and LAMP1 followed by incubation with mixtures of goat antibody to mouse coupled to 18-nm gold (LAMP1) and goat antibody to rabbit coupled to 12-nm gold (EGFP-tagged LMBD1).

Functional assays. Rescue of cellular function in immortalized fibroblasts of subjects P2 and P9 and controls, transfected with the above described LMBD1 wild-type cDNA construct in pcDNA3 or the modified pEGFP-N1 vector, was tested by measuring the synthesis of methylcobalamin and adenosylcobalamin, formation of methionine, and incorporation of propionate, as described earlier[3]. Background activities were measured in cells transfected with pcDNA3 vector without insert.

URLs. PCR primer design for Pyrosequencing, http://www.Pyrosequencing.com; Primer3 software, http://frodo.wi.mit.edu/; prediction of membrane spanning helices with TMHMM Server v.2.0, http://www.cbs.dtu.dk/services/TMHMM/; sequence homology, http://pfam.sanger.ac.uk/.

Accession codes. GenBank: LMBRD1, 55788; LMBD1, NP_060058.2; LIMR, NP_060583; LMBR1, NP_071905.

Note: Supplementary information is available on the Nature Genetics website.

ACKNOWLEDGMENTS

We thank the following individuals who provided subject samples and/or clinical information: D. Applegarth, J. Bess, S. Cederbaum, G. Davidson, B.S. Dowton, G. Hoganson, R. Lafrenière, U. Lichter, M. Lindner, M. Seashore, V. Shih, G.R.A. Scott, J. Yoddley and H.E. White. We thank E. Kinz, C. Kluck and U. Retzlaff for expert technical assistance. E.R. and S.G. were supported by the fund "Innovative Medical Research" of University of Münster Medical School. B.G. and C.S. were supported by the Centre National de la Recherche Scientifique, the Institut national de la santé et de la recherche médicale and the Agence Nationale de la Recherche – Programme Fluriamed de Recherche sur les Maladies Rares. I.R.M. was supported by a studentship from the Fonds de la Recherche en Santé du Québec. D.S.R. and I.R.M. were supported by funds from the Canadian Institutes of Health Research and the Hess B. and Diane Finestone Laboratory in memory of Jacob and Jenny Finestone. Financial support was further given by the Swiss National Foundation and the German Federal Ministry of Education and Research through the National Genome Research Network.

AUTHOR CONTRIBUTIONS

E.R. and P.N. designed the study, analyzed the data and wrote the manuscript. S.G. designed primers, collected data, performed sequencing analysis, LMBD1 expression analysis and biochemical rescue experiments. I.R.M. collected subject information and performed microcell-mediated chromosome transfer. T.S. performed biochemical rescue experiments with the wild-type construct. C.S., I.B., A.S., H.R. and B.G. analyzed the subcellular localization of the tagged construct. M.R.T. performed pyrosequencing of the control chromosomes. G.N. performed the bioinformatic analysis and analyzed the haplotype data. T.W. performed sequencing analysis and edited the manuscript. M.S. and M.B. cloned the construct. C.B. performed the genome scan. T.M., B.G., D.S.R. and B.F. were involved in study design. W.H. and B.G. analyzed the structure and homology of LMBD1. All authors discussed the results and commented on the manuscript.

Published online at http://www.nature.com/naturegenetics/
Reprints and permissions information is available online at http://npg.nature.com/reprintsandpermissions/

1. Chanarin, I., Deacon, R., Lumb, M., Muir, M. & Perry, J. Cobalamin-folate interactions: a critical review. *Blood* 66, 479–489 (1985).
2. Rosenblatt, D.S., Hosack, A., Matiaszuk, N.V., Cooper, B.A. & Laframboise, R. Defect in vitamin B12 release from lysosomes: newly described inborn error of vitamin B12 metabolism. *Science* 228, 1319–1321 (1985).
3. Vassiliadis, A., Rosenblatt, D.S., Cooper, B.A. & Gregoire, J.J. Lysosomal cobalamin accumulation in fibroblasts from a patient with an inborn error of cobalamin metabolism (cblF complementation group): visualization by electron microscope autoradiography. *Exp. Cell Res.* 195, 295–302 (1991).
4. Coelho, D. *et al.* Gene identification for the cblD defect of vitamin B12 metabolism. *N. Engl. J. Med.* 358, 1454–1464 (2008).
5. Suormala, T. *et al.* The cblD defect causes either isolated or combined deficiency of methylcobalamin and adenosylcobalamin synthesis. *J. Biol. Chem.* 279, 42742–42749 (2004).
6. Morral, N. *et al.* The origin of the major cystic fibrosis mutation (delta F508) in European populations. *Nat. Genet.* 7, 169–175 (1994).
7. Varon, R. *et al.* Nibrin, a novel DNA double-strand break repair protein, is mutated in Nijmegen breakage syndrome. *Cell* 93, 467–476 (1998).
8. Dacke, D.S. *et al.* tRNA splicing endonuclease mutations cause pontocerebellar hypoplasia. *Nat. Genet.* 40, 1113–1118 (2008).
9. Abecasis, G.R. & Wigginton, J.E. Handling marker-marker linkage disequilibrium: pedigree analysis with clustered markers. *Am. J. Hum. Genet.* 77, 754–767 (2005).
10. Konrad, M. *et al.* Mutations in the tight-junction gene claudin 19 (CLDN19) are associated with renal magnesium wasting, renal failure, and severe ocular involvement. *Am. J. Hum. Genet.* 79, 949–957 (2006).
11. Crispoi, L. *et al.* Gaspery syndrome is caused by mutations in the GNL3 gene and is allelic to cold-induced sweating syndrome type 1. *Am. J. Hum. Genet.* 80, 971–981 (2007).
12. Gutbert, A.P. *et al.* Construction and characterization of a highly stable human–rodent monochromosomal hybrid panel for genetic complementation and genome mapping studies. *Cytogenet. Cell Genet.* 71, 68–76 (1995).
13. Watkins, D., Matiaszuk, N. & Rosenblatt, D.S. Complementation studies in the cblA class of inborn error of cobalamin metabolism: evidence for intralocic complementation and for a new complementation class (cblE). *J. Med. Genet.* 37, 510–513 (2000).
14. Wang, Y.H. *et al.* Novel nuclear export signal-interacting protein, HCSI, critical for the assembly of hepatitis delta virus. *J. Virol.* 79, 8113–8120 (2005).
15. Clark, R.H., Stanier, P.C. & Kingsley, D.M. A novel candidate gene for mouse and human preaxial polydactyly with altered expression in limbs of Hemimelic extra-toes mutant mice. *Genomics* 67, 19–27 (2000).
16. Wojnar, P., Lechner, M., Merschak, P. & Redl, B. Molecular cloning of a novel lipocalin-1 interacting human cell membrane receptor using phage display. *J. Biol. Chem.* 276, 26015–26012 (2001).
17. Lattier, L.A. *et al.* Disruption of a forkhead-box-containing regulator for SIN causes precocial polydactyly. *Proc. Natl. Acad. Sci. USA* 99, 7549–7553 (2002).
18. Flower, D.R. The lipocalin protein family: structure and function. *Biochem. J.* 318, 1–14 (1996).
19. Flutsinger, M., Merschak, P., Hermann, M., Hantle, T. & Redl, B. Lipocalin-interacting membrane receptor (LIMR) mediates cellular internalization of β-lactoglobulin. *Biochim. Biophys. Acta* 1778, 340–347 (2008).
20. Wojnar, P., Lechner, M. & Redl, B. Antisense down-regulation of lipocalin-interacting membrane receptor expression inhibits cellular internalization of lipocalin-1 in human HEK cells. *J. Biol. Chem.* 278, 16209–16215 (2003).
21. Gutiez, C., Mercier, M.C. & Hantle, T. β-lactoglobulin binds retinol and protoporphyrin IX at two different binding sites. *FEBS Lett.* 277, 223–226 (1990).
22. Schuh, S. *et al.* Homocystinuria and megaloblastic anemia responsive to vitamin B12 therapy. An inborn error of metabolism due to a defect in cobalamin metabolism. *N. Engl. J. Med.* 310, 686–690 (1984).
23. Abecasis, G.R., Cherny, S.S., Cookson, W.O. & Cardon, L.R. GRR: graphical representation of relationship errors. *Bioinformatics* 17, 742–743 (2001).
24. Abecasis, G.R., Cherny, S.S., Cookson, W.O. & Cardon, L.R. Merlin–rapid analysis of dense genetic maps using sparse gene flow trees. *Nat. Genet.* 30, 97–101 (2002).
25. Thiele, H. & Nürnberg, P. HaploPainter: a tool for drawing pedigrees with complex haplotypes. *Bioinformatics* 21, 1730–1732 (2005).
26. Rüschendorf, F. & Nürnberg, P. ALOHOMORA: a tool for linkage analysis using 10K SNP array data. *Bioinformatics* 21, 2123–2125 (2005).
27. Lichter, P., Jha, K.K. & Ganz, H.L. Efficient transfer of cloned DNA into human diploid cells: protoplast fusion in suspension. *Mol. Cell. Biol.* 4, 2549–2552 (1984).
28. Takizawa, K.T. Immunocytochemistry on ultrathin frozen section. *Histochem. J.* 12, 381–403 (1980).
29. Rohrbach, H. & Severs, N.J. Recent advances in freeze-fracture electron microscopy: the replica immunolabeling technique. *Biol. Prevet. Online* 10, 9–19 (2008).
30. Rohrbach, H., Blum, I., Hofnagel, O., Lutkowski, S. & Severs, N.J. GFP-tagged protein visualized by freeze-fracture immuno-electron microscopy: a new tool in cellular and molecular medicine. *J. Cell. Mol. Med.* advance online publication, doi:10.1111/j.1582-4934.2008.00407.x (27 June 2008).

Molecular Genetics and Metabolism 102 (2011) 505–507

Contents lists available at ScienceDirect

Molecular Genetics and Metabolism

journal homepage: www.elsevier.com/locate/ymgme

Brief Communication

Novel splice site mutations and a large deletion in three patients with the *cblF* inborn error of vitamin B_{12} metabolism

Isabelle R. Miousse *, David Watkins, David S. Rosenblatt

Department of Human Genetics, McGill University, Montreal, Canada

ARTICLE INFO

Article history:
Received 23 November 2010
Received in revised form 6 January 2011
Accepted 6 January 2011
Available online 14 January 2011

Keywords:
cblF
Cobalamin
Lysosome
LMBRD1
Homocysteine
Methylmalonic acid

ABSTRACT

The *cblF* disorder, characterized by accumulation of internalized cobalamin in the lysosome, is caused by mutations in the *LMBRD1* gene which encodes an integral lysosomal membrane protein. We describe novel mutations in *LMBRD1* in three patients: two splice site mutations, c.916-1G>T and c.1339-1G>T, and a 6785 bp deletion encompassing exon 2, c.70-4298_246+231 1del8785. The three patients are compound heterozygotes for one novel mutation and the common c.1056delG mutation.

1. Introduction

Vitamin B_{12} (cobalamin) acts as a coenzyme for two reactions in mammalian cells: the conversion of homocysteine to methionine by the cytoplasmic enzyme methionine synthase, which utilizes methylcobalamin as cofactor, and the conversion of methylmalonyl-CoA to succinyl-CoA by the mitochondrial enzyme methylmalonyl-CoA mutase, which requires adenosylcobalamin [1]. The *cblF* inborn error of intracellular cobalamin metabolism is characterized by the accumulation of free cobalamin in lysosomes as a result of the failure to export the vitamin to the cytoplasm [2]. This results in decreased synthesis of both cobalamin coenzymes and decreased activity of the two cobalamin-dependent enzymes. Patients accumulate homocysteine and methylmalonic acid in blood and urine. The altered gene in this disorder is *LMBRD1*, which encodes an integral lysosomal membrane protein [3]. There are thirteen reported *cblF* patients [4]. One mutation (c.1056delG, p.L352SX18) is common to 18 of 26 mutant alleles, although the patients are not known to be related and come from a variety of different ethnic groups. Five other mutations have been described, one nonsense mutation and four that result in frameshifts [5]. All are predicted to lead to a truncated protein. We have analyzed the *LMBRD1* gene in three *cblF* patients and describe three novel mutations.

2. Material and methods

2.1. Patients

Fibroblasts from the patients were grown at the Repository for Human Mutant Cells at the Montreal Children's Hospital. Patient 1 presented at two months of age with severe gastritis and failure to thrive, and was subsequently found to have hyperhomocysteinemia and methylmalonic acidemia that responded to therapy with hydroxocobalamin (Patient 11 in reference [3]). Patients 2 and 3 were identified on newborn screening with elevated C3 acylcarnitines, leading to identification of methylmalonic acidemia and hyperhomocysteinemia. Fibroblasts from patients 1 and 3 had decreased function of methylmalonyl CoA mutase and methionine synthase and an abnormal cobalamin distribution indicative of *cblF*. The *cblF* disorder was confirmed by complementation analysis [6,7]. Fibroblasts from patient 2 had an abnormal cobalamin distribution but mutase and methionine synthase function were normal; complementation analysis could not be performed for this patient. Detailed clinical descriptions for patients 2 and 3 will be published separately.

2.2. Mutation analysis

DNA and RNA were extracted using the Puregene DNA purification kit (Qiagen) and Tri reagent (Molecular Research Center, Inc.). cDNA was generated using MMLV reverse transcriptase (USB, Cleveland, OH). PCR amplification was performed with Hot Star Taq (Qiagen). PCR products were visualized on 2% agarose gels with GelPilot 100 bp Plus Ladder (Qiagen) and analyzed by Sanger sequencing at the

* Corresponding author. Department of Human Genetics, MUHC/Montreal General Hospital, 1650 Cedar Avenue, Room L3-319, Montreal, Quebec, Canada H3G 1A4. Fax: +1 514 936 8536.
E-mail address: isabelle.radomiousse@mail.mcgill.ca (I.R. Miousse).

1096-7192/$ – see front matter © 2011 Elsevier Inc. All rights reserved.
doi:10.1016/j.ymgme.2011.01.003

Genome Quebec Innovation Center (Montreal, Canada). Primers were designed with the program Primer3 to amplify *IMBRD1* from gDNA and cDNA. Real-time quantitative amplification using the SYBR green reagent (Invitrogen) was performed on a RotorGene RG 3000 (Corbett Research). Long range PCR was performed using LA Taq with Mg^{2+} buffer (TaKaRa).

3. Mutation analysis

3.1. Patient 1

A heterozygous c.1056delG mutation was previously reported in patient 1 [3]. On gDNA sequencing of *IMBRD1*, a G>T change was observed at the position -1 of exon 10, corresponding to the splice acceptor site (c.916-1G>T). PCR amplification of cDNA using primers located in exons 9 (forward) and 13 (reverse) resulted in two products, one migrating at 335 bp, the expected size for full-length product, and a second migrating at 270 bp, consistent with loss of exon 10 (Fig. 1A, patient 1). The omission of exon 10 from the transcript leads to a frameshift creating a stop codon two amino acids after exon 9 (p.I306Sfs*2).

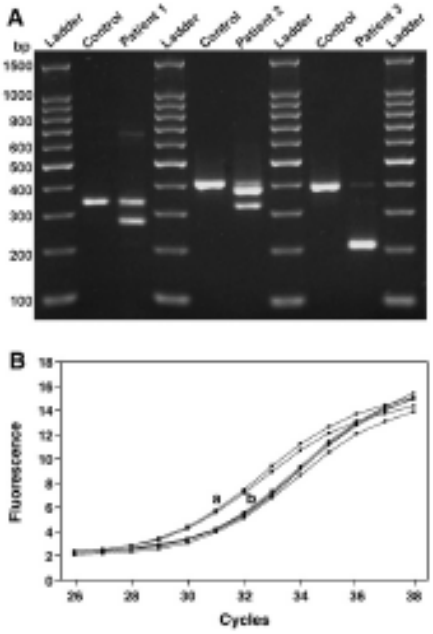

Fig. 1. A. Agarose gel electrophoresis of cDNA PCR products. In patient 1 (c.887-1221), there were two products: one of control length (335 bp) and a shorter band lacking the residues of exon 10 (270 bp). Investigations on the faint band seen at 700 bp were inconclusive. In patient 2 (c.1220–1696), there were three products: one of control length (400 bp) and a shorter band (321 bp) lacking the residues of exon 14. A third band of intermediate size is composed of mutant and normal product. In patient 3 (c.70-246), there was a band of 305 bp, in addition to the control band of 182 bp; this reflects a deletion of exon 2. Only a small amount of control product was detected. B. Quantitative real-time PCR analysis of exon 2 in patient 3. a) 100 ng control gDNA ($\Delta CT = 1.4$) and b) 100 ng patient gDNA ($\Delta CT = 3.0$), superimposed with 50 ng (one half) control gDNA ($\Delta CT = 2.6$), delayed by 1.25 cycle compared to a), supporting evidence for the loss of one allele. All samples were run in duplicate. For exon 1, control gDNA showed a delay of 0.4 cycles compared to patient gDNA (data not shown).

3.2. Patient 2

The c.1056delG mutation was identified in the heterozygous state by digestion of the PCR product of exon 11 in gDNA with the restriction endonuclease TspRI and confirmed by sequencing. A G>T change was observed at the position -1 of exon 14, corresponding to the splice acceptor site (c.1339-1G>T). Amplification of cDNA using primers in exons 13 (forward) and 16 (reverse) resulted in two products, one migrating at 400 bp, the expected size for full-length product, the second migrating at 321 bp, consistent with the loss of exon 14 (Fig. 1A, patient 2). Sequencing of the cDNA confirmed the loss of exon 14 in the message. A product of intermediate size is also visible, which is a mixture of normal and truncated product. The splicing defect leads to a frameshift creating a stop codon 33 amino acids after exon 13 (p.T447Sfs*33).

3.3. Patient 3

For patient 3, the c.1056delG mutation was identified on one allele by sequencing and TspRI digestion. PCR amplification of a cDNA fragment containing exons 1 to 5 showed a transcript consistent in size with the absence of the 177-bp exon 2 (Fig. 1A, patient 3). cDNA sequencing confirmed the skipping of exon 2 but failed to detect any product from the allele bearing the common mutation. No mutation affecting the exon 1 splice donor or exon 2 splice acceptor site was detected on gDNA sequencing. Real-time quantitative PCR of *IMBRD1* from gDNA showed similar amplification of exon 1 in control and patient. The onset of fluorescence was delayed by 1.25 cycle for the patient compared to the control for exon 2, consistent with loss of one copy of exon 2 in patient gDNA (Fig. 1B). SNP analysis identified a heterozygous SNP (rs3799120 C/A) in intron 2, reducing the DNA segment potentially affected by the deletion from 17 to 11 kb. Sequencing of gDNA using primers flanking this segment identified a 6785 bp deletion extending from 4298 bp upstream to 2311 bp downstream of exon 2 (c.70–4298_246+2311del6785, p.A24_K82del).

4. Discussion

This work describes three novel mutations in *cIIF* patients. In all three cases, the novel mutation was found in combination with the common c.1056delG mutation and resulted in the absence of one exon in cDNA derived from patient cells. These are the first splice site mutations and large deletion to be described in *cIIF* patients. The splice mutations result in frameshifts leading to premature stop codons after exons 9 and 13 in patients 1 and 2, respectively. The third patient displays a heterozygous deletion of 6.8 kb leading to the absence of exon 2 in the transcript. In this case, the deletion conserves the frame of the transcript but is predicted to result in loss of parts of two transmembrane domains and the intervening cytoplasmic loop in the gene product.

The presence of the common c.1056delG mutation in 13 out of 15 known patients underlines the relevance of testing for this mutation in suspected *cIIF* cases. However, caution should be taken in the analysis of cDNA, since we have observed variable detection of this allele in four patients, including a failure to detect any product in patient 3 in the present study. This report brings the number of mutations described in *cIIF* patients to nine. Mutations other than the common c.1056delG mutation have been unique to each patient. All known mutations are predicted to cause a shortened protein, through nonsense mutation, frameshift, or exon deletion; no missense mutations have yet been found.

Acknowledgments

This study was supported by a grant from the CIHR to DSR and a graduate studentship to IRM from the Fonds de Recherche en Santé du

Québec. We would like to thank Dr. Christine Armour and Dr. Marwan Shinawi for the referral of patients 2 and 3.

References

[1] E.V. Quadros, Advances in the understanding of cobalamin assimilation and metabolism, Br. J. Haematol. 148 (2009) 195–204.
[2] D.S. Rosenblatt, A. Hosack, N.V. Matiaszuk, B.A. Cooper, R. Laframboise, Defect in vitamin B_{12} release from lysosomes: newly described inborn error of vitamin B_{12} metabolism, Science 228 (1985) 1319–1321.
[3] F. Rutsch, S. Gailus, I.R. Miousse, T. Suormala, C. Sagné, M.R. Toliat, G. Nurnberg, T. Wittkampf, I. Buers, A. Sharifi, M. Studer, C. Becker, M. Baumgartner, H. Rosenberg, T. Marquardt, W. Höhne, B. Garnier, D.S. Rosenblatt, B. Fowler, P. Nürnberg, Identification of a putative lysosomal cobalamin exporter altered in the *cblF* defect of vitamin B_{12} metabolism, Nat. Genet. 41 (2009) 234–239.
[4] S. Gailus, T. Suormala, A.C. Malerczyk-Aktar, M.R. Toliat, T. Wittkampf, M. Studer, R. Nürnberg, B. Fowler, J.B. Hennermann, F. Rutsch, A novel mutation in *LMBRD1* causes the *cblF* defect of vitamin B_{12} metabolism in a Turkish patient, J. Inherit. Metab. Dis. 33 (2010) 17–24.
[5] S. Gailus, W. Höhne, B. Garnier, P. Nürnberg, B. Fowler, F. Rutsch, Insights into lysosomal cobalamin trafficking: lessons learned from *cblF* disease, J. Mol. Med. 88 (2010) 459–466.
[6] B.A. Cooper, D.S. Rosenblatt, D. Watkins, Methylmalonic aciduria due to a new defect in adenosylcobalamin accumulation by cells, Am. J. Hematol. 34 (1990) 115–120.
[7] D. Watkins, D.S. Rosenblatt, Failure of lysosomal release of vitamin B_{12}: a new complementation group causing methylmalonic aciduria (*cblF*), Am. J. Hum. Genet. 39 (1986) 404–408.

Clinical and Molecular Heterogeneity in Patients with the *CblD* Inborn Error of Cobalamin Metabolism

Isabelle R. Miousse, BSc, David Watkins, PhD, David Coelho, PhD, Tony Rufar, PhD, Eric A. Crombez, MD, Eric Vilain, MD, Jonathan A. Bernstein, MD, PhD, Tina Cowan, PhD, Christopher Lee-Messer, MD, PhD, Gregory M. Enns, MB, ChB, Brian Fowler, PhD, and David S. Rosenblatt, MD

Objectives To describe 3 patients with the *cblD* disorder, a rare inborn error of cobalamin metabolism caused by mutations in the *MMADHC* gene that can result in isolated homocystinuria, isolated methylmalonic aciduria, or combined homocystinuria and methylmalonic aciduria.

Study design Patient clinical records were reviewed. Biochemical and somatic cell genetic studies were performed on cultured fibroblasts. Sequence analysis of the *MMADHC* gene was performed on patient DNA.

Results Patient 1 presented with isolated methylmalonic aciduria, patient 3 with isolated homocystinuria, and patient 2 with combined methylmalonic aciduria and homocystinuria. Studies of cultured fibroblasts confirmed decreased synthesis of adenosylcobalamin in patient 1, decreased synthesis of methylcobalamin in patient 3, and decreased synthesis of both cobalamin derivatives in patient 2. The diagnosis of *cblD* was established in each patient by complementation analysis. Mutations in the *MMADHC* gene were identified in all patients.

Conclusions The results emphasize the heterogeneous clinical, cellular and molecular phenotype of the *cblD* disorder. The results of molecular analysis of the *MMADHC* gene are consistent with the hypothesis that mutations affecting the N terminus of the MMADHC protein are associated with methylmalonic aciduria, and mutations affecting the C terminus are associated with homocystinuria. *(J Pediatr 2009;154:551-6)*

Derivatives of cobalamin (vitamin B_{12}) are required for the activity of 2 enzymes in mammalian cells. 5'-deoxyadenosylcobalamin (AdoCbl) is required for activity of the mitochondrial enzyme methylmalonyl-CoA mutase (EC 5.3.99.2), which catalyzes the conversion of methylmalonyl-CoA, generated during catabolism of branched-chain amino acids and odd-chain fatty acids, to succinyl-CoA. Methylcobalamin (MeCbl) is required for activity of the cytoplasmic enzyme methionine synthase (EC 2.1.1.13), which catalyzes the methylation of homocysteine to form methionine, with 5'-methyltetrahydrofolate (methylTHF) as its source of methyl groups. A series of inborn errors of cobalamin metabolism have been identified, designated *cblA-cblG*, which affect the ability of cells to generate these cobalamin derivatives. Disorders that affect synthesis of AdoCbl result in accumulation of methylmalonic acid in the blood and urine because of decreased activity of methylmalonyl-CoA mutase, disorders that affect synthesis of MeCbl result in hyperhomocysteinemia and homocystinuria because of decreased methionine synthase activity. Disorders that affect synthesis of both cobalamin coenzyme derivatives result in accumulation of both methylmalonic acid and homocysteine.[1]

The *cblD* disorder (OMIM 277410) was originally described in 1970 in 2 siblings, a 14-year-old boy with psychiatric and neurologic problems and his younger symptom-free brother. Both patients had combined methylmalonic aciduria and homocystinuria.[2] Somatic cell complementation studies demonstrated that the defect in these siblings affected a different locus than the more common *cblC* disorder, which also results in combined methylmalonic aciduria and homocystinuria.[3] No additional patients with the *cblD* disorder were reported until 2004, when 3 patients, 2 with isolated homocystinuria (*cblD variant 1*) and 1 with isolated methylmalonic aciduria (*cblD variant 2*), were shown by complementation analysis to have the *cblD* disorder[4] despite having markedly different clinical and laboratory findings from the original patients with *cblD* disorders.

AdoCbl	5'-deoxyadenosylcobalamin	MethylTHF	5'-methyltetrahydrofolate
MeCbl	Methylcobalamin	PCR	Polymerase chain reaction

From the Department of Human Genetics (IM, DW, DR) and the Division of Medical Genetics, Department of Medicine (DR), McGill University Health Centre, Montreal, Quebec, the Departments of Pediatrics, Biochemistry and the Children's Health Research Institute, University of Western Ontario (TR), London, Ontario, Canada, the Metabolic Unit, University Children's Hospital (DC, BF), Basel, Switzerland, the Departments of Pediatrics (EC, EV), Urology (EV) and Human Genetics (EV), University of California Los Angeles, Los Angeles, the Department of Pediatrics, Division of Genetics (JB, GE), Neurology (CM) and Pathology (TC), Stanford University, Palo Alto, CA.

The authors declare no conflicts of interest, real or perceived.

Submitted for publication May 21, 2008; last revision received Oct 3, 2008; accepted Oct 27, 2008.

Reprint requests: David Watkins, PhD, Division of Medical Genetics, Room L3-319, McGill University Health Centre, Montreal General Hospital, 1650 Cedar Avenue, Montreal, Quebec, Canada, H3G 1A4. E-mail: davidwatkins@mcgill.ca.

0022-3476/$ - see front matter

10.1016/j.jpeds.2008.10.043

Recently, mutations at the *MMADHC* gene on chromosome 2q23.2 were shown to underlie the *cblD* disorder in seven unrelated patients.[5] Function of the product of this gene remains unknown; it shows homology to the putative ATPase component of a bacterial ABC transporter. Mutations in the C-terminal region were identified in patients with *cblD variant 2*, mutations in the N-terminal region were identified in patients with *cblD variant 1*, and truncating mutations were associated with the classic *cblD* phenotype.[5] This supports suggestions that the *MMADHC* gene product plays a role in directing cobalamin to the 2 cobalamin-dependent enzymes of mammalian cells. This report describes 3 additional patients with the *cblD* disorder, one with classic *cblD*, 1 with *cblD variant 2* and 1 with *cblD variant 1*, and reports the *MMADHC* mutations that underlie *cblD* disease in these patients.

METHODS

Patient 1 (WG3280) was a boy of Lebanese descent, the nonconsanguineous child of a healthy 39-year-old father and 32-year-old mother. An older brother was well. No other members of the family appeared to be affected, although a cousin of the father died at 28 years of age with a myelopathic process. The child was born at term in Beirut after an uneventful pregnancy. Birth weight was 3.2 kg; other measurements at birth are not available. During the first days of life, he developed poor feeding and lethargy and was subsequently admitted to hospital with what was believed to be an infection, but cultures were negative. Profound metabolic acidosis was identified and treated. He was released after 1 week.

Beyond the neonatal period the patient was generally well, although he had muscle weakness. There were occasional episodes of wheezing associated with respiratory infections and treated with bronchodilators. At 4.5 years, he presented with a 2-month history of weakness and reported poor weight gain; however, the weight was between the 90th and 95th percentile and height was at the 50th percentile. Investigation revealed a metabolic acidosis and a diagnosis of renal tubular acidosis was considered.

At about 5 10/12 years he returned to hospital after several episodes of vomiting precipitated by physical activity. He had generalized weakness, metabolic acidosis, and a self-imposed reduced dietary protein intake. Investigation of the metabolic acidosis resulted in a diagnosis of methylmalonic acidemia on the basis of plasma acyl carnitine profile and urine organic acids. There was no evidence of homocystinuria. Methylmalonic acidemia (0.45-0.8 mmol/L; normal: not detected) and aciduria (5.4-7.5 mg per mg creatinine; normal: not detected) were present. Treatment with intramuscular vitamin B_{12} (cyanocobalamin) 1 mg every second day, carnitine (900 mg 2 times daily), and Polycitra (20 mL 3 times daily) was initiated. Intramuscular vitamin B_{12} was replaced with oral vitamin B_{12} (5 mg daily). This resulted in reduction of urine methylmalonic acid to near-normal levels (0.45 mg per mg creatinine).

At 6 years of age, the patient was developmentally normal with appropriate milestones, although he exhibited poor social skills and behavioral problems. He spoke 2 languages well. Physical and neurologic examination results were normal.

Patient 2 (WG3583) was a girl of Mexican descent born to a 34-year-old mother. Both parents were from the same city in Mexico, but consanguinity was denied. Two older brothers were apparently healthy. The pregnancy was complicated by gestational diabetes, treated by diet alone. Labor was induced because of poor fetal growth, with birth by caesarian section when induction failed. Birth weight was 2.5 kg; other measurements were not available. The perinatal period was otherwise uncomplicated. The patient was subsequently admitted to the hospital at 3 months of age for respiratory syncytial virus bronchiolitis with secondary bacterial pneumonia, right hip dysplasia, and poor weight gain. At 4 months, there was concern about possible developmental delay because of hypotonia and poor head control. Physical and neurologic examination results were otherwise normal.

There was evidence of methylmalonic acidemia on newborn screening. The original C3 measurement was below the established cutoff in use at the time, but by a subsequently adopted secondary criterion that used C3/C2 ratios for values above a lower cutoff, the screening result would have been positive. Thus this patient was not diagnosed on the basis of the newborn screen. Further workup revealed megaloblastic anemia, and elevated homocysteine (157.8 μmol/L; normal < 20 μmol/L) and methylmalonic acid (26 μmol/L; normal < 0.41 μmol/L) were confirmed. The patient has been treated with a low protein diet, intramuscular hydroxycobalamin 0.5 mg 4 times daily, oral betaine 250 mg/kg day, baby aspirin half a tablet daily, and folic acid 2 mg 4 times daily.

At 2 years of age the patient remains developmentally delayed but is making progress in cognitive and motor skills. Response to hydroxycobalamin has been good but is hampered by the parents' reluctance to give the injections as frequently as required. Megaloblastic anemia has disappeared.

Patient 3 (WG3745) was a girl of Mexican descent. Her parents are first cousins. No family history of significant childhood illness or developmental difficulty was identified. Her only sibling, a 3-year-old sister, was in good health. The patient was born at 38 weeks gestation. The birth weight was 3.1 kg, length 45.5 cm, and occipitofrontal circumference 33 cm. In the newborn period, an anteriorly displaced anus was identified. At 4 months of age the patient was admitted to the hospital for respiratory distress and altered mental status. Respiratory syncytial virus pneumonia was diagnosed. She had delayed development with a history of significant head lag and was not yet rolling over. Reportedly she fed well at the breast. Visual tracking was inconsistent, and there was limited responsiveness to voice. A computed tomography scan of the head revealed 4-ventricle, nonobstructive hydrocephalus (Figure).

Two weeks after admission to the hospital, significant hair loss was noted. Metabolic investigation revealed an elevated total plasma homocysteine of 52.2 μmol/L (normal <

Figure. Computed tomography scan of head for patient 3 performed at 4 months of age, demonstrating 4-ventricle hydrocephalus.

14 μmol/L); the plasma methylmalonic acid level was normal. Plasma methionine was not detected, cystine was low (8 μmol/L; normal 16 to 84 μmol/L), and cobalamin and folate levels were normal. Mean corpuscular volume was also normal (97.5 fL; normal 74-108 fL).

The patient was started on a regimen of hydroxycobalamin, folate, and betaine. Although biochemical measures improved, there was no clinical improvement. Subsequently, the patient developed a nearly obstructive inferior vena cava clot. Medical support was ultimately withdrawn because of progressive hydrocephalus and prolonged ventilator dependence. Retrospective evaluation of the patient's newborn screening bloodspot demonstrated decreased methionine (5.5 μmol/L; abnormal less than 10 μmol/L) and elevated total homocysteine levels (64.4 μmol/L; abnormal greater than 15 μmol/L). Total homocysteine levels were normal for both the patient's parents and sibling.

Tissue Culture

Fibroblasts were obtained from patients and were maintained in culture at 37°C in minimum essential medium (InVitrogen Canada, Burlington, Ontario) supplemented with nonessential amino acids and 10% fetal bovine serum (Cansera International, Etobicoke, Ontario, Canada). The research protocol was approved by the Royal Victoria Hospital Research Ethics board.

Ability of fibroblasts in culture to incorporate label from [1-^{14}C]propionate (New England Nuclear, Waltham, Massachusetts, or MP Biomedicals, Solon, Ohio) and 5-[^{14}C]methylTHF; Amersham Life Sciences, GE Healthcare, Chalfont St. Giles, United Kingdom) into trichloroacetic acid-precipitable cellular macromolecules (measures of function of methylmalonyl-CoA mutase and methionine synthase, respectively) were performed as previously described.[3,6] Synthesis of the 2 cobalamin coenzyme derivatives, AdoCbl and MeCbl, was assessed by growth of fibroblasts in medium containing [^{57}Co]cyanocobalamin (MP Biomedicals) 25 pg/mL bound to human transcobalamin, followed by hot ethanol extraction and separation of cobalamin derivatives by high-performance liquid chromatography.[6,7] For complementation analysis, equal numbers of 2 fibroblast lines were plated. Half of cultures were fused by exposure for 60 seconds to 40% polyethylene glycol 1000 (JT Baker Inc., Mallinckrodt Baker, Phillipsburg, New Jersey) in phosphate buffered saline solution. Incorporation of propionate or methylTHF into cellular macromolecules was assessed in parallel fused and unfused cultures as described above.[8]

Sequencing Studies

DNA was amplified by polymerase chain reaction (PCR) from genomic DNA or cDNA. Genomic DNA was extracted from fibroblasts with the QIAamp DNA mini kit (Qiagen AG, Basel, Switzerland) and amplified by PCR with specific primers.[5] The cDNA was prepared by total RNA extraction from fibroblast cultures with RNeasy kit (Qiagen AG), followed by reverse transcription with the 1-step RT-PCR kit (Qiagen AG) and specific primers.[5] PCR products were purified with the NucleoSEQ kit (Macherey-Nagel, Düren, Germany). Sequencing reaction products were analyzed on an ABI Prism 3100 sequencer (Applied Biosystems, Foster City, California). Sequencing files were processed with Sequence Analysis software (Applied Biosystems) and were assembled and analyzed with the Autoassembler v.2.1.1 software (Applied Biosystems).

RESULTS

Fibroblast line WG3280 (patient 1) had decreased incorporation of label from propionate into cellular macromolecules compared with control fibroblasts (Table I); incorporation was stimulated by incubation of cells in the presence of 3.75 μmol/L hydroxycobalamin (OHCbl). Incorporation of label from 5-methylTHF into cellular macromolecules fell within the normal range and was not stimulated in the presence of OHCbl. There was decreased synthesis of AdoCbl from labeled cyanocobalamin (CNCbl), with 1.6% of labeled intracellular cobalamin present as AdoCbl (normal: 15.3% ± 4.2%); the proportion of intracellular cobalamin present as MeCbl was greater than normal (Patient: 81%; normal 58% ± 7). The finding of deficient AdoCbl synthesis and decreased function of methylmalonyl-CoA mutase suggested a diagnosis of *cblA* or *cblB* disease. This was investigated by cell complementation analysis (Table II). There was clear complementation of the defect in WG3280 by *mut* and *cblB* fibroblasts. Results with *cblA* fibroblasts were initially difficult

Table I. Propionate incorporation, methyltetrahydrofolate incorporation and cobalamin coenzyme synthesis in patient fibroblasts

	Propionate incorporation (nmol/mg/18 h)		MethylTHF incorporation (pmol/mg/18 h)			
	w/o OHCbl	+ OHCbl	w/o OHCbl	+ OHCbl	AdoCbl (% total)	MeCbl (% total)
WG3280	1.0 ± 0.5	3.2 ± 0.3	118 ± 7	119 ± 5	2	81
WG3583	1.5 ± 0.1	4.5 ± 0.4	24 ± 0.6	45 ± 3	7	3
WG3745	11.5 ± 0.3	11.1 ± 0.5	30 ± 0.6	43.0; 43.6	50	1
Control	10.8 ± 3.7	10.9 ± 3.5	225 ± 165	305 ± 125	15 ± 4	58 ± 7

Values for propionate and methylTHF without added OHCbl and in the presence of 3.75 μmol/L OHCbl in the culture medium. Values are the means of triplicate determinations except for methylTHF incorporation in the presence of added OHCbl for WG3745, where there were duplicate determinations. Values for AdoCbl and MeCbl, expressed as a percentage of total labeled cellular cobalamin, were determined once. Control values are the means of 12 determinations in 3 control fibroblast lines.

Table II. Complementation analysis of patient with cblD fibroblasts

	w/o PEG	+ PEG
Propionate Incorporation (nmol/mg/18 h)		
WG3280	0.9 ± 0.2	
× WG2951 (*cblA*)	1.0 ± 0.2	3.6 ± 0.9
× WG1191 (*cblA*)	1.1 ± 0.2	5.1 ± 0.2
× WG3287 (*cblA*)	1.0 ± 0.1	1.3 ± 0.3
× WG3322 (*cblA*)	1.8 ± 0.1	11.0 ± 0.5
× WG3470 (*cblA*)	1.1 ± 0.2	4.9, 4.9
× WG3185 (*cblB*)	1.4 ± 0.1	6.8 ± 0.9
× WG3224 (*cblB*)	0.9 ± 0.1	3.3 ± 0.3
× WG3293 (*cblB*)	0.8 ± 0.1	2.1 ± 0.1
× WG3200 (*mut*)	1.0 ± 0.1	4.9 ± 0.6
× WG3205 (*mut*)	1.4 ± 0.1	3.1 ± 0.3
× WG3207 (*mut*)	1.1 ± 0.1	2.4 ± 0.2
× WG3191 (*mut*)	1.0 ± 0.2	2.0 ± 0.1
× WG1437 (*cblD*)	1.1 ± 0.1	1.0 ± 0.1
WG3583	1.0 ± 0.1	
× WG3480 (*cblC*)	1.2 ± 0.1	4.8 ± 0.2
× WG3560 (*cblC*)	0.9 ± 0.1	3.3 ± 0.1
× WG2025 (*cblD*)	1.9 ± 0.1	1.9 ± 0.1
× WG3377 (*cblF*)	3.5 ± 0.1	9.1 ± 0.4
MethylTHF Incorporation (pmol/mg/18 h)		
WG3745	63 ± 3	
× WG3728 (*cblC*)	68 ± 1	196 ± 11
× WG3583 (*cblD*)	60 ± 6	61 ± 3
× WG3732 (*cblE*)	63 ± 6	209 ± 6
× WG3589 (*cblE*)	57 ± 1	134 ± 8
× WG3298 (*cblG*)	64 ± 4	155 ± 8
× WG3412 (*cblG*)	68 ± 2	218 ± 5

Values are the means of triplicate determinations except where otherwise indicated.

to interpret, with 1 *cblA* line (WG3287) apparently not complementing the defect in WG3280. However, 5 additional *cblA* lines did complement the defect in WG3280, whereas a *cblD variant 2* line (WG1437) did not complement the defect. These results established that the defect in this patient was *cblD variant 2*.

The fibroblast line WG3583 (Patient 2) showed decreased incorporation of label from both propionate and methylTHF into cellular macromolecules (Table I), and decreased synthesis of both AdoCbl and MeCbl (7% and 3% of cellular cobalamin, respectively). On complementation analysis, the defect in WG3583 was complemented by *cblC* and *cblF* fibroblasts, whereas *cblD* fibroblasts failed to complement the defect, establishing the diagnosis of *cblD* in this patient.

The fibroblast line WG3745 (Patient 3) had normal incorporation of label from propionate into cellular macromolecules, and significantly decreased incorporation of label from methylTHF. Synthesis of MeCbl was decreased (1.4% of total cellular cobalamin) in the presence of normal AdoCbl. The cell line complemented *cblE* and *cblG* cell lines but failed to complement a *cblD variant 1* cell line.

Sequence analysis revealed that WG3280 was a compound heterozygote for 2 novel mutations in the *MMADHC* gene, an insertion and a duplication that both resulted in frame shifts and a truncated protein: c.60insAT (p.L20fsX21) in exon 3 and c.455dupC (p.T152fsX162) in exon 5. WG3583 was homozygous for a novel nonsense mutation in exon 7, c.683C>G (S228X). WG3745 was homozygous for a novel mutation in exon 8 of the *MMADHC* gene, c.737A>G, that results in conversion of a conserved aspartate residue to a glycine (D246G).

DISCUSSION

The *cblD* disorder has been the rarest of the inborn errors of cobalamin metabolism, with only a single sibship identified before 2004. The recent recognition that the clinical and biochemical variability of this disorder is greater than previously realized has been accompanied by identification of additional affected individuals.[4] These include patients with the classic presentation of combined homocystinuria and methylmalonic aciduria, as well as *cblD variant 1* (isolated homocystinuria) and *cblD variant 2* (isolated methylmalonic aciduria). Some previously studied patients that could not be confidently assigned to any of the known classes of inborn

error of cobalamin metabolism have been shown to in fact belong to the *cblD* class. For example, a patient with isolated methylmalonic acidemia that was assigned to the novel *cblH* class[9] has been shown to be a *cblD variant 2*.[5] Similarly, patient 1 (WG3280) in this study was tentatively assigned to the *cblA* complementation class before recognition of the heterogeneity of the *cblD* class. There was no apparent complementation with 1 of the 3 *cblA* fibroblast lines (WG3287) used in the initial complementation studies, a result attributed at the time to interallelic complementation, which is known to occur within the *cblA* complementation class.[9] The finding of complementation with additional *cblA* lines and the recognition of the *cblD variant 2* phenotype led to the correct diagnosis of this patient. Diagnosis of the genetic defect in patient 2 (WG3583), who had the classic presentation of the *cblD* disorder, was straightforward, as was diagnosis in patient 3 (WG3745) who came to medical attention after the recognition of heterogeneity in the *cblD* class.

The cloning of the *MMADHC* gene and the identification of mutations in the gene in several patients with *cblD* disorder has allowed for the first time investigation of the relationship between genotype and phenotype in this disorder. It was noted that missense mutations affecting the C-terminal region of the *MMADHC* protein product resulted in isolated homocystinuria, and mutations in the N-terminal region were associated with isolated methylmalonic aciduria, and it was suggested that the protein consisted of 2 domains: an N-terminal domain that was required for synthesis of AdoCbl; and a C-terminal domain required for MeCbl synthesis.[5] Mutations that result in either a completely inactive protein or decreased mRNA levels because of nonsense-mediated mRNA decay would be associated with decreased synthesis of both cobalamin coenzyme derivatives. The mutations identified in our patients appear consistent with this hypothesis. The 2 mutations present in the patient with *cblD* disorder *variant 2* WG3280 (c.60insAT and c.455dupC) both result in introduction of a frame shift and creation of a stop codon in the 5′-region of the mRNA. It has been predicted that in cases in which there is premature termination, translation starting from an alternate start site at codon 62 produces a truncated protein, lacking the putative mitochondrial leader sequence, which supports synthesis of MeCbl only.[5] The homozygous mutation identified in the patient with *cblD* disorder *variant 1* WG3745 is a missense mutation (c.737A>G) in the 3′ domain of the gene, and results in an amino acid change of aspartic acid to glycine at position 246 in the domain of the *MMADHC* protein associated with MeCbl synthesis. The homozygous mutation in the classic patient with *cblD* disorder WG3583 is a nonsense mutation (c.683C>G), resulting in creation of a stop codon at position 228 of the protein. This mutation falls in the same region of the gene previously associated truncating mutations associated with the classic *cblD* phenotype.[5]

With the recognition of the variants 1 and 2 of *cblD* disease and the causative role of the *MMADHC* gene, the biochemical and molecular diagnosis of *cblD* disease has become increasingly straightforward. However, it should be noted that although, in theory, patients with the *cblD* disorder should be detected on newborn screening, levels of methylmalonic acid excretion are sufficiently low that patients have been missed. In addition, most screening programs do not usually screen for low methionine levels that are associated with the hyperhomocysteinemia seen in the classic and variant 1 (isolated hyperhomocysteinemia) forms of *cblD*. With respect to patients suspected of having increased blood levels of homocysteine, if plasma amino acids are being investigated, the blood collected for plasma amino acids assay should be placed on ice and the plasma separated immediately to prevent binding of free homocysteine, resulting in a false-normal homocysteine level. Alternatively, measurement of total plasma homocysteine should be specifically requested. The clinical variability of the condition remains a barrier to its recognition in patients not identified by newborn screening. The range of presenting features in patients described here and those previously reported[2,4,5] include developmental delay, focal neurologic signs, megaloblastic anemia, marfanoid appearance, venous thrombosis, cerebral atrophy and hydrocephalus. Several patients demonstrated only 1 of these manifestations at the time of diagnosis. Therefore the clinician needs to recognize each as a potential indicator of disturbance in methylmalonic acid or homocysteine metabolism. Notably, cerebral atrophy and hydrocephalus have also been observed in *cblC* disease and severe methylenetetrahydrofolate reductase deficiency.[10–12] Because these patients generally respond well to treatment with vitamin B_{12}, it is essential for clinicians to be aware of the possibility of this diagnosis.

We thank Dr. S. Cederbaum and Dr. J. T. R. Clarke for referral of patients and for review of the manuscript, and Dr. J. Lavallée for performing studies on cultured fibroblasts. This is a publication of the Hess B. and Diane Finestone Laboratory in the memory of Jacob and Jenny Finestone.

REFERENCES

1. Rosenblatt DS, Fenton WA. Inherited disorders of folate and cobalamin transport and metabolism. In: Scriver CR, Beaudet AL, Sly WS, Valle D, Childs B, Kinzler KW, et al, editors. The metabolic and molecular bases of inherited disease. 8th ed. New York: McGraw-Hill; 2001. p. 3897–933.

2. Goodman SI, Moe PG, Hammond KB. Homocystinuria with methylmalonic aciduria: two cases in a sibship. Biochem Med 1970;4:500–25.

3. Willard HF, Mellman IS, Rosenberg LE. Genetic complementation among inherited deficiencies of methylmalonyl-CoA mutase activity: evidence for a new class of human cobalamin mutant. Am J Hum Genet 1978;30:1–13.

4. Suormala T, Baumgartner MR, Coelho D, Zavadakova P, Kozich V, Koch HG, et al. The cblD defect causes either isolated or combined deficiency of methylcobalamin and adenosylcobalamin synthesis. J Biol Chem 2004;279:42742–9.

5. Coelho D, Suormala T, Stucki M, Lerner-Ellis JP, Rosenblatt DS, Newbold RF, et al. Gene identification for the cblD defect of vitamin B_{12} metabolism. N Engl J Med 2008;358:1454–64.

6. Rosenblatt DS, Cooper BA, Pottier A, Lue-Shing H, Matiaszuk N, Gravel K. Altered vitamin B_{12} metabolism in fibroblasts from a patient with megaloblastic anemia and homocystinuria due to a new defect in methionine biosynthesis. J Clin Invest 1984;74:2149–56.

7. Jacobsen DW, Green R, Quadros EV, Moestrup YD. Rapid analysis of cobalamin coenzymes and related corrinoid analogs by high-performance liquid chromatography. Anal Biochem 1992;120:394-403.
8. Watkins D. Cobalamin metabolism in methionine-dependent human tumour and leukemia cell lines. Clin Invest Med 1998;21:151-8.
9. Watkins D, Matiaszuk N, Rosenblatt DS. Complementation studies in the *cblE* class of inborn error of cobalamin metabolism: evidence for intracellular complementation and for a new complementation class (*cblX*). J Med Genet 2000;37:510-3.
10. Baethmann M, Wendel U, Hoffmann GF, Goblich-Ratmann G, Kleinlein B, Seiffert P, et al. Hydrocephalus internus in two patients with 5,10-methylenetetrahydrofolate reductase deficiency. Neuropediatrics 2000;32:314-7.
11. Bianchetti R, Carrese R, Schiaffino MC, Caruso U, Vezzulli E, Perrone MV, et al. Cobalamin (Cbl) C/D deficiency: clinical, neurophysiological and neuroradiologic findings in 14 cases. Neuropediatrics 2001;32:14-22.
12. Andersson HC, Marble M, Shapiro E. Long-term outcome in combined methylmalonic acidemia and homocystinuria (cblC). Genet Med 1999;1:346-50.

50 Years Ago in *The Journal of Pediatrics*

The Protein Requirement of Infants

Holt EM. J Pediatr 1959;54:496-502.

One hundred years ago, attempts at artificial feeding of young infants still were challenged by the frequent contamination of food, water, and vessels by germs and toxins. In addition, there was little understanding of the nutrient needs of infants for growth and development or of the nutrient composition of human and substitute animal milks. By the middle of the 20th century, there was relatively good information on the nutrient composition of human milk, safe infant formulas were available to support the growth of healthy infants, and balance studies were helping to define the needs for both macronutrients and micronutrients. However, the nutritional science available had not yet definitively determined the daily protein requirement for growing infants. The non-protein nitrogen content of human milk and its contribution to protein requirements and to the health and growth of the infant were not appreciated, and energy expenditure and body composition data were at best approximations. As a result, at the end of the 1950s, Holt was unable to conclude from available evidence whether protein intakes <3 to 4 g/kg/day were adequate to support the growth of young infants.

In the 50 years since then, the question that puzzled Dr. Holt has been answered, through the use of modern analytic techniques. The use of stable isotope tracers, neutron activation, photon and x-ray absorptiometry, air-displacement plethysmography, total body electrical conductivity, and other techniques pioneered since the 1950s has led to much more accurate estimations of daily nutrient requirements and body composition.

The adequate intake for infants aged 0 to 6 months is 1.52 g/kg/day, based on the protein intake consumed from human milk. Protein quality must be considered when sources of protein other than human milk are consumed. Thus, infant formula should provide 1.68 g/kg/day of protein. For older infants, the reference value is estimated by using the factorial method to be 1.0 g/kg/day, and the value that meets the requirements of 97% of the population is 1.2 g/kg/day. Holt can now rest easy as we shift our attention away from daily requirements and focus on infant feeding and its effects on later health, nutrient-gene interactions, and more effective ways to support the nutritional needs of special populations, such as premature infants.

This is dedicated to Dr. Sam Fomon, whose friendship, counsel, and advice are dearly missed.

Ronald E. Kleinman, MD
Chair, Department of Pediatrics
Massachusetts General Hospital
Charles Wilder Professor of Pediatrics
Harvard Medical School
Boston, Massachusetts
10.1016/j.jpeds.2008.09.046